Label Transfer Reagents for the Study of Protein Kinase Complexes

Simeon Andrews

A dissertation

submitted in partial fulfillment of the

requirements for the degree of

Doctor of Philosophy

University of Washington

2012

Reading Committee:

Dustin J. Maly, Chair

Forrest Michael

Gojko Lalic

Program Authorized to Offer Degree:

Department of Chemistry

University of Washington

Abstract

Label Transfer Reagents for the Study of Protein Kinase Complexes

Simeon Andrews

Chair of the Supervisory Committee:

Assistant Professor Dustin J. Maly

Department of Chemistry

Protein kinases are essential enzymes for cellular signaling, and are often regulated by participation in protein complexes. The mitogen-activated protein kinase (MAPK) p38 is involved in multiple pathways, and its regulation depends on its interactions with other signaling proteins. However, the weak and transient nature of these interactions makes the identification of p38 interacting proteins challenging. For this reason, we have developed label transfer reagents (LTRs) which allow labeling of p38 signaling complexes. These LTRs leverage the potency and selectivity of known p38 inhibitors to place a photo-crosslinker and tag in the vicinity of p38 and its binding partners. Upon UV irradiation, proteins that are in close proximity to p38 are covalently crosslinked, and labeled proteins are detected and/or purified through an orthogonal chemical handle. Here we demonstrate that p38-selective LTRs efficiently label a diversity of p38 binding partners, including substrates and activators. Furthermore, these LTRs can be used in immunoprecipitations for study of proteins not exogenously expressible. Several limitations of LTRs are also explored. Finally, copper-catalyzed click chemistry is optimized in a quantitative fashion for the labeling and purification of alkynylated proteins.

Table of Contents

Introduction

Protein phosphorylation is a key posttranslational modification in eukaryotic organisms, in which the γ-phosphate of ATP is covalently attached to a serine, threonine, or tyrosine residue. This modification is critical for intracellular signaling and can both positively and negatively affect enzyme activity and protein-protein interactions. Phosphorylation is carried out by a class of enzymes known as protein kinases, while the removal of the phosphate is performed by phosphatases.[1,2] Given the diversity and complex specificity requirements of intracellular signaling, it is unsurprising that there is a large number kinases in the human genome – 518.[3] Most cellular processes are affected by protein phosphorylation, and misregulation of phosphorylation has been linked to many diseases, including cancer and inflammation.

Although protein kinases are quite diverse and are often contain multiple domains, the kinase domain of all kinases is highly conserved in structure, with a β-strand-rich N-terminal lobe and an α-helix-rich C-terminal lobe (Figure 1). The cleft between these two lobes represents the active site of the kinase, where adenine of the ATP substrate binds in a deep pocket, leaving its phosphates solvent-exposed and coordinated by a magnesium ion. This metal is crucial in the catalytic step, coordinating the β- and γ-phosphates of ATP to minimize charge repulsion as the γ-phosphate is transferred to the substrate.[4]

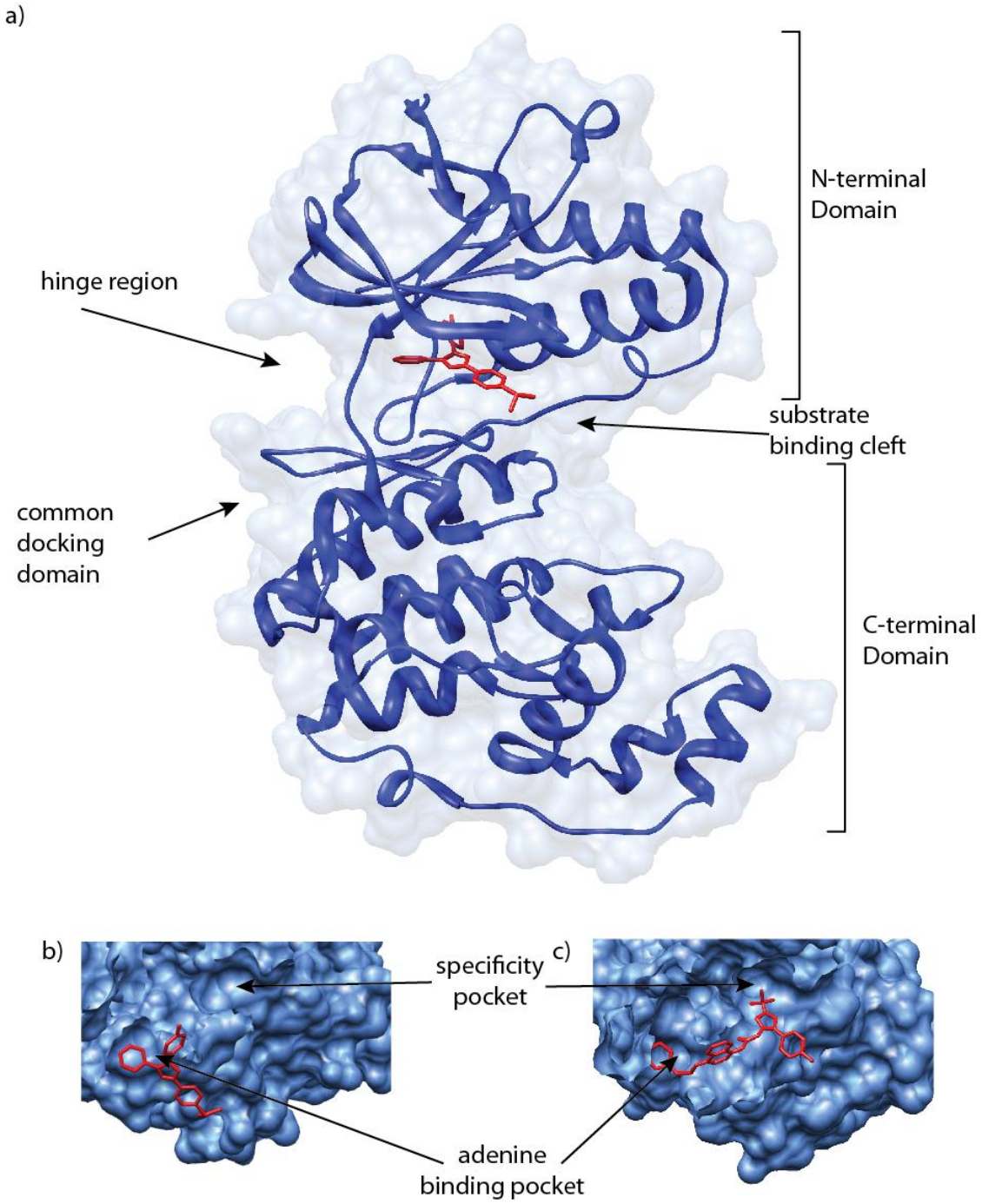

***Figure 1*:** General structure of protein kinases. a) p38α kinase, crystallized with the inhibitor SB203580 (PDB ID 3GCP. B) Expansion of the ATP-binding pocket of p38α with the inhibitor SB203580 bound. c) Expansion of the ATP-binding pocket of p38α with the inhibitor BIRB796 bound.

The mitogen-activated protein kinase (MAPK) family of kinases includes 4 subfamilies: ERK, JNK, BMK, and p38.[5-8] This family of kinases is relatively simple structurally, consisting of a single catalytic domain. Their activation loops contain both a tyrosine and a serine or threonine residue, which must be phosphorylated by a dual-specificity kinase, a MAPK kinase (or MKK, also known as MEKs), in order to gain full catalytic activity. The MKKs in turn are phosphorylated by MAPK kinase kinases (MKKKs or MEKKs); in some cases there is even a MAPK kinase kinase kinase (MKKKK). These MAPK cascades are often initiated by the same signal, such as mitogens and cell stress. JNK and p38 family members, in particular, are often called stress-activated protein kinases (SAPKs) for their critical role in responding to osmotic shock, UV DNA damage, heat shock, and other stressors.

MAPKs are involved in highly diverse pathways (*e.g.*, differentiation vs stress response), and consequently the outcomes from activating the MAPKs must be commensurate with the initial trigger. Indeed, it is clear that different stimuli will produce different phenotypes in spite of acting through the same MAPK.[9] The mechanism of this pathway specificity is poorly understood. It is likely that, as a given stimulus often activates multiple pathways, the crosstalk between the pathways will regulate the outcome of the other pathways. Another way of maintaining pathway integrity is through the use of pathway-specific complexes.

Protein kinase A (PKA, a non-MAPK) is particularly well known for this, as there are a variety of A-kinase anchoring proteins (AKAPs) known to compartmentalize PKA and other proteins – both substrates and activators – in diverse parts of the cell. Among the MAPKs, scaffolding proteins have been described for all families except BMK1.[10,11] KSR, MORG1, Paxillin, and

Arrestin B all scaffold ERK with its upstream MKK and MKKK. JIPs, similarly, bind to both JNK and its upstream activators. For p38, PKN has been shown to bind p38 (both α and γ), its upstream kinases MKK3 and MKK6, and their activator MLTK.[12-14] Additionally, OSM is known to interact with p38-specific MKK3, MEKK3, and Rac, though binding to p38 itself was not observed.[15] Thus, it is clear that the particular subset of proteins that a kinase interacts with during a signaling event can vary, and that the determination of these interacting partners is an important issue to address.

The p38 sub-family of protein kinases has four members, designated α, β, γ, and δ.[16] Proteins p38α and p38β are quite similar to each other in sequence, while proteins p38γ and p38δ are also quite similar to each other; this is reflected in the specificity of inhibitors, as some inhibitors can potently inhibit p38α and p38β, but not p38γ and p38δ. While some signaling events seem to preferentially use one p38 family member over the others, the majority of signaling events lead to activation of all p38 family members. p38α is by far the most ubiquitously expressed and is expressed at higher levels. Consequently, it is generally the most studied member of the p38 family, and hereafter "p38" will refer to p38α, unless otherwise noted.

p38 is involved in a wide variety of cellular processes. Aside from its response to the cellular stresses mentioned above, this kinase is also involved in development, growth, and inflammatory responses. It has been implicated in cancer, heart disease, and neurodegenerative disorders.[17] These signals can act though a variety of MKKKs, leading to activation of MKK6 or MKK3 (or in some cases MKK4). p38 is activated by an MKK via dual phosphorylation on its activation loop tyrosine and threonine. This greatly enhances the enzymatic activity of p38, leading to rapid

phosphorylation of its substrates. Alternately, p38 can also be activated by association with the protein TAB1, which appears to induce auto-phosphorylation, again leading to activated p38.[18] p38 has a wide diversity of substrates, including downstream kinases (like MAPKAP-K2, otherwise known as MK2), enzymes (*e.g.*, PLA2), and transcription factors (*e.g.*, MEF2A/C/D).

p38 has been the focus of multiple drug development programs, in particular due to its role in inflammation. While to date there are no clinically approved p38 inhibitors, there are several potent, selective, and structurally diverse p38 inhibitors that have been used extensively to study p38.[19-22] SB203580 is the most widely used p38 inhibitor, and it is a classic "type I" inhibitor, as it binds to p38 in the adenine binding site, maintaining all catalytic residues in their active conformations.[23] BIRB796, another common inhibitor of p38, is a "type II" inhibitor, inducing the so-called "DFG-out" conformation.[24] In this conformation, the aspartate-phenylalanine-glycine (DFG) motif of the activation loop is rotated into a catalytically incompetent conformation, as the inhibitor binds to a "specificity pocket" as well as the adenine pocket, displacing the phenylalanine of the DFG motif.

Aside from structures of p38 bound to small molecule inhibitors, it has also been crystallized with its substrate MAPKAP-K2 (also known as MK2).[25,26] This structure reveals multiple points of contact between p38 and MK2, as the active sites of the two kinases face each other. However, the majority of the binding energy for the MK2-p38 interaction comes from the 30 C-terminal residues of MK2, where it interacts with a patch near the active site of p38 known as the "common docking" domain (see Figure 1).[27] Binding to the common docking domain is also

seen in structures of p38 with peptides derived from its substrate MEF2A and its activator MKK3.[28]

Given the importance of p38 in cellular function, as well as in disease, we desired to develop a method of determining which proteins it interacts with under different conditions. A wide variety of methods have already been developed to study protein-protein interactions, and all have their advantages and disadvantages. Our original goal was to develop a method that would work with endogenous levels of untagged proteins, and would require no protein purification that might disrupt protein-protein interactions. Moreover, since we wanted to observe the complement of p38 binding partners under different conditions, this method needed to function on a time-scale commensurate with kinase signaling events.

The approach we chose is to create a label transfer reagent. Label transfer reagents (LTRs) are tri-functional probes: one component binds the bait protein, one component labels proteins bound to the bait, and a tag that can be used to identify or purify the proteins labeled by the reagent. Many LTRs have been developed, but generally are limited by their delivery to the bait protein.[29,30] Most LTRs are conjugated to the bait protein through non-specific reactions, such as a succinimide labeling of surface-exposed lysines. This means that there is little structural information about where the target proteins interact with the bait protein, unless the sites of modification can be identified. Moreover, because the bait and target are covalently linked, analysis of the crosslinked product can be particularly challenging. Some groups have used bis-arsenical tags on the bait protein as the site of attachment for the LTR.[30] This avoids these two problems – the LTR is attached to a specific site, and can be dissociated with an excess of

chelating thiols – but require a non-endogenous tag. Not only is there a risk of interfering with native protein-protein interactions, but he N and C termini of the protein, where bis-arsenical tags are normally placed, may not be near the site of protein-protein interaction.

We have therefore made a critical modification to the normal LTR approach by choosing to attach the LTR to the bait protein through an inhibitor of the kinase. The potency of the inhibitor can assure a strong connection to the bait protein, yet this is fully reversible upon denaturation of the proteins. Furthermore, this places the LTR near the active site of the enzyme, where many proteins interact. This positioning is particularly true of MAPKs, as both the common docking domain and substrate binding areas of the kinase are located near the adenine-binding pocket.

Both type I and II inhibitors would be of interest for use in an LTR, as the conformation of the protein may alter the proteins it interacts with. The MPAQ inhibitor has been structurally characterized as a type II inhibitor.[31,32] Conveniently, this inhibitor has already been characterized as a fairly selective inhibitor, and an easily derivitizable piperidine moiety extends out of the active site near the common docking site of p38.[33] During the course of this work, a phthalazine-based inhibitor of p38 was also described.[34-36] This inhibitor also contains a portion that exits the active site near the common docking domain. The phthalazine core binds in a conformation that requires a glycine in the hinge region of the kinase, which is present in very few kinases. As a result, this inhibitor is highly selective, as has been shown in both other labs and our own.[37] A crystal structure of p38 complexed with a phthalazine inhibitor shows the kinase in an active conformation, indicating this is a type I inhibitor.[34] Given that these are both potent and selective inhibitors, these were selected for our initial LTRs.

The crosslinking moiety was another critical choice for the LTR. Diazirines and perfluoro aryl azides are effective UV-triggered crosslinkers. However, when they are activated, they have short lifetimes; if they do not interact productively with a protein of interest in that time frame, they relax and are no longer of use. Benzophenones have been used as photocrosslinkers for many years.[38] Aside from being fairly efficient, they have the added advantage of being able to relax back to the ground state if they do not insert into a bond when excited, and can be re-excited. This is a particular advantage for use in an LTR, as the crosslinker is expected to need to diffuse through space around the bait protein, and thus often when the crosslinker is excited it may not be near a protein of interest during its lifetime. Benzophenones have been shown to insert into a wide variety of carbon-hydrogen bonds, making them more general than many crosslinkers that require a specific residue type. We also chose to explore L-3,4-dihydroxyphenylalanine (DOPA) as a crosslinker. Incubation of DOPA with a strong oxidizing agent like sodium periodate can create a diketone which is highly reactive to nucleophilic side chains.[39] While sodium periodate is incompatible with living biological systems, it would be useful for work in lysate or with purified proteins.

The third component of the LTR is the label. We have considered a diversity of labels, and describe them in detail in chapter 2. However, we have focused on an alkyne label. An alkyne is small, highly cell permeable, and unreactive to biological molecules. Moreover, it increases the flexibility of the LTRs synthesized, allowing for the inclusion of almost any label of interest through copper-mediated click chemistry.

This thesis is divided into three chapters. The first describes the most productive work we have had with LTRs, showing their utility to study protein-protein interactions of exogenously expressed proteins, as well as their use to probe complexes that are immunoprecipitated from mammalian cells. The second chapter explores a diversity of other LTRs that were less effective than those described in the first chapter, as well as some applications we attempted with the LTRs which were not ultimately successful. In an effort to improve click chemistry – particularly our ability to purify proteins labeled with our LTRs – we desired to optimize click chemistry. The third chapter describes our efforts to quantitatively compare several ligands for click chemistry and improve recovery of low-abundance alkynylated proteins.

Refernces

(1) Fischer, E. H.; Krebs, E. G. *J. Biol. Chem.* **1955**, *216*, 121-32.

(2) Krebs, E. G.; Fischer, E. H. *J. Biol. Chem.* **1955**, *216*, 113-20.

(3) Manning, G.; Whyte, D. B.; Martinez, R.; Hunter, T.; Sudarsanam, S. *Science* **2002**, *298*, 1912-34.

(4) Adams, J. A. *Chem. Rev.* **2001**, *101*, 2271-90.

(5) de Paula, R. M.; Lamb, T. M.; Bennett, L.; Bell-Pedersen, D. *Cell Cycle* **2008**, *7*, 2630-4.

(6) Dent, P.; Yacoub, A.; Fisher, P. B.; Hagan, M. P.; Grant, S. *Oncogene* **2003**, *22*, 5885-96.

(7) Pimienta, G.; Pascual, J. *Cell Cycle* **2007**, *6*, 2628-32.

(8) Raman, M.; Chen, W.; Cobb, M. H. *Oncogene* **2007**, *26*, 3100-12.

(9) Lu, G.; Kang, Y. J.; Han, J.; Herschman, H. R.; Stefani, E.; Wang, Y. *J Biol. Chem.* **2006**, *281*, 6087-95.

(10) Dhanasekaran, D. N.; Kashef, K.; Lee, C. M.; Xu, H.; Reddy, E. P. *Oncogene* **2007**, *26*, 3185-202.

(11) Morrison, D. K.; Davis, R. J. *Annu. Rev. Cell Dev. Biol.* **2003**, *19*, 91-118.

(12) Cariolato, L.; Cavin, S.; Diviani, D. *J. Biol. Chem.*, *286*, 7925-37.

(13) Marinissen, M. J.; Chiariello, M.; Gutkind, J. S. *Genes Dev.* **2001**, *15*, 535-53.

(14) Takahashi, M.; Gotoh, Y.; Isagawa, T.; Nishimura, T.; Goyama, E.; Kim, H. S.; Mukai, H.; Ono, Y. *J. Biochem.* **2003**, *133*, 181-7.

(15) Hilder, T. L.; Malone, M. H.; Johnson, G. L. *Methods Enzymol.* **2007**, *428*, 297-312.

(16) Cuadrado, A.; Nebreda, A. R. *Biochem. J.*, *429*, 403-17.

(17) Cuenda, A.; Rousseau, S. *Biochim. Biophys. Acta* **2007**, *1773*, 1358-75.

(18) Kang, Y. J.; Seit-Nebi, A.; Davis, R. J.; Han, J. *J. Biol. Chem.* **2006**, *281*, 26225-34.

(19) Boldt, S.; Kolch, W. *Curr. Pharm. Des.* **2004**, *10*, 1885-905.

(20) Dominguez, C.; Powers, D. A.; Tamayo, N. *Curr. Opin. Drug Discov. Devel.* **2005**, *8*, 421-30.

(21) Lee, M. R.; Dominguez, C. *Curr. Med. Chem.* **2005**, *12*, 2979-94.

(22) Xu, J. J.; Hendriks, B. S.; Zhao, J.; de Graaf, D. *FEBS Lett.* **2008**, *582*, 1276-82.

(23) Simard, J. R.; Getlik, M.; Grutter, C.; Pawar, V.; Wulfert, S.; Rabiller, M.; Rauh, D. *J. Am. Chem. Soc.* **2009**, *131*, 13286-96.

(24) Pargellis, C.; Tong, L.; Churchill, L.; Cirillo, P. F.; Gilmore, T.; Graham, A. G.; Grob, P. M.; Hickey, E. R.; Moss, N.; Pav, S.; Regan, J. *Nat. Struct. Biol.* **2002**, *9*, 268-72.

(25) White, A.; Pargellis, C. A.; Studts, J. M.; Werneburg, B. G.; Farmer, B. T., 2nd *Proc. Natl. Acad. Sci. U S A* **2007**, *104*, 6353-8.

(26) ter Haar, E.; Prabhakar, P.; Liu, X.; Lepre, C. *J. Biol. Chem.* **2007**, *282*, 9733-9.

(27) Lukas, S. M.; Kroe, R. R.; Wildeson, J.; Peet, G. W.; Frego, L.; Davidson, W.; Ingraham, R. H.; Pargellis, C. A.; Labadia, M. E.; Werneburg, B. G. *Biochemistry* **2004**, *43*, 9950-60.

(28) Chang, C. I.; Xu, B. E.; Akella, R.; Cobb, M. H.; Goldsmith, E. J. *Mol. Cell.* **2002**, *9*, 1241-9.

(29) Fancy, D. A. *Curr. Opin. Chem. Biol.* **2000**, *4*, 28-33.

(30) Liu, B.; Archer, C. T.; Burdine, L.; Gillette, T. G.; Kodadek, T. *J. Am. Chem. Soc.* **2007**, *129*, 12348-9.

(31) Sullivan, J. E.; Holdgate, G. A.; Campbell, D.; Timms, D.; Gerhardt, S.; Breed, J.; Breeze, A. L.; Bermingham, A.; Pauptit, R. A.; Norman, R. A.; Embrey, K. J.; Read, J.; VanScyoc, W. S.; Ward, W. H. *Biochemistry* **2005**, *44*, 16475-90.

(32) Cumming, J. G.; McKenzie, C. L.; Bowden, S. G.; Campbell, D.; Masters, D. J.; Breed, J.; Jewsbury, P. J. *Bioorg. Med. Chem. Lett.* **2004**, *14*, 5389-94.

(33) Perera, B. G.; Maly, D. J. *Mol. Biosyst.* **2008**, *4*, 542-50.

(34) Herberich, B.; Cao, G. Q.; Chakrabarti, P. P.; Falsey, J. R.; Pettus, L.; Rzasa, R. M.; Reed, A. B.; Reichelt, A.; Sham, K.; Thaman, M.; Wurz, R. P.; Xu, S.; Zhang, D.; Hsieh, F.;

Lee, M. R.; Syed, R.; Li, V.; Grosfeld, D.; Plant, M. H.; Henkle, B.; Sherman, L.; Middleton, S.; Wong, L. M.; Tasker, A. S. *J. Med. Chem.* **2008**, *51*, 6271-9.

(35) Pettus, L. H.; Xu, S.; Cao, G. Q.; Chakrabarti, P. P.; Rzasa, R. M.; Sham, K.; Wurz, R. P.; Zhang, D.; Middleton, S.; Henkle, B.; Plant, M. H.; Saris, C. J.; Sherman, L.; Wong, L. M.; Powers, D. A.; Tudor, Y.; Yu, V.; Lee, M. R.; Syed, R.; Hsieh, F.; Tasker, A. S. *J. Med. Chem.* **2008**, *51*, 6280-92.

(36) Tasker, A. Z., Dawei; Pettus, Liping H.; Rzasa, Robert M.; Sham, Kelvin K. C.; Xu, Shimin; Chakrabarti, Partha Pratim 2008; Vol. WO 2008030466 A1 20080313.

(37) Hill, Z. B.; Perera, B. G.; Andrews, S. S.; Maly, D. J. *ACS Chem. Biol.* **2012**, *7*, 487-95.

(38) Dorman, G.; Prestwich, G. D. *Biochemistry* **1994**, *33*, 5661-73.

(39) Liu, B.; Burdine, L.; Kodadek, T. *J. Am. Chem. Soc.* **2006**, *128*, 15228-35.

Chapter 1

Label Transfer Reagents for Labeling and Purification of Proteins Associated with p38 Kinase

Abstract

Protein kinases are essential enzymes for cellular signaling, and are often regulated by participation in protein complexes. The mitogen-activated protein kinase (MAPK) p38 is involved in multiple pathways, and its regulation depends on its interactions with other signaling proteins. However, the weak and transient nature of these interactions makes the identification of p38 interacting proteins challenging. For this reason, we have developed label transfer reagents (LTRs) which allow labeling of p38 signaling complexes. These LTRs leverage the potency and selectivity of known p38 inhibitors to place a photo-crosslinker and tag in the vicinity of p38 and its binding partners. Upon UV irradiation, proteins that are in close proximity to p38 are covalently crosslinked, and labeled proteins are detected and/or purified through an orthogonal chemical handle. Here we demonstrate that p38-selective LTRs efficiently label a diversity of p38 binding partners, including substrates and activators. Furthermore, these LTRs can be used in immunoprecipitations for study of proteins not exogenously expressible.

Introduction

Protein phosphorylation is a post-translational modification that is essential for intracellular signaling in all eukaryotic organisms. Indeed, the human genome encodes over 500 different protein kinases.[25] Consequently, the regulation of these kinases is both important and complex. One key way that kinases are regulated is by their sequestration in signaling complexes. These complexes can bring together activators or substrates of kinases, permitting rapid and complex-specific transmission of a cellular signal.[26,27]

p38α (hereafter referred to as p38) is a MAPK involved in cellular responses to inflammatory cytokines, growth factors, and stresses such as osmotic shock and DNA damage.[28] These signals trigger the activation of MKK6 and/or MKK3, which activate p38 by dual activation loop phosphorylation. In addition, p38 can be activated by MAPKK-independent pathways, such as TAB1-induced autophosphorylation of p38 in response to some extracellular signals.[29,30] The substrates of p38 are varied, including downstream kinases, enzymes, and transcription factors. Importantly, while diverse stimuli activate p38, the substrates that are phosphorylated by p38 vary with the specific stimulus.[30,31] Thus, there exists a means of correlating the activation of p38 with the substrates it phosphorylates. This specificity may be accomplished, in part, by the activity of other signaling molecules triggered by that stimulus. It is also likely that a significant component of this regulation is through sequestering p38 into stimulus-specific complexes. Therefore, the complement of proteins bound to p38 will vary under different cellular conditions. Surprisingly, few p38 complexes have been described.[32] It is likely that this lack of knowledge is due to the weak and transient nature of these complexes.

For these reasons, we have developed a novel method to study protein kinase signaling complexes that enables us to detect p38-interacting proteins. This method relies on the use of highly selective ATP-competitive inhibitors to position a photo-crosslinker and tag in the vicinity of p38 protein complexes (Figure 1). These label transfer reagents (LTRs) contain three modular components (Figure 1a): (1) an ATP-competitive kinase inhibitor that targets the labeling reagent to a kinase target of interest; (2) a photo-crosslinker, which allows covalent labeling of any proteins that are in proximity to the LTR; and (3) an orthogonal chemical handle for visualization and/or purification of proteins that have been labeled. When the LTR is introduced to a sample containing p38, the ATP-competitive inhibitor will bind to the kinase, positioning the crosslinker in the vicinity of p38 and the proteins with which it is complexed. Upon ultraviolet (UV) irradiation, the LTR covalently labels proteins in a p38 complex. The use of a selective p38 inhibitor allows LTRs to be used in complex protein mixtures, and the covalent nature of the labeling reaction should enable detection of even weak and transient interactions.

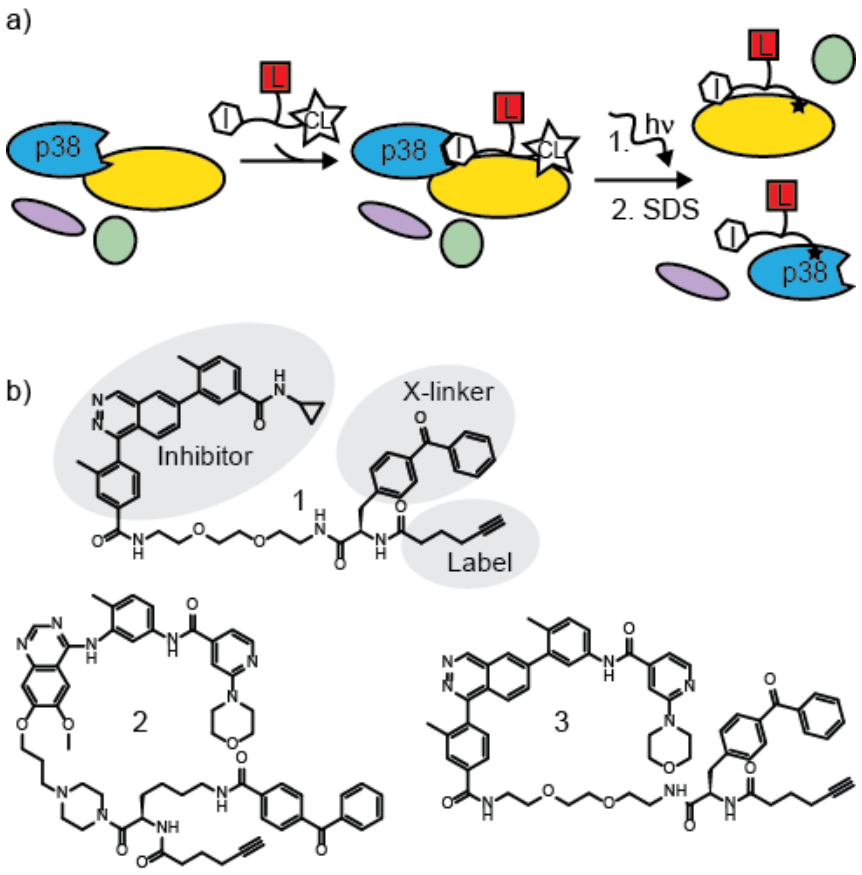

Figure 1. a) Label transfer reagent (LTR) strategy. An ATP-competitive p38 inhibitor (I) directs the LTR to the active site of p38, placing a photo-crosslinker (CL) in the vicinity of p38 and proteins that interact with p38. UV irradiation covalently labels proteins in p38 signaling complexes with a label (L) that can be used for detection or purification. b) Structures of LTRs **1**-**3** that were generated and used in this study.

Results & Discussion

Three different LTRs were designed for labeling p38 complexes (**1**-**3**, Figure 1b). All three LTRs contain a benzophenone photo-crosslinker and an alkyne tag that are connected to an ATP-competitive inhibitor through a flexible linker. Upon ultraviolet irradiation, the benzophenone

crosslinker is able to label proteins that are in close proximity to the bound inhibitor.[33] The alkyne tag allows conjugation of labeled proteins to a reporter group for visualization (fluorophore) or affinity enrichment (biotin) through a "click" chemistry reaction.[34] Three different inhibitors that are highly potent and selective for p38 were used as the directing groups for the LTRs (Figure 1b). All three inhibitors occupy the ATP-binding site of p38 and make key hydrogen bonds with the hinge region of this kinase. Furthermore, the inhibitor scaffolds of **1** and **2** have been structurally characterized with p38 (Figure 2).[35,36]

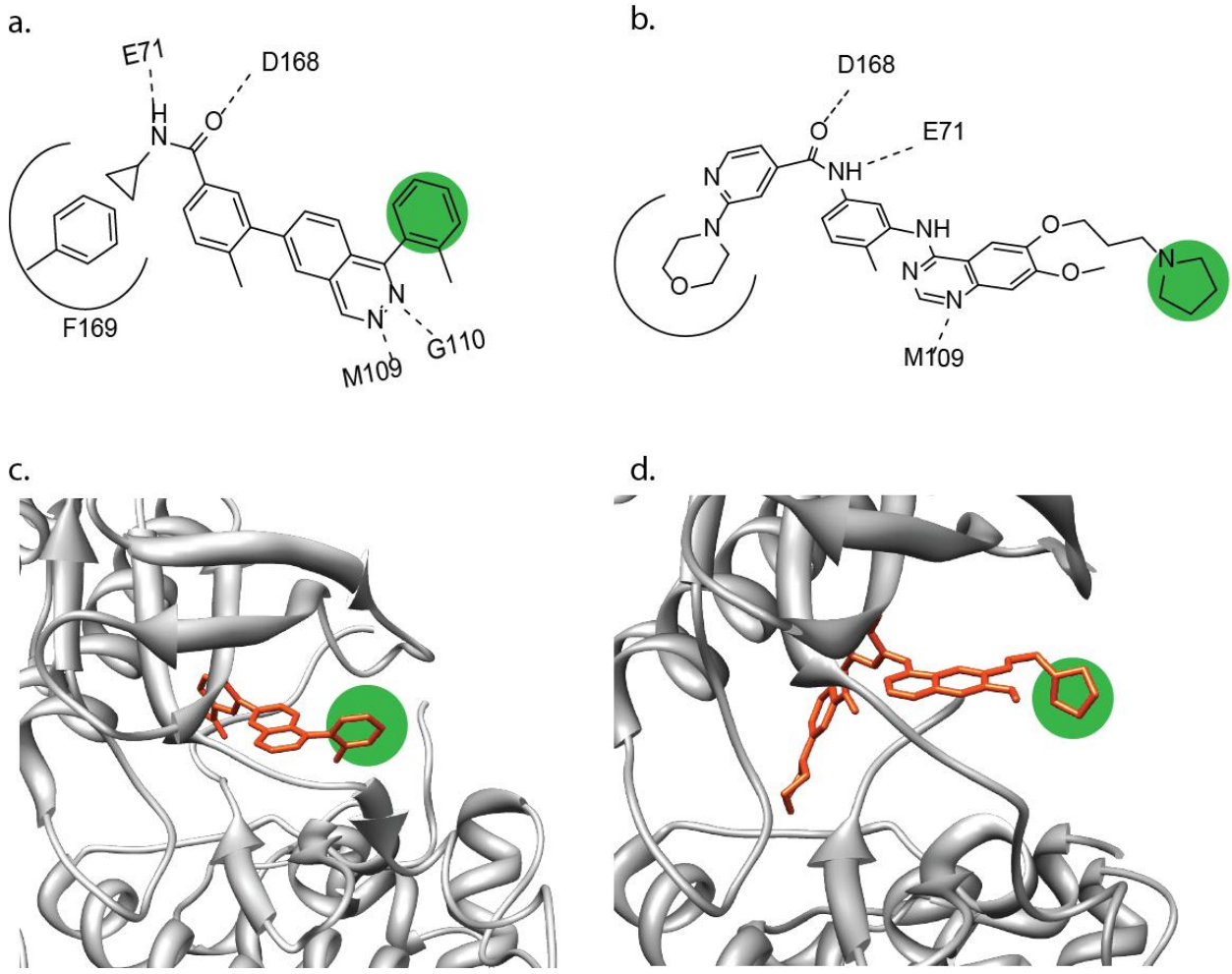

Figure 2 **a.** Phthalazine scaffold described in literature. The phthalazine scaffold occupies the purine binding site of ATP, making key hydrogen bonds with the backbone hinge region residues M109 and G110, as well as hydrogen bonds to D168 and E71. The cyclopropyl group of the inhibitor packs against F169 of the "DFG" motif. **b.** The published quinazoline compound and its crystal structure contacts. The quinazoline has similar contacts to the phthalazine scaffold, though it lacks one hinge region hydrogen bond. Importantly, the morpholine moiety displaces F169, leading to a "DFG-out" conformation which is catalytically inactive. **c.** Crystal structure of phthalazine scaffold bound to p38 (PDB ID: 2DS6), showing the site chosen for modification, highlighted in green. **d.** Crystal structure of the quinazoline scaffold bound to p38 (PDB ID: 2BAK), showing the site chosen for modification, highlighted in green.

LTR **1** is based on a phthalizine inhibitor that contains a cyclopropyl group that packs against the activation loop of p38, stabilizing this kinase in an active conformation.[35] LTR **2** is based on a quinazoline inhibitor that contains an extended morpholino-pyridine moiety that occupies a pocket formed by movement of the activation loop.[36] Combined with a hydrogen bond donor–acceptor pair, this forces p38 to adopt an inactive conformation known as "DFG-out." We synthesized a third scaffold, **3**, which retains the core phthalazine scaffold of **1**, but substitutes the morpholino pyridine moiety of **2** for the cyclopropyl group. We expect this hybrid molecule will be a highly selective and potent inhibitor that binds analogously to **1**, but induces the DFG-out conformation. These three scaffolds have different interactions with p38, and thus, their selectivity profiles are expected to differ from one another.[37] Consequently, LTRs with complementary scaffolds can be used to demonstrate that the results obtained are due to interaction with p38, and not an off-target kinase.

a)

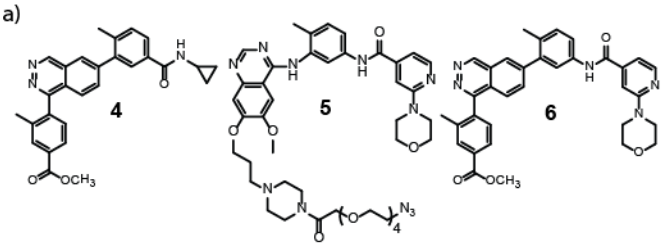

b)

Compound	p38α	JNK1	JNK3	ERK1	ERK2
1	< 1.0	> 10,000	> 10,000	> 10,000	> 10,000
2	15 ± 1	> 10,000	> 10,000	> 10,000	> 10,000
3	< 1.0	> 10,000	> 10,000	> 10,000	> 10,000
4	< 1.0	NT	NT	NT	NT
5	7.9 ± 1.2	NT	NT	NT	NT
6	< 1.0	NT	NT	NT	NT

Figure 3. a) Structures of the selective p38 inhibitors that were used as competitors in these studies. b) *In vitro* activities (in nM) of LTRs **1**-**3** and competitors **4**-**6** against the MAPKs p38, JNK1, JNK3, ERK1, and ERK2. Values shown are the average of at least three assays ± SEM.

To attach the benzophenone crosslinker and alkyne tag, each inhibitor scaffold was modified at a site that has been shown to be solvent-exposed. Importantly, this site of derivitization should project the photo-crosslinker in the direction of the docking and substrate-binding sites of p38 (Figure 2 c,d). To ensure that the LTRs maintained their potency and selectivity for p38, they were tested in an *in vitro* activity assay against this kinase and several other MAPKs (JNK1, JNK3, ERK1, and ERK2). We were gratified to see that LTRs **1**-**3** have low to sub-nanomolar IC_{50}s for p38 and show no detectable inhibition of the other MAPKs tested (Figure 3a). This level of potency and selectivity is similar to the parent inhibitors from which these LTRs were derived (Figure 3b). [35,36]

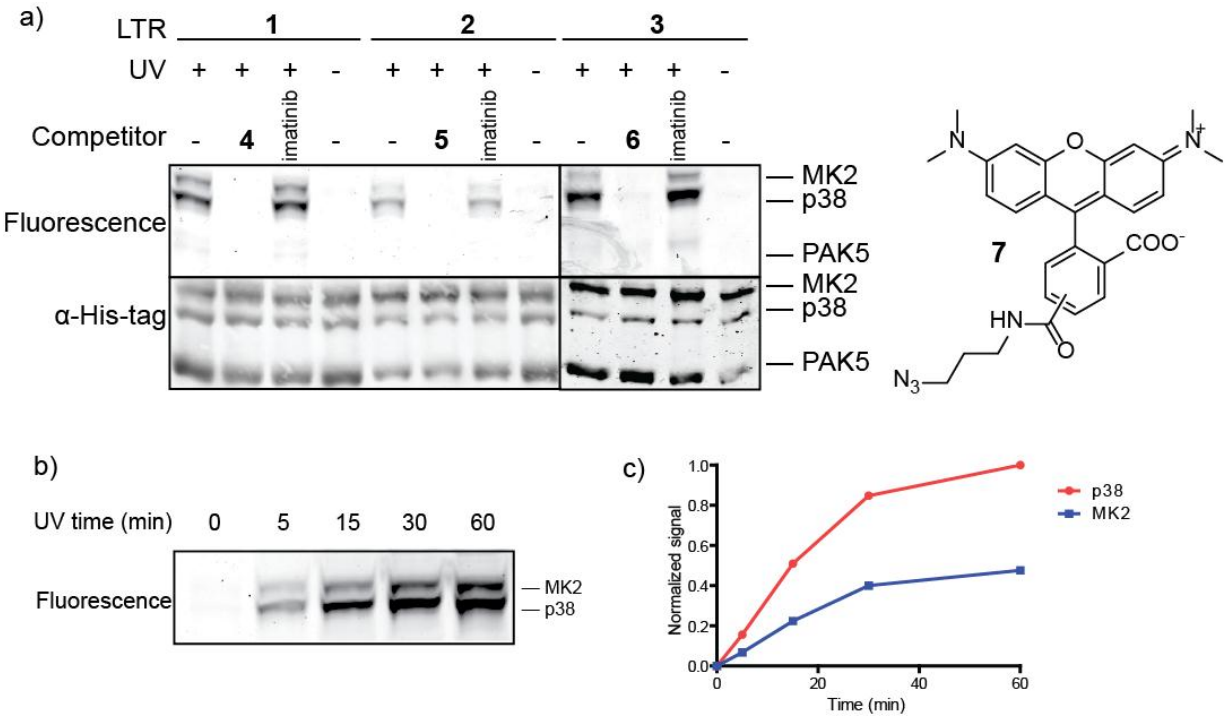

Figure 4. LTR labeling of p38 and its substrate MK2. Each protein mixture was irradiated with UV light for 30 minutes, and then conjugated to rhodamine-azide **7**, followed by SDS-PAGE analysis and in-gel fluorescence scanning. Total protein loading for each sample was determined with an α-His6 antibody. a) Characterization of LTRs **1-3**. Each LTR (500 nM) was incubated with p38 (400 nM), MK2 (400 nM), and PAK5 (400 nM) in the absence or presence of a competitor (**4-6** or imatinib at 10 μM) b) UV irradiation time-dependence of LTR labeling with probe **2**: fluorescence labeling of p38 and MK2 shows an increase over time. c) Quantitation of bands in b) shows that the labeling ratio of p38 and MK2 remains constant, and begins to plateau at 30 min.

To test the ability of our LTRs to label proteins that interact with p38, we performed cross-linking experiments with p38 and MK2 (a p38 substrate, also known as MAPKAP-K2) in the presence of a control kinase, PAK5, that does not interact with p38, MK2, or the LTRs (Figure 4a). p38, MK2, and PAK5 were incubated with a LTR (**1-3**), irradiated with UV light, and coupled to rhodamine-azide **7** with click chemistry. LTRs **1-3** all successfully labeled both p38 and MK2, with probes **1** and **3** demonstrating more robust labeling than probe **2** (lanes 1, 5 and

9, Figure 4a). However, PAK5 kinase is not labeled, confirming that it does not bind to p38 and does not interact with any of the LTRs. Importantly, the presence of an ATP-competitive p38 inhibitor that does not contain a photo-crosslinking moiety blocks labeling of both p38 and MK2 (lanes 2, 6, and 10, Figure 4a). In contrast, the ABL-selective kinase inhibitor imatinib, which has no significant affinity for p38, was unable to prevent photo-crosslinking. For all three LTRs, labeling was found to be UV dependent, with no signal observed in the absence of UV light (lanes 4, 8, and 12, Figure 4a). Furthermore, labeling with probe **2** is dose-dependent on UV irradiation time, achieving a plateau after 30 minutes (Figure 4b). At all time points, the ratio of p38 to MK2 labeling remains constant (~3:1 p38 to MK2).

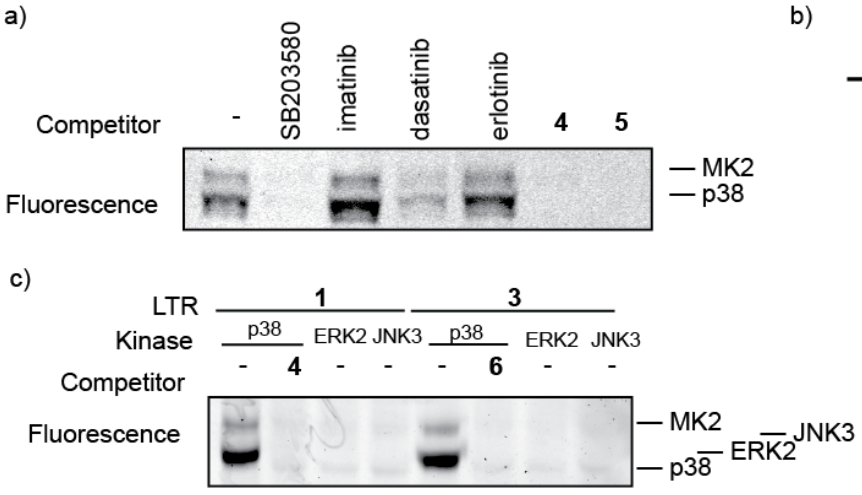

b)

Compound	IC_{50}
SB203580	61 ± 1
Imatinib	> 10,000
Dasatinib	330 ± 10
Erlotinib	> 10,000

Figure 5. Labeling by LTRs is specific. a) Selective p38 inhibitors block p38 and MK2 labeling. LTR **2** (500 nM) was incubated with p38 (400 nM), MK2 (400 nM), and an ATP-competitive inhibitor (10 μM). b) Known kinase inhibitors were tested for their ability to inhibit the activity of p38α. Numbers represent the IC_{50} values in nM concentration. c) Labeling is dependent on the presence of p38 MAPK. LTRs **1** and **3** (250 nm) were incubated with MK2 (200 nM) and p38 (200 nM), ERK2 (200 nM), or JNK3 (200 nM).

The use of highly selective p38 inhibitors as competitors in photo-crosslinking experiments allows further confirmation that protein labeling is due to association with p38 complexes. To demonstrate this, photo-crosslinking experiments were performed in the presence of ATP-competitive inhibitors that have a range of affinities for p38 (Figure 5a,b). As expected, the EGFR- and ABL-selective inhibitors erlotinib and imatinib (p38 IC_{50} >10,000 nM), do not block labeling of p38 or MK2. The presence of the ABL and SRC inhibitor dasatinib, which is a moderately potent inhibitor of p38 (p38(IC_{50}) = 330 nM) does not completely block labeling. Conversely, potent and selective p38 inhibitors such as SB203580 (p38 IC_{50} = 61 nM), **4**, and **5** completely prevent labeling at 10 μM.

MK2 is a substrate for p38 and not of other MAPKs and, therefore, should only be labeled by our LTRs in the presence of p38. To demonstrate this, labeling experiments were performed with MK2 in the presence of p38, ERK2, or JNK3. Significantly, MK2 is not labeled by LTRs **1** and **3** in the presence of ERK2 or JNK3 (Figure 5c). This further establishes that protein labeling is mediated by association with p38. Furthermore, JNK3 and ERK2 are also not labeled, which is consistent with the low affinity of these LTRs for ERK2 and JNK3.

MK2 is a substrate for p38 that interacts with both the substrate-binding cleft and the common docking domain. However, many p38 interacting proteins may only interact with one site of this kinase. Therefore, the diversity of binding partners that can be labeled with p38-selective LTRs was further examined. To determine whether proteins that only interact with the common docking domain of p38 can be identified, a fusion construct that contains the 30 *C*-terminal residues of MK2 (AGT-MK2) was generated. These 30 *C*-terminal residues bind to the common

docking domain of p38 and do not interact with the substrate-binding site.[38] As expected, the AGT-MK2 fusion protein was labeled by LTR **1** (lane 1, Figure 6a), while an AGT construct that lacks the MK2 peptide was not (lane 3, figure 6a). Next, we determined whether a weak-binding activator of p38, MKK6, can be labeled with our LTRs. GST-MKK6 was labeled with LTRs **1** and **3** when incubated in the presence of p38 (lanes 1 and 3, Figure 6b). Labeling of GST-MKK6 and p38 was prevented in the presence of selective p38 inhibitors (lanes 2 and 4, Figure 6b). Similarly, the dual-specificity phosphatase DUSP10 is known to dephosphorylate p38 and binds to both phosphorylated and dephosphorylated p38 with a low-micromolar affinity.[39-41] We investigated whether our LTR would be effective in labeling DSUP10. Even with unphosphorylated p38, DUSP10 was labeled in the presence of p38, but not in the absence of p38 or when a competitor was added. Together, these data demonstrate that a broad diversity of p38-interacting partners can be identified with p38-selective LTRs.

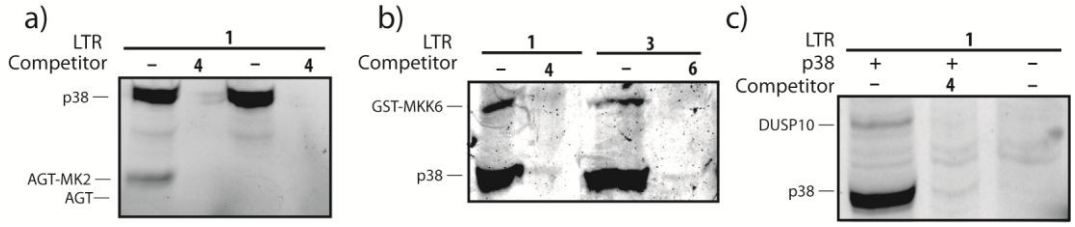

Figure 6. LTRs label a diversity of p38 binding partners. Each protein mixture was irradiated with UV light for 30 minutes, conjugated to rhodamine-azide, followed by SDS-PAGE analysis and in-gel fluorescence scanning. Total protein loading for each sample was determined with a His6 antibody. a) Labeling of a construct, AGT-MK2, that only interacts with the common docking domain of p38. LTR **1** (500 nM) was incubated with p38 (400 nM) and AGT-MK2 (800 nM) or AGT (800 nM). [competitor **4**] = 10 μM. b) Labeling of p38 activator GST-MKK6. LTRs **1** and **3** (500 nM) were incubated with p38 (400 nM) and GST-MKK6 (1 μM) in the absence or presence of competitors **4** and **6** (10 μM). c) Labeling of p38 phosphatase DUSP10. LTR **1** (500 nM) was incubated with p38 (400 nM) and DUSP10 (400 nM) in 0.2 mg/mL HEK293 lysate in the presence or absence of competitor **4** (10 μM).

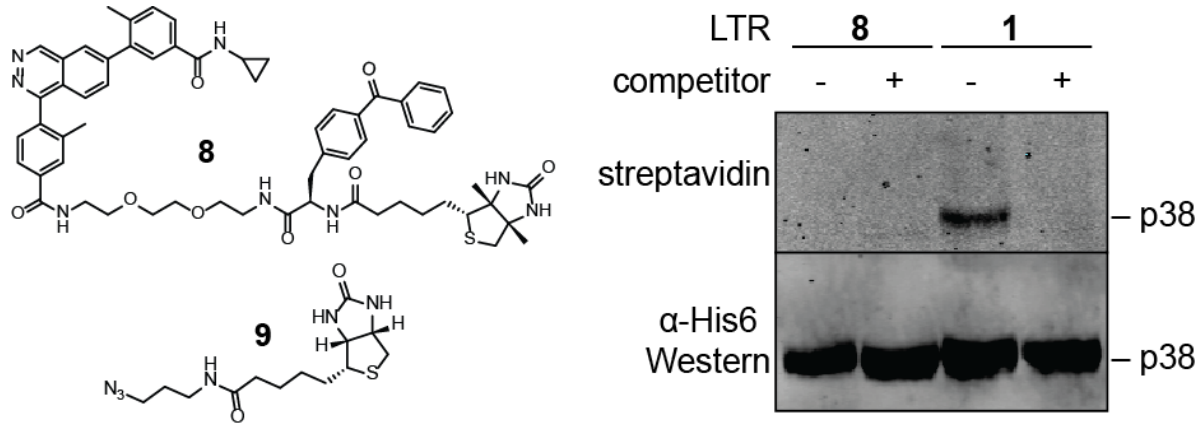

Figure 7. Biotinylated LTR fails to biotinylate proteins of interest. LTR **1** or **8** (500 μM) were incubated with p38 (400 nM) in the presence or absence of competitor **4** and irradiated with UV light (365 nm) for 30 min. Samples with LTR **1** were subjected to click chemistry with biotin-azide **9**. All samples were then precipitated and resuspended in loading buffer before being run on a gel and subjected to Western blot analysis with anti-His6 antibody or fluorophore-conjugated streptavidin.

We next sought to use the LTR in a purification scheme to identify labeled proteins. Synthesis of LTR **8**, which contains a biotin already attached, was unable to label proteins with biotin (or could not be detected by streptavidin), whereas LTR **1** could produce biotinylated proteins after click chemistry with biotin-azide **9** (Figure 7**)**.

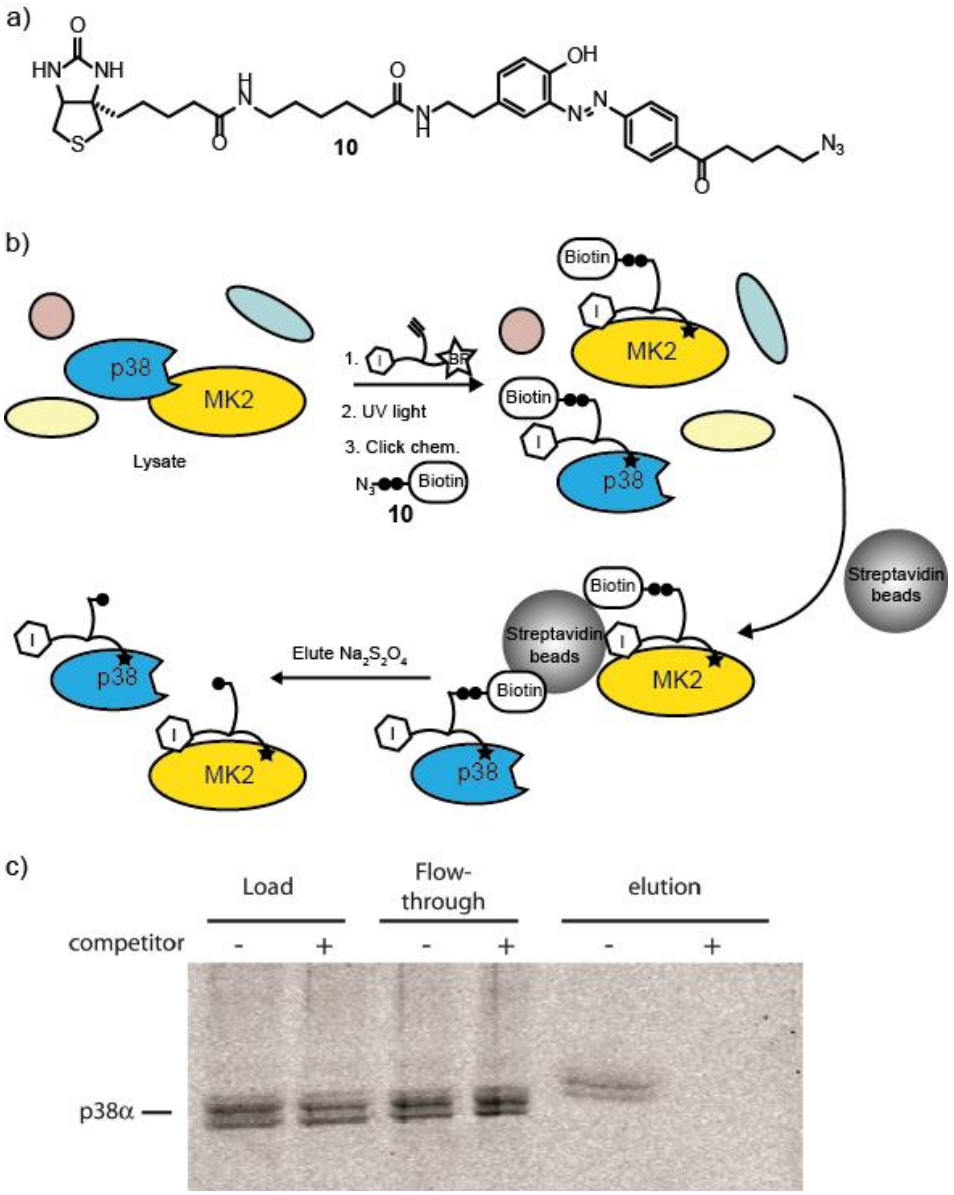

Figure 8. Attempted labeling of endogenous p38 and its substrate MK2 in HeLa cell lysate. a) Structure of biotin-azide **10** which can be efficiently cleaved with sodium dithionite. b) Schematic diagram demonstrating how cleavable biotin-azide was used to attempt labeling and purification of p38 and its binding partners. HeLa cell lysate was first incubated with DMSO or competitor **4** (10 μM), then LTR **1** (1 μM). After 10 minutes of incubation, HeLa lysate was irradiated with UV light for 10 minutes, then incubated with streptavidin beads. After extensive washes, labeled proteins were eluted with sodium dithionite. c) anti-p38 Western of the experiment described in b), showing p38 is selectively labeled in the absence of competitor, though most of the protein from the lysate ("load") is present in the flow-through from the streptavidin beads.

Consequently, we chose to use click chemistry with biotin-azide for purification. Due to the very high affinity of biotin and streptavidin, it can be challenging to selectively elute from regular streptavidin beads. Therefore, it was desirable to use a biotin-azide which contained a cleavable moiety. We attempted a purification strategy using a cleavable biotin-azide molecule **10** that had been previously described.[16] After crosslinking and click chemistry with the cleavable biotin-azide, streptavidin beads could be extensively washed before the protein was selectively eluted with sodium dithionite. While *in vivo* labeling showed no cross-linking, labeling reactions in lysate revealed that p38 was selectively labeled and enriched by the LTR (Figure 8). However, the signal for this kinase was very weak, and there was no evidence of labeling of the high-affinity p38 binding partner MK2.

The attempts at enrichment reveal that the LTRs used in this study are inefficient at labeling the desired proteins in environments where the proteins of interest are only a small fraction of all proteins present. Consequently, we have sought to perform a crude purification of the proteins of interest before attempting cross-linking. To do so, we performed an immunoprecipitation (IP) of a p38-containing complex of interest before adding the LTR (Figure 9).

Flag-MK2 or Flag-MKK6 was expressed alone or in conjunction with GFP-tagged p38. After an overnight incubation with the lysate, anti-flag beads were briefly washed with PBS before being exposed to the LTR and being subjected to UV irradiation. After elution with flag peptide, the eluates were subjected to click chemistry with rhodamine-azide **7** to fluorescently tag all LTR-labeled proteins. A fluorescence gel separated the proteins and revealed which were labeled with fluorophore. When co-expressed with MK2 and MKK6, both p38 and its binding partner are labeled in the presence of overexpressed p38, and this labeling is selectively competed away with a p38 inhibitor (Figure 9). MK2 efficiently co-precipitates p38, such that even endogenous levels of p38 are sufficient to provide labeling of MK2. MKK6 has a significantly weaker interaction with p38, and endogenous p38 levels provide no detectable MKK6 labeling.

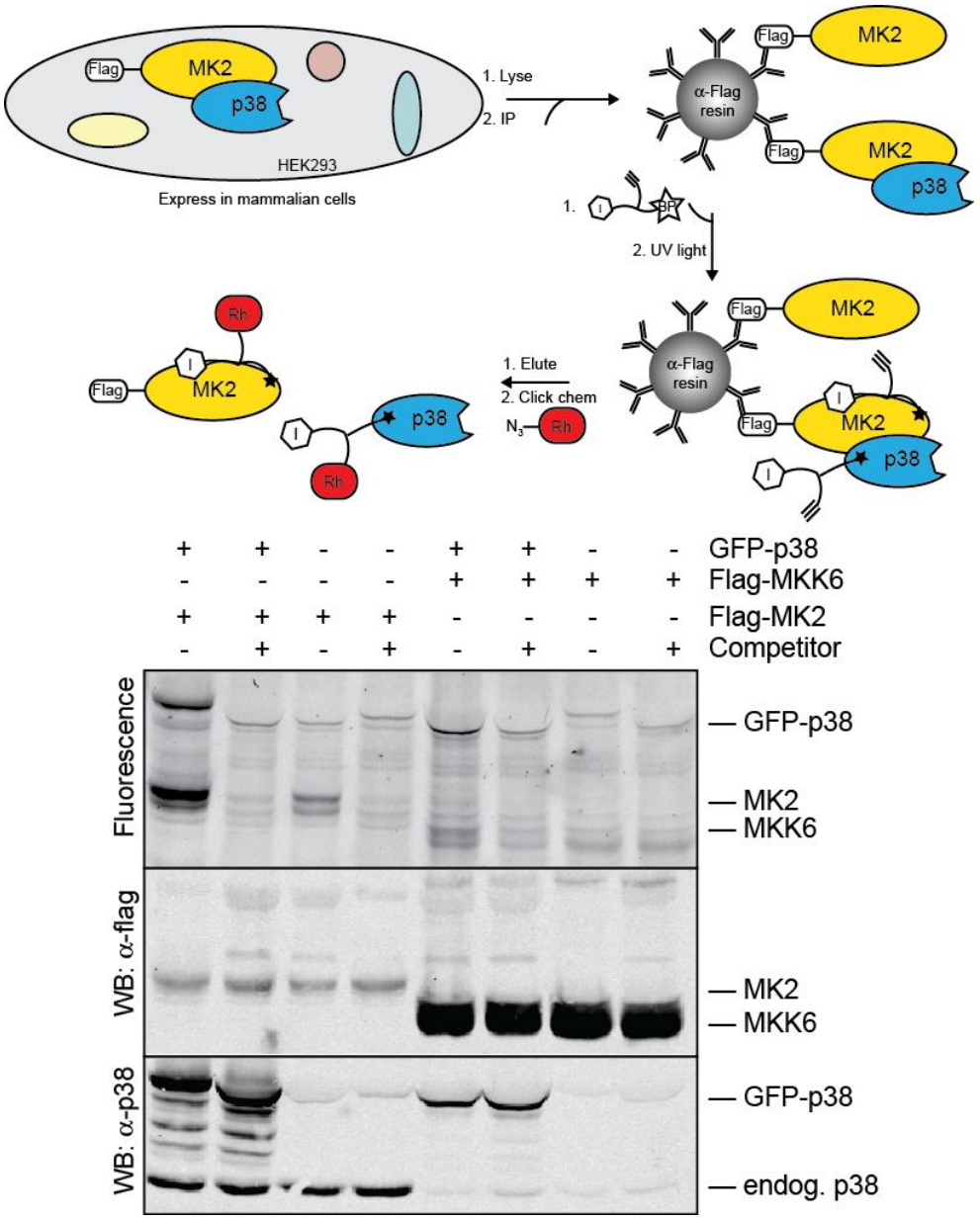

Figure 9. Crosslinking experiments with immunoprecipitated p38 complexes. HEK293 cells were transfected with flag-tagged MK2 or MKK6, and with no exogenous p38, or with GFP-p38, as indicated. Cells were lysed, and the lysate subjected to an α-flag immunoprecipitation. Beads were transferred to a 96-well plate and received cross-linking reagents as for figure 4. Proteins were eluted with flag peptide and were subjected to click chemistry with rhodamine-azide. After precipitation, proteins were run on an SDS-PAGE gel which was scanned for fluorescence before being transferred to nitrocellulose and probed with α-flag or α-p38 antibodies.

Conclusion

We have developed a set of label transfer reagents that facilitate the identification of proteins that are involved in p38 MAPK signaling complexes. These LTRs use a potent and selective ATP-competitive inhibitor to target a photo-crosslinker and tag to the active site of p38. Upon UV irradiation, proteins that are in close proximity to p38 are covalently crosslinked to an LTR, and an orthogonal chemical handle allows visualization and purification of labeled proteins. We have shown that these LTRs are highly selective for p38 and its binding partners, with no observed cross-reactivity, even with proteins that are at high concentrations. Moreover, the use of competitors with different selectivity profiles should provide even greater confidence that labeled proteins are associated with p38. Besides identifying substrates of p38, p38-directed LTRs also label activators, repressors, and other binding partners. The LTRs are therefore expected to be effective with any p38 binding partner. However, we cannot exclude the possibility that some binding partners of p38 may interact with sites distant from the active site, or have extremely weak binding affinities for p38, and these may not be labeled by our LTRs. Thus, while absence of labeling can provide little data on p38 interactions, labeling of a protein by the LTR should provide substantial confidence that it interacts with p38.

The LTRs appear to be ineffective in lysate or in vivo. We speculate that the low concentration of proteins of interest leads to extremely poor efficiency of labeling. However, by eliminating most undesired proteins though immuno-precipitation, we are able to study any protein that can

be overexpressed in mammalian cells. A traditional co-IP is a widely used technique, and very useful. However, co-IPs require extensive washes to eliminate non-specifically bound proteins; when combined with an LTR, extensive washes can be eliminated, as we rely on labeling by the LTR to establish connectivity. Additionally, a co-IP alone can demonstrate that two proteins are associated, but that interaction may be mediated by one or more proteins. LTRs, on the other hand, will only label proteins in close proximity to the kinase active site, effectively providing structural information about the complex. Thus, we believe these LTRs have the potential to expose the structural arrangement of p38-containing complexes, providing a significant advance on currently available methods.

Methods

Synthesis of LTRs

A. General Information

Unless otherwise noted, all reagents were obtained from commercial suppliers and used without further purification. ^{1}H-NMR spectra were obtained on a Bruker DRX-499 or AV500 instrument at room temperature. Chemical shifts are reported in ppm, and coupling constants are reported in Hz. Mass spectrometry was performed on a Bruker Esquire Ion Trap MS instrument.

General HPLC Purification Conditions: Preparatory reverse-phase C18 column (250 x 21 mm), Acetonitrile/Water–0.1% CF_3CO_2H gradient: 1:99 to 100:0 over 60 min; 8 mL/min; 254 nm detection for 65 min.

General Analytical HPLC Conditions: C18 column (250 x 4.6 mm), Acetonitrile/Water-0.1% CF_3CO_2H gradient: 1:99 to 100:0 over 40 min. Methanol/Water–0.1% CF_3CO_2H gradient: 1:99 to 100:0 over 30 or 40 min. Flow rate = 1 mL/min; 220 and 254 nM detection for 45 min.

B. Synthetic Scheme for Synthesis of 1, 4, and 8.

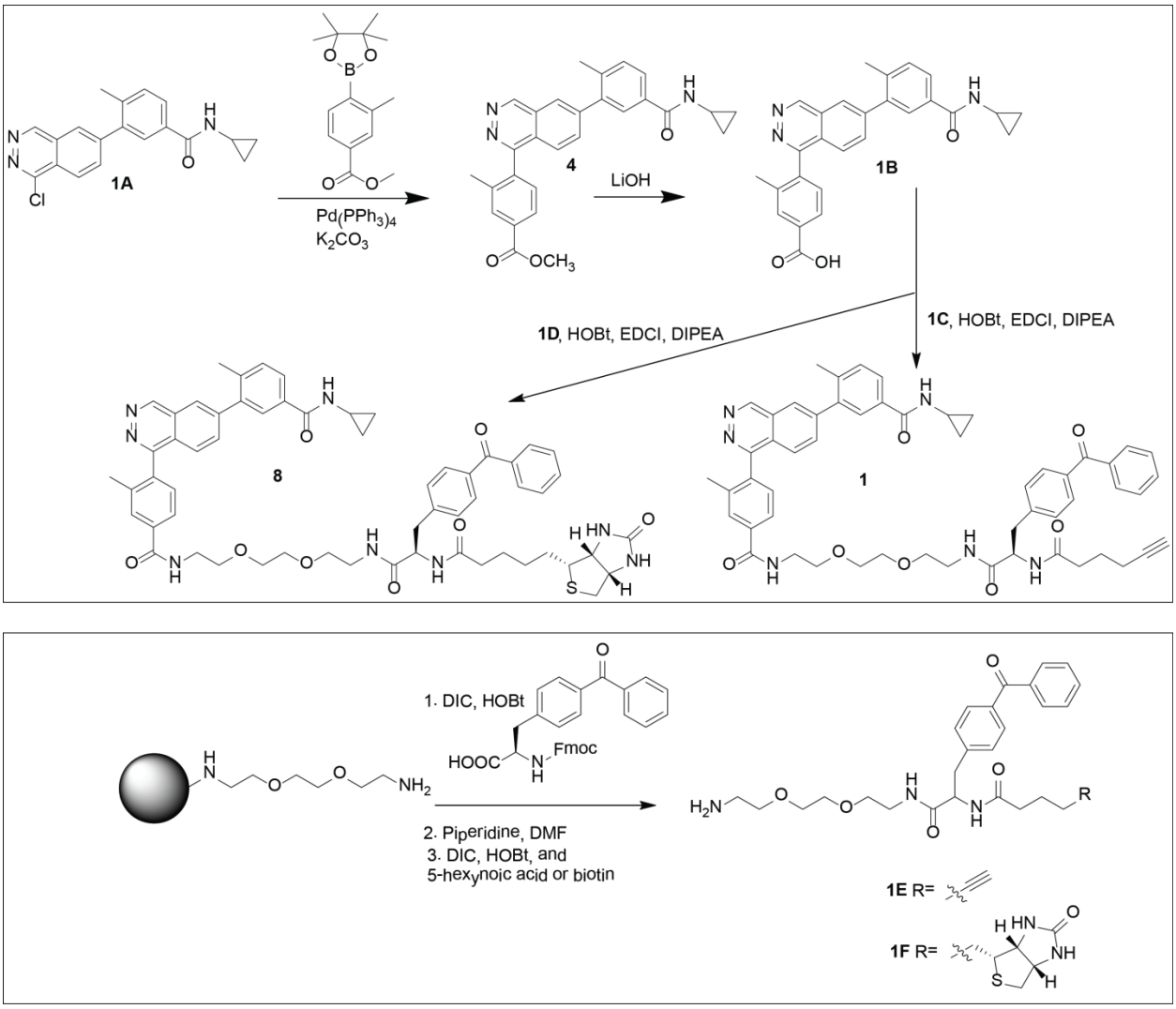

[4]: **1A** was synthesized as previously reported.[35,42] **1A** (35 mg, 0.104 mmol), (4-methoxycarbonyl)-2-methylphenyl boronic acid pinacol ester (29 mg, 0.104 mmol), $Pd(PPh_3)_4$ (6.0 mg, 0.0052 mmol), and 2 M aqueous K_2CO_3 (155 μL, 0.311 mmol) were dissolved in 1.0 mL of 1:4 EtOH:DME. The reaction was stirred at 95 °C for 4 hours under N_2. The reaction mixture was then concentrated *in vacuo*, taken up in EtOAc/H_2O, washed with H_2O (3×) and

brine (2×), dried over Na_2SO_4, and evaporated. 53 mg of crude product was purified by flash column chromatography (12g silica column, gradient: 100% CH_2Cl_2 to 1.25% Et_3N/3.75% MeOH/95% CH_2Cl_2 over 35 min), providing 25 mg (53% yield) of pure product. ^{1}H NMR (500 MHz, $CDCl_3$) δ 9.63 (s, 1H), 8.12 (s, 1H), 8.06 (s, 1H), 8.00 (s, 1H), 7.81 (d, *J* = 6.8 Hz, 1H), 7.73 – 7.66 (m, 2H), 7.64 (d, *J* = 8.3 Hz, 1H), 7.51 (d, *J* = 7.9 Hz, 1H), 7.40 (d, *J* = 7.9 Hz, 1H), 6.22 (s, 1H), 4.00 (s, 3H), 2.97 – 2.89 (m, 1H), 2.35 (s, 3H), 2.23 (s, 3H), 0.90 (m, *J* = 5.9 Hz, 2H), 0.63 (m, 2H). Calc'd for $C_{28}H_{26}N_3O_3$ $(M+H)^+$: 452.2; found 452.4.

[1B]: $LiOH•H_2O$ (11.4 mg, 0.27 mmol) was added to a solution of **4** (41 mg, 0.091 mmol) dissolved in 1.7 mL of 1:1 THF:H_2O. The reaction mixture was stirred at rt overnight. The mixture was then dissolved in EtOAc/saturated Na_2CO_3 and extracted with saturated Na_2CO_3 (3×). The aqueous layer was then acidified with concentrated HCl and extracted with EtOAc (with a few drops of MeOH). The aqueous layer was then extracted with EtOAc (6×). The combined organic layer was washed with brine (2×), dried over Na_2SO_4, and evaporated to give 33 mg of crude product which was purified by HPLC using General HPLC Purification (see above). 28.1 mg (71% yield) of pure product was obtained. ^{1}H NMR (300 MHz, MeOD) δ 9.76 (s, 1H), 8.31 (d, *J* = 1.2 Hz, 1H), 8.17 (s, 1H), 8.11 (d, *J* = 7.9 Hz, 1H), 8.05 (dd, *J* = 8.5, 1.7 Hz, 1H), 7.85 – 7.79 (m, 2H), 7.75 (d, *J* = 8.6 Hz, 1H), 7.57 (d, *J* = 7.9 Hz, 1H), 7.49 (d, *J* = 9.1 Hz, 1H), 2.93 – 2.82 (m, 1H), 2.39 (s, 3H), 2.21 (s, 3H), 0.86 – 0.78 (m, 2H), 0.69 – 0.60 (m, 2H). Calc'd for $C_{27}H_{23}N_3O_3$ $(M+H)^+$: 438.2; found 438.4.

[1C]: 0.08 mmol of *O*-Bis(aminoethyl)ethylene glycol trityl resin was swelled in ~ 1 mL CH_2Cl_2, and washed with CH_2Cl_2 and DMF. A solution of Fmoc-benzoylphenylalanine (98 mg,

0.2 mmol), HOBt (31 mg, 0.2 mmol), and DIC (31 μL, 0.2 mmol) was added to the filtered resin. The reaction mixture was twirled ~24h. The Fmoc group was removed (2 treatements with 25% piperidine in DMF for 25 min each), and the resin was filtered and washed with DMF. Next, a solution of 5-hexynoic acid (22 μL, 0.2 mmol), HOBt (31 mg, 0.2 mmol), and DIC (31 μL, 0.2 mmol) in DMF was added to the resin. The reaction mixture was twirled for ~24 hours. The reaction was drained and washed sequentially with DMF, CH_2Cl_2, MeOH, and CH_2Cl_2. 1 mL of cleavage cocktail (95% TFA, 2.5 % H_2O, 2.5% TIS) was added and incubated for 1 hour. The resin was then drained, washed with CH_2Cl_2, and resubjected to cleavage cocktail for 10 min, then washed with CH_2Cl_2. Elutions were concentrated and purified by HPLC, using General HPLC Purification (see above). 39 mg (54% yield) of pure **1C** were obtained. Calc'd for $C_{28}H_{36}N_3O_5$ $(M+H)^+$: 494.3; found 494.4.

[1D]: 0.08 mmol of *O*-Bis(aminoethyl)ethylene glycol trityl resin was swelled in ~1 mL CH_2Cl_2, and washed with CH_2Cl_2 and DMF. A solution of Fmoc-benzoylphenylalanine (98 mg, 0.2 mmol), HOBt (31 mg, 0.2 mmol), and DIC (31 μL, 0.2 mmol) was added to the filtered resin. The reaction mixture was twirled for ~24 hours. The Fmoc group was removed (2 treatments with 25% piperidine in DMF for 25 min each), and the resin was filtered and washed with DMF. Next, a solution of biotin (49 mg, 0.2 mmol), HOBt (31 mg, 0.2 mmol), and DIC (31 μL, 0.2 mmol) in DMF was added to the resin. The reaction mixture was twirled ~24 hours. The reaction was drained and washed sequentially with DMF, CH_2Cl_2, MeOH, and CH_2Cl_2. 1 mL of cleavage cocktail (95% TFA, 2.5 % H_2O, 2.5% TIS) was added and incubated for 1 hour. The resin was then drained, washed with CH_2Cl_2, and resubjected to cleavage cocktail for 10 min, then washed with CH_2Cl_2. Elutions were concentrated and purified by HPLC, using General HPLC

Purification (see above). 27 mg (54% yield) of pure **1D** were obtained. Calc'd for $C_{32}H_{43}N_5O_6S$ $(M+H)^+$: 626.3; found 626.6.

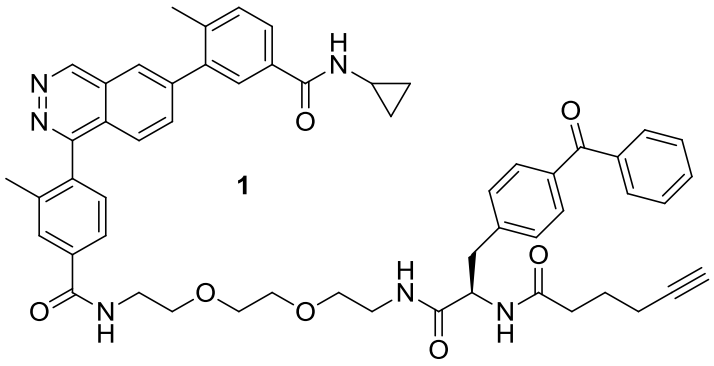

[1]: **1B** (16.5 mg, 0.038mmol), **1C** (11.5 mg, 0.016 mmol), DIPEA (11.5 μL, 0.066 mmol), HOBt (3.3 mg, 0.021 mmol), and EDCI (4.1 mg, 0.021 mmol) were combined in 45 μL of DMF and stirred at rt for ~ 36 hours. The crude reaction was taken up in MeOH/H_2O and purified using General HPLC Purification (see above), obtaining 1.95 mg of pure product. ^{1}H NMR (500 MHz, MeOD) δ 9.81 (s, 1H), 8.35 (d, *J* = 1.3 Hz, 1H), 8.06 (dd, *J* = 8.5, 1.7 Hz, 1H), 7.96 (s, 1H), 7.90 (dd, *J* = 7.9, 1.5 Hz, 1H), 7.89-7.90 (m, 2H), 7.76 (d, *J* = 8.5 Hz, 1H), 7.72 – 7.69 (m, 2H), 7.67 (d, *J* = 8.3 Hz, 2H), 7.61 (t, *J* = 7.5 Hz, 1H), 7.53 (d, *J* = 7.9 Hz, 1H), 7.49 (m, 3H), 7.40 (d, *J* = 8.2 Hz, 2H), 4.70 (dd, *J* = 9.1, 6.0 Hz, 1H), 3.72 (t, *J* = 5.5 Hz, 2H), 3.68 – 3.59 (m, 6H), 3.55 – 3.44 (m, 2H), 3.40 – 3.34 (m, 2H), 3.24 – 3.18 (m, 1H), 2.97 (dd, *J* = 13.7, 9.1 Hz, 1H), 2.88 – 2.83 (m, 1H), 2.36 (s, 3H), 2.28 (t, *J* = 7.4 Hz, 2H), 2.19 (dd, *J* = 5.6, 2.9 Hz, 4H), 2.06 – 2.01 (m, 2H), 1.70 – 1.63 (m, 2H), 0.83 – 0.78 (m, 2H), 0.65 – 0.61 (m, 2H). Calc'd for $C_{55}H_{57}N_6O_7$ $(M+H)^+$: 913.4; found 914.0.

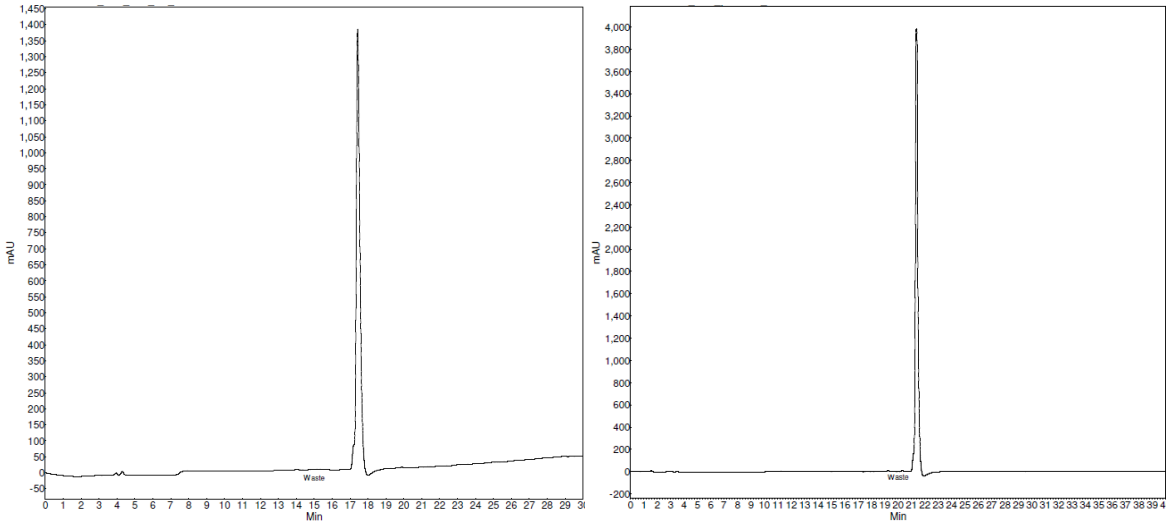

Figure i: Analytical HPLC traces for **1**. (Acetonitrile – Right; MeOH – Left)

[8]: **1B** (5.4 mg, 0.012 mmol), **1D** (9.0 mg, 0.012 mmol), DIPEA (8.6 µL, 0.049 mmol), HOBt (2.5 mg, 0.016 mmol), and EDCI (3.1 mg, 0.016 mmol) were combined in 123 µL of DMF and stirred at rt for 4 days. The crude reaction was taken up in MeOH/H_2O and purified using General HPLC Purification (see above), obtaining at least 1.55 mg of pure product. ^{1}H NMR (500 MHz, Methanol-d4) δ 9.72 (s, 1H), 8.27 (d, *J* = 1.3 Hz, 1H), 7.99 (dd, *J* = 8.5, 1.7 Hz, 1H), 7.95 (s, 1H), 7.89 (dd, *J* = 8.0, 1.5 Hz, 1H), 7.84 – 7.78 (m, 2H), 7.73 – 7.65 (m, 5H), 7.62 (t, *J* = 7.5 Hz, 1H), 7.53 – 7.45 (m, 4H), 7.41 (d, *J* = 8.2 Hz, 2H), 4.72 (dd, *J* = 9.6, 5.7 Hz, 1H), 4.41 (dd, *J* = 7.9, 4.6 Hz, 1H), 4.16 (dd, *J* = 7.9, 4.5 Hz, 1H), 3.72 (t, *J* = 5.5 Hz, 2H), 3.69 – 3.60 (m, 6H), 3.57 – 3.43 (m, 4H), 3.29 – 3.27 (m, 1H), 3.22 (dd, *J* = 13.7, 5.7 Hz, 2H), 3.06 – 3.00 (m, 1H), 2.96 (dd, *J* = 13.6, 9.5 Hz, 2H), 2.90 – 2.80 (m, 2H), 2.36 (s, 3H), 2.23 – 2.12 (m, 5H), 1.66 – 1.56 (m, 2H), 1.56 – 1.41 (m, 2H), 1.26 – 1.13 (m, 2H), 0.84 – 0.76 (m, 2H), 0.67 – 0.60 (m, 2H). Calc'd for $C_{59}H_{64}N_8O_8S$ $(M+H)^+$: 1045.5; found 1045.9.

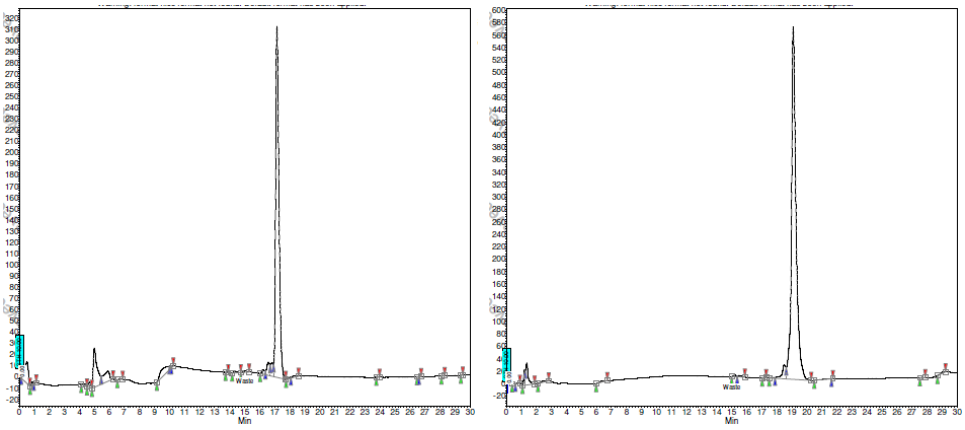

Figure ii: Analytical HPLC traces for **8**. (Acetonitrile – Right; MeOH – Left)

C. Synthetic Scheme for synthesis of 2

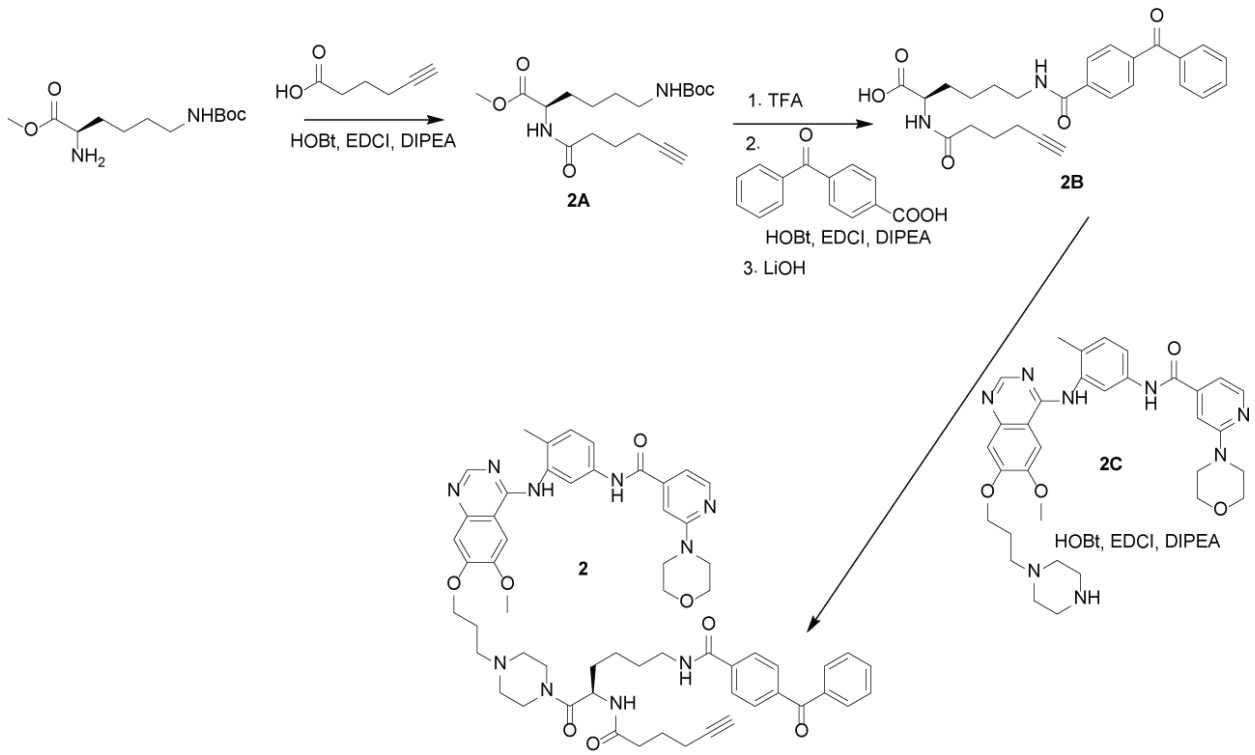

[2A]: MeO-Lys(Boc)-NH_2•HCl (100 mg, 0.337 mmol), 5-hexynoic acid (48.4 μL, 0.438 mmol), HOBt (68 mg, 0.44 mmol), DIPEA (117 μL, 0.674 mmol), and EDCI (92 mg, 0.44 mmol) were combined in 1.7 mL of DMF and stirred overnight at rt under N_2. The reaction was dissolved in EtOAc and washed with saturated Na_2CO_3 (2×), saturated NH_4Cl (2×), and brine (2×), then dried over Na_2SO_4. Evaporation gave a crude oil that was purified by flash column chromatography (4 g silica column, gradient: 100% Hexanes to 80% EtOAc/20% Hexanes over 20 min). Pure fractions were evaporated to obtain 80 mg (67% yield) of pure **2A**. ^{1}H NMR (300 MHz, $CDCl_3$) δ 6.15 – 6.05 (m, 1H), 4.64 – 4.52 (m, 1H), 3.74 (s, 3H), 3.15 – 3.05 (m, 2H), 2.38 (t, *J* = 7.4 Hz, 2H), 2.32 – 2.23 (m, 2H), 1.99 (t, *J* = 2.6 Hz, 1H), 1.94 – 1.79 (m, 4H), 1.76 – 1.63 (m, 2H), 1.54 – 1.46 (m, 2H), 1.44 (s, 9H).

[2B]: **2A** (80 mg, 0.23 mmol) was dissolved in 2.3 mL of 30% TFA in CH_2Cl_2 and stirred at rt for 2 hours under N_2. The reaction was evaporated and placed on a vacuum line for several hours. The deprotected amine was then taken up in 1 mL of DMF and mixed with 4-benzoyl benzoic acid (67 mg, 0.30 mmol), DIPEA (79.1 μL, 0.454 mmol), HOBt (46 mg, 0.30 mmol), and EDCI (57 mg, 0.30 mmol). The mixture was stirred overnight at rt under N_2. The reaction was then dissolved in EtOAc and washed with saturated Na_2CO_3 (2×), saturated NH_4Cl (2×), and brine (2×), then dried over Na_2SO_4. The residue was evaporated to give a clear oil. The oil was dissolved in 1mL of a 1:1 THF:H_2O mixture, along with 5 drops MeOH. LiOH•H_2O (26.5 mg, 0.632 mmol) was then added and the mixture was stirred overnight at rt. The reaction was dissolved in EtOAc and H_2O, and extracted with saturated $NaHCO_3$. The combined aqueous layers were acidified, then extracted with EtOAc (3×). Extractions were combined and dried over Na_2SO_4, then evaporated to give 88 mg (86% yield after three steps) of pure **2B**. ^{1}H NMR (300

MHz, $CDCl_3$) δ 7.99 – 7.74 (m, 6H), 7.62 (t, *J* = 7.4 Hz, 1H), 7.50 (t, *J* = 7.5 Hz, 2H), 6.71 (s, 1H), 6.63 (d, *J* = 7.2 Hz, 1H), 4.56 (m, 1H), 3.66 – 3.38 (m, 2H), 2.45 – 2.34 (m, 2H), 2.29 – 2.18 (m, 2H), 1.93 (t, *J* = 2.6 Hz, 1H) 1.82 (dt, *J* = 14.2, 7.2 Hz, 4H), 1.70 (dd, *J* = 13.1, 6.7 Hz, 2H), 1.49 (d, *J* = 7.3 Hz, 2H).

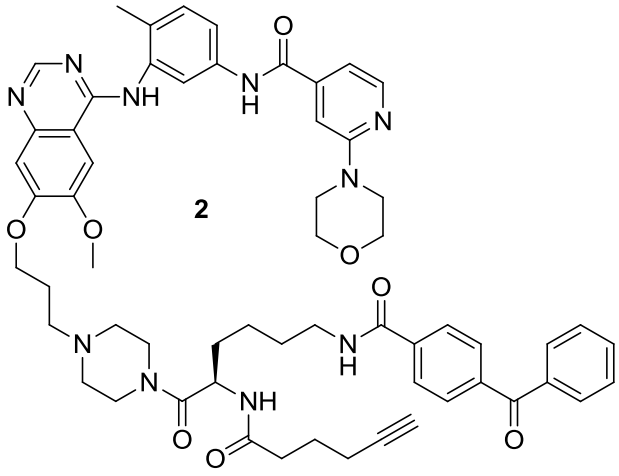

[2]: The synthesis of **2C** has been described elsewhere.[43] **2C** (9.2 mg, 0.012 mmol), **2B** (7.4 mg, 0.016 mmol), DIPEA (6.6 μL, 0.038 mmol), HOBt (2.7 mg, 0.016 mmol), and EDCI (3.7 mg, 0.016 mmol) were combined in 200 μL of DMF and stirred at rt for 3 days. The crude reaction mixture was diluted in MeOH/H_2O and purified using General HPLC Purification (see above), yielding 0.74 mg of pure product. ^{1}H NMR (500 MHz, MeOD) δ 8.56 (s, 1H), 8.25 (d, *J* = 4.7 Hz, 1H), 7.95 (d, *J* = 8.4 Hz, 4H), 7.82 (d, *J* = 6.7 Hz, 2H), 7.77 (d, *J* = 7.3 Hz, 2H), 7.66 (t, *J* = 7.0 Hz, 1H), 7.57 – 7.51 (m, 3H), 7.40 (d, *J* = 8.5 Hz, 1H), 7.26 (d, *J* = 9.4 Hz, 2H), 7.12 (d, *J* = 5.1 Hz, 1H), 4.78 (m, 1H), 4.41 (s, 2H), 4.07 (s, 3H), 3.84 – 3.78 (m, 4H), 3.60 – 3.55 (m, 4H), 3.48 – 3.35 (m, 8H), 3.16 (m, 4H), 2.37 (t, *J* = 7.8 Hz, 2H), 2.26 (s, 3H), 2.24 – 2.17 (m, 3H), 1.82 – 1.58 (m, 10H). Calc'd for $C_{59}H_{67}N_{10}O_8$ $(M+H)^+$: 1043.5; found 1044.0.

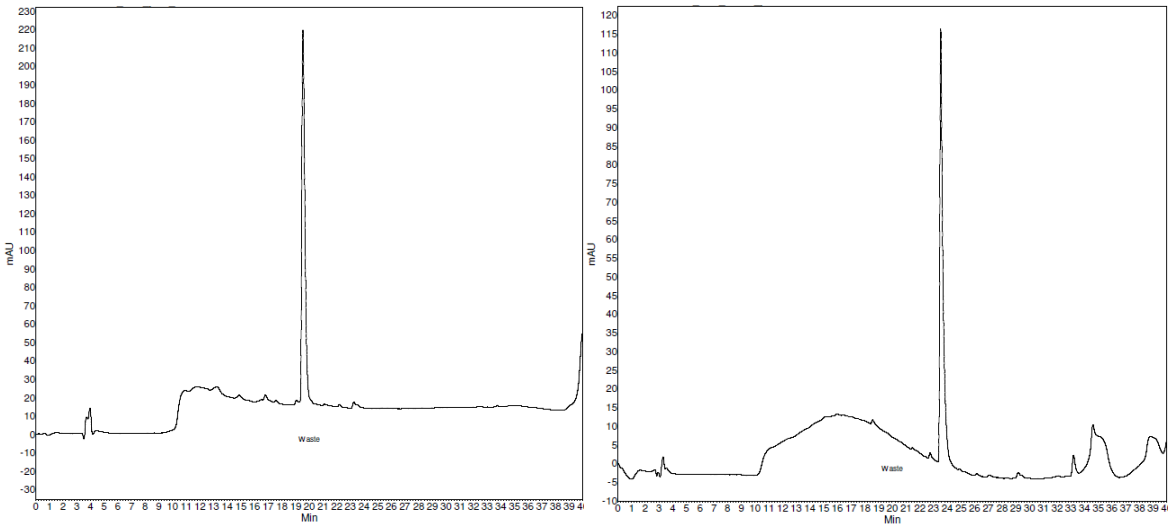

Figure ii: Analytical HPLC traces for **2**. (Acetonitrile – Right; MeOH – Left)

D. Synthetic Scheme for synthesis of 3 and 6.

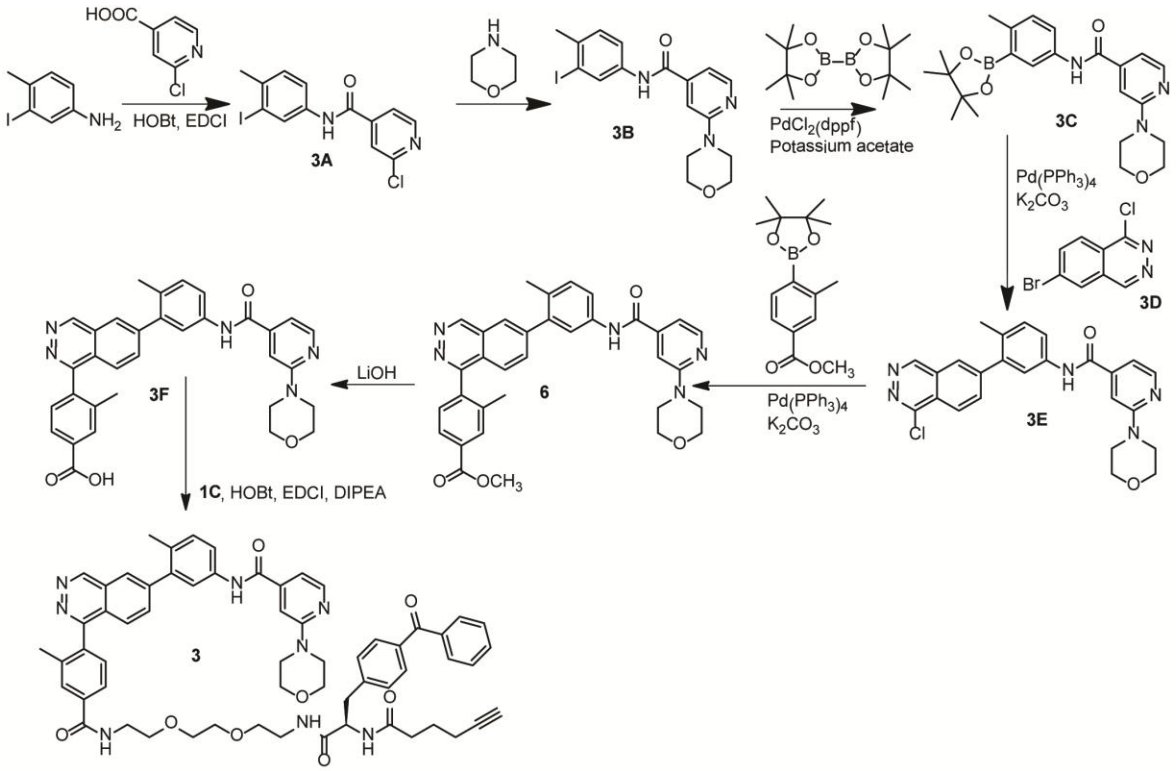

[3A] 2-chloroisonicotinic acid (0.50 g, 3.2 mmol), 3-iodo-4-methylaniline (888 mg, 3.81 mmol), DIPEA (1.66 mL, 9.52 mmol), HOBt (595 mg, 3.81 mmol), and EDCI (730 mg, 3.81 mmol) were combined in 8.0 mL of DMF and stirred at rt overnight. The reaction was dissolved in EtOAc and washed with saturated Na_2CO_3 (2×), saturated NH_4Cl (2×), and brine (2×), and then dried over Na_2SO_4. The product was triturated with EtOAc, and the solid was dried to obtain 572 mg (42% yield) of pure **3A**. ^{1}H NMR (300 MHz, $CDCl_3$) δ 8.59 (d, *J* = 5.1 Hz, 1H), 8.10 (d, *J* = 2.2 Hz, 1H), 7.74 (s, 1H), 7.68 (s, 1H), 7.62 (dd, *J* = 5.1, 1.5 Hz, 1H), 7.56 (dd, *J* = 8.2, 2.2 Hz, 1H), 2.44 (s, 3H).

[3B]: **3A** (750 mg, 2.0 mmol) was suspended in morpholine (8.3 mL, 96 mmol), and the mixture was stirred at 80 °C overnight. The reaction was cooled to rt, then it was poured into 8.3 mL of DI H_2O and stirred for 10 min. 1 mL of $CHCl_3$ was added and the reaction was stirred for another 30 min. The slurry was filtered, washed with H_2O and minimal $CHCl_3$, and then dried with high vacuum overnight to give 766 mg (90% yield) of pure **3B**. ^{1}H NMR (300 MHz, $CDCl_3$) δ 8.33 (d, *J* = 5.1 Hz, 1H), 8.10 (d, *J* = 2.3 Hz, 1H), 7.71 (s, 1H), 7.58 (dd, *J* = 8.1, 2.1 Hz, 1H), 7.11 (s, 1H), 6.90 (dd, *J* = 5.2, 1.3 Hz, 1H), 3.88 – 3.79 (m, 4H), 3.65 – 3.57 (m, 4H), 2.43 (s, 3H).

[3C]: **3B** (766 mg, 1.8 mmol), bis(pinacolato) diboron (1.01 g, 2.7 mmol), potassium acetate (888 mg, 9.05 mmol), and $PdCl_2$(dppf) (149 mg, 0.180 mmol) were mixed in 9.05 mL of DMF and heated to 80°C overnight. After cooling, the reaction was dissolved in EtOAc/H_2O and washed with H_2O (2×). The solution was filtered through Celite, and then the filtrate was washed extensively with H_2O. The organic layer was dried over Na_2SO_4 and evaporated to give a crude

solid. This solid was taken up in CH_2Cl_2 and purified by flash column chromatography (silica column, gradient: 100% Hexanes to 100% EtOAc). Evaporation of pure fractions gave 466 mg (61% yield) of pure product. ^{1}H NMR (500 MHz, $CDCl_3$) δ 8.33 (d, *J* = 5.0 Hz, 1H), 7.99 (d, *J* = 8.8 Hz, 1H), 7.76 (s, 1H), 7.65 (d, *J* = 2.3 Hz, 1H), 7.23 (d, *J* = 9.2 Hz, 1H), 7.14 (s, 1H), 6.93 (d, *J* = 5.0 Hz, 1H), 3.90 – 3.83 (m, 4H), 3.66 – 3.58 (m, 4H), 2.55 (s, 3H), 1.36 (d, *J* = 9.7 Hz, 12H).

[3E]: **3D** was synthesized as described elsewhere.[35,42] **3C** (466 mg, 1.1 mmol), **3D** (268 mg, 1.1 mmol), 2 M aqueous K_2CO_3 (550 μL, 1.1 mmol), and $Pd(PPh_3)_4$ (63.6 mg, 0.055 mmol) were dissolved in 11 mL of a 1:4 EtOH:DME solution and heated to 70 °C overnight. The reaction was concentrated, and the residue was dissolved in EtOAc/H_2O. The mixture was washed with H_2O (3×), dried over Na_2SO_4, and evaporated to give ~600 mg of crude product. The crude product was purified by flash column chromatography (silica column, gradient: 100% Hexanes to 100% EtOAc) to give 147 mg (29% yield) pure **3E**. ^{1}H NMR (300 MHz, $CDCl_3$) δ 9.43 (s, 1H), 8.32 (dd, *J* = 12.8, 6.8 Hz, 2H), 8.16 (s, 1H), 8.01 (d, *J* = 8.5 Hz, 1H), 7.94 (s, 1H), 7.73 (d, *J* = 2.0 Hz, 1H), 7.58 (dd, *J* = 8.3, 2.1 Hz, 1H), 7.35 (d, *J* = 8.3 Hz, 1H), 7.13 (s, 1H), 6.95 (d, *J* = 5.1 Hz, 1H), 3.87 – 3.75 (m, 4H), 3.62 – 3.54 (m, 4H), 2.28 (s, 3H). Calc'd for $C_{25}H_{23}ClN_5O_2$ $(M+H)^+$: 460.2; found 460.3.

[6]: **3E** (147 mg, 0.32 mmol), 4-methoxycarbonyl-2-methylphenyl boronic acid pinacol ester (88 mg, 0.32 mmol), 2 M aqueous K_2CO_3 (479 μL, 0.959 mmol), and $Pd(PPh_3)_4$ (18 mg, 0.016 mmol) were combined in 3.2 mL of a 1:4 EtOH:DME solution and stirred under N_2 for 30 min. The reaction was heated to 95 °C for 2.5 hours, then cooled and dissolved in EtOAc/H_2O. The

mixture was washed with H_2O (3×) and brine (1×) before being dried over Na_2SO_4 and evaporated to give ~150 mg of crude product. This solid was purified by flash column chromatography (40 g silica column, gradient: 100% hexanes to 100% EtOAc over 40 min, then constant at 100% EtOAc for 35 min), giving 130 mg (70% yield) of pure product. ^{1}H NMR (300 MHz, $CDCl_3$) δ 9.62 (s, 1H), 8.33 (d, *J* = 4.6 Hz, 1H), 8.07 (dd, *J* = 18.4, 11.0 Hz, 2H), 7.88 – 7.80 (m, 2H), 7.75 (s, 1H), 7.63 (d, *J* = 8.5 Hz, 1H), 7.56 – 7.48 (m, 2H), 7.36 (d, *J* = 8.4 Hz, 1H), 7.13 (s, 1H), 6.92 (d, *J* = 5.2 Hz, 1H), 4.00 (s, 3H), 3.89 – 3.76 (m, 4H), 3.64 – 3.55 (m, 4H), 2.30 (s, 3H), 2.23 (s, 3H). Calc'd for $C_{34}H_{32}N_5O_4$ $(M+H)^+$: 574.3; found 574.4.

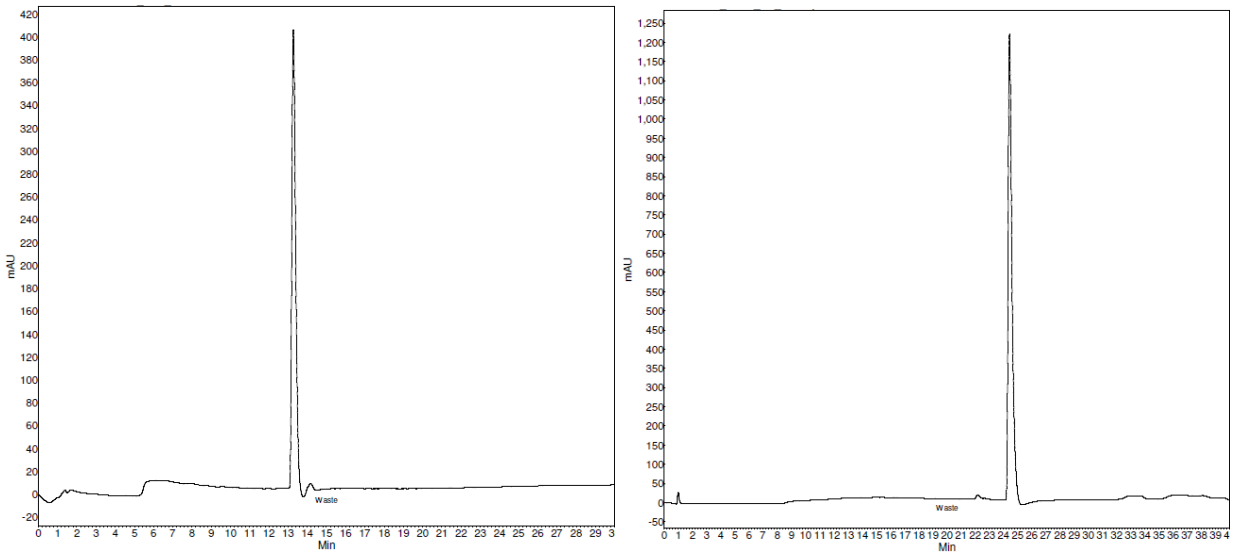

Figure iv: Analytical HPLC traces for **6**. (Acetonitrile – Right; MeOH – Left)

[3F]: LiOH•H_2O (29 mg, 0.68 mmol) was added to **6** (130 mg, 0.23 mmol) in 2.2 mL of a 1:1 THF:H_2O mixture. The reaction was stirred at rt for 3 hours, then dissolved in EtOAc and saturated NH_4Cl. This mixture was basified with 1 M NaOH, and the organic layer was

evaporated, then taken up in MeOH and filtered through glass wool. The cleared solution was evaporated, dissolved in MeOH/H_2O, filtered, and purified using General HPLC Purification (see above), which yielded ~ 20 mg of pure product. ^{1}H NMR (500 MHz, MeOD) δ 9.73 (s, 1H), 8.31 – 8.22 (m, 2H), 8.15 (d, *J* = 17.1 Hz, 1H), 8.11 – 8.05 (m, 1H), 8.03 – 7.97 (m, 1H), 7.78 – 7.65 (m, 3H), 7.55 (dd, *J* = 15.5, 6.3 Hz, 1H), 7.37 (d, *J* = 8.4 Hz, 1H), 7.25 (s, 1H), 7.12 (s, 1H), 3.87 – 3.75 (m, 4H), 3.63 – 3.53 (m, 4H), 2.30 (s, 3H), 2.18 (s, 3H). Calc'd for $C_{33}H_{30}N_5O_4$ $(M+H)^+$: 560.2; found 560.4.

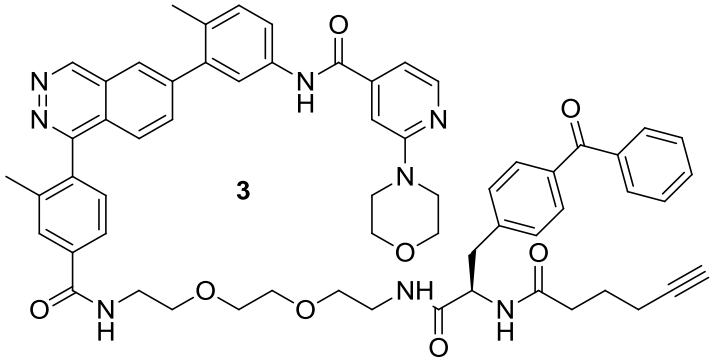

[3]: **3F** (5.0 mg, 0.0089 mmol), **1C** (12.5 mg, 0.021 mmol), DIPEA (7.8 μL, 0.045 mmol), HOBt (2.1 mg (0.013 mmol), and EDCI (2.6 mg, 0.013 mmol) were combined in 44.7 μL of DMF and stirred overnight at rt. The crude reaction mixture was diluted in MeOH/H_2O and purified by HPLC using General HPLC Purification (see above), yielding about 2 mg of pure product. ^{1}H NMR (500 MHz, MeOD) δ 9.87 (s, 1 H), 8.40 (d, *J* = 1.1 Hz, 1H), 8.19 (d, *J* = 5.9 Hz, 1H), 8.12 (dd, *J* = 8.5, 1.6 Hz, 2H), 7.93 (d, *J* = 7.9 Hz, 1H), 7.85 (d, *J* = 2.2 Hz, 1H), 7.82 (d, *J* = 8.5 Hz, 1H), 7.72 (dd, *J* = 8.3, 1.3 Hz, 2H), 7.68 (m, 3H), 7.62 (t, *J* = 7.5 Hz, 1H), 7.59 – 7.54 (m, 2H), 7.51 (t, *J* = 7.7 Hz, 2H), 7.46 – 7.38 (m, 3H), 7.27 (dd, *J* = 5.9, 1.3 Hz, 1H), 4.72 (dd, *J* = 9.1, 6.0 Hz, 1H), 3.89 – 3.84 (m, 4H), 3.77 – 3.60 (m, 12H), 3.58 – 3.45 (m, 2H), 3.44 – 3.34 (m, 2H),

3.22 (dd, *J* = 13.6, 5.9 Hz, 1H), 2.96 (dt, *J* = 10.8, 6.4 Hz, 1H), 2.34 (s, 3H), 2.29 (t, *J* = 7.4 Hz, 3H), 2.23 – 2.19 (m, 4H), 2.08 – 2.01 (m, 2H), 1.72 – 1.63 (m, 2H). Calc'd for $C_{61}H_{63}N_8O_8$ $(M+H)^+$: 1035.5; found 1036.0.

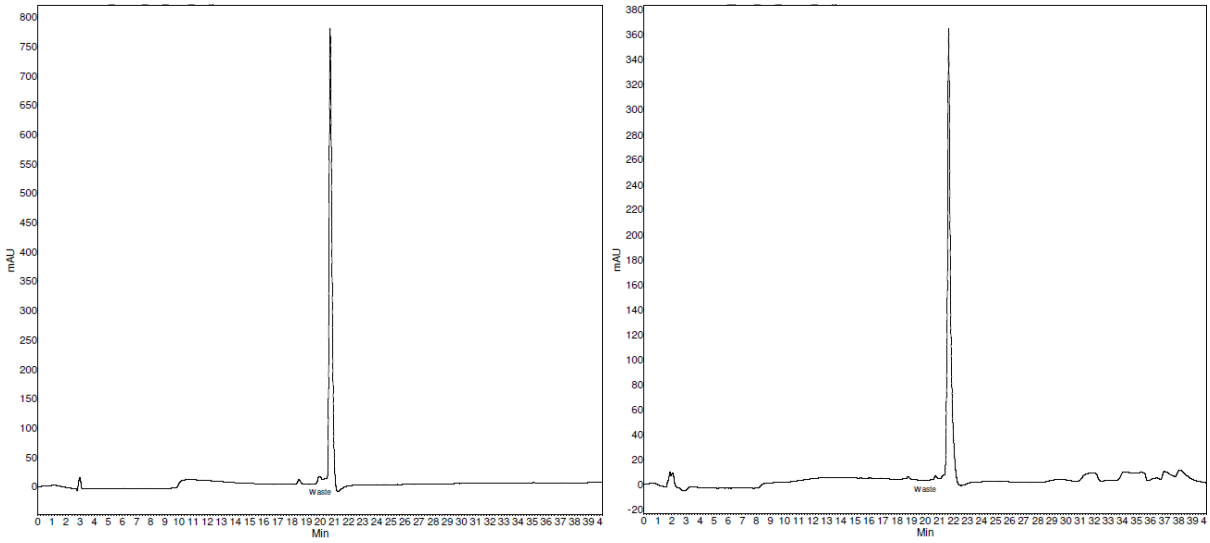

Figure v: Analytical HPLC traces for **3**. (Acetonitrile – Right; MeOH – Left)

Rhodamine-azide [**7**] and biotin-azide [**9**] were synthesized according to previously published protocols.[20,44]

IV. Kinase Activity Assays

A. Activation of MAP Kinases

p38α was activated by MKK6 according to a previously published protocol.[45]

ERK1 was activated by incubating the following mixture at rt for 1 hour: 50 mM MOPS pH 7.4, 10 mM $MgCl_2$, 0.001% Tween-20, 1 mM DTT, 0.10 mg/mL BSA, 1.3 mM ATP, 2 μM ERK1, 1 μL MKK2 (activating enzyme was of insufficient purity and concentration for accurate protein concentration determination).

ERK2 was activated by incubating the following mixture at rt for 1 hour: 50 mM MOPS pH 7.4, 10 mM $MgCl_2$, 0.001% Tween-20, 1 mM DTT, 0.10 mg/mL BSA, 1.3 mM ATP, 2 μM ERK2, 1 μL MKK2 (activating enzyme was of insufficient purity and concentration for accurate protein concentration determination).

JNK1α2 was activated by incubating the following mixture at rt for 1 hour: 50 mM MOPS pH 7.4, 10 mM $MgCl_2$, 0.001% Tween-20, 1 mM DTT, 0.10 mg/mL BSA, 1.3 mM ATP, 2 μM JNK1α2, 1 μL MKK4, 1 μL MKK7, and 2 μL MAP3K1 (all activating enzymes were of insufficient purity and concentration for accurate protein concentration determination).

JNK3α1 was activated by incubating the following mixture at rt for 1 hour: 50 mM MOPS pH 7.4, 10 mM $MgCl_2$, 0.001% Tween-20, 1 mM DTT, 0.10 mg/mL BSA, 1.3 mM ATP, 2 μM JNK3α1, 1 μL MKK4, 1 μL MKK7, and 2 μL MAP3K1 (all activating enzymes were of insufficient purity and concentration for accurate protein concentration determination).

B. Activity assays with MAP Kinases

p38 assay. Inhibitors (initial concentration: 10 μM, 3-fold dilutions: 9 dilutions) were assayed in triplicate or quadruplicate against recombinant full-length activated p38α (final concentration = 1 nM) in an assay also containing 50 mM Tris-HCl, pH 7.5, 20 mM $MgCl_2$, 1 mM EGTA, 1 mM Na_3VO_4, 0.1% Triton x-100, 0.2 mg/mL BSA, 0.2 mg/mL myelin basic protein, and 0.5 μCi of γ-^{32}P-ATP ([ATP] ≪ K_m (ATP)) in a final volume of 30.2 μL. The reactions were incubated for 2 hours at rt and terminated by transferring 4.6 μL of the reaction mixture to a phosphocellulose membrane. The membranes were washed with 0.5% phosphoric acid (4×) and acetone (1×) and quantitated by phosphorimaging. The scanned membranes were quantified with ImageQuant and converted to percent inhibition. Data was analyzed using Prism Graphpad software and IC_{50} values were determined using non-linear regression analysis.

ERK1. Inhibitors (initial concentration: 10 μM, 3-fold dilutions: 9 dilutions) were assayed in triplicate against recombinant full-length activated ERK1 (final concentration = 1 nM) in an assay also containing 30 mM HEPES, pH 7.5, 10 mM $MgCl_2$, 0.6 mM EGTA, 1 mM Na_3VO_4, 0.05 mg/mL BSA, 0.2 mg/mL myelin basic protein, and 0.5 μCi of γ-^{32}P-ATP ([ATP] ≪ K_m (ATP)) in a final volume of 30.2 μL. The reactions were incubated for 1 hour at rt and terminated by transferring 4.6 μL of the reaction mixture to a phosphocellulose membrane. The membranes were washed with 0.5% phosphoric acid (4×) and acetone (1×) and quantitated by phosphorimaging. The scanned membranes were quantified with ImageQuant and converted to percent inhibition. Data was analyzed using Prism Graphpad software and IC_{50} values were determined using non-linear regression analysis.

ERK2. Inhibitors (initial concentration: 10 μM, 3-fold dilutions: 9 dilutions) were assayed in triplicate against recombinant full-length activated ERK2 (final concentration = 1 nM) in an assay also containing 30 mM HEPES, pH 7.5, 10 mM $MgCl_2$, 0.6 mM EGTA, 1 mM Na_3VO_4, 0.05 mg/mL BSA, 0.2 mg/mL myelin basic protein, and 0.5 μCi of γ-^{32}P-ATP ([ATP] $\ll K_m$ (ATP)) in a final volume of 30.2 μL. The reactions were incubated for 1 hour at rt and terminated by transferring 4.6 μL of the reaction mixture to a phosphocellulose membrane. The membranes were washed with 0.5% phosphoric acid (4×) and acetone (1×) and quantitated by phosphorimaging. The scanned membranes were quantified with ImageQuant and converted to percent inhibition. Data was analyzed using Prism Graphpad software and IC_{50} values were determined using non-linear regression analysis.

JNK1. Inhibitors (initial concentration: 10 μM, 3-fold dilutions: 9 dilutions) were assayed in triplicate against recombinant full-length activated JNK1α2 (final concentrations = 5 nM) in an assay also containing 30 mM HEPES, pH 7.5, 10 mM $MgCl_2$, 0.6 mM EGTA, 1 mM Na_3VO_4, 0.05 mg/mL BSA, 0.2 mg/mL myelin basic protein, and 0.5 μCi of γ-^{32}P-ATP ([ATP] $\ll K_m$ (ATP)) in a final volume of 30.2 μL. The reactions were incubated for 1 hour at rt and terminated by transferring 4.6 μL of the reaction mixture to a phosphocellulose membrane. The membranes were washed with 0.5% phosphoric acid (4×) and acetone (1×) and quantitated by phosphorimaging. The scanned membranes were quantified with ImageQuant and converted to percent inhibition. Data was analyzed using Prism Graphpad software and IC_{50} values were determined using non-linear regression analysis.

JNK2. Inhibitors (initial concentration: 10 μM, 3-fold dilutions: 9 dilutions) were assayed in triplicate against recombinant full-length activated JNK3α1 (final concentrations = 20 nM) in an assay also containing 30 mM HEPES, pH 7.5, 10 mM $MgCl_2$, 0.6 mM EGTA, 1 mM Na_3VO_4, 0.05 mg/mL BSA, 0.2 mg/mL myelin basic protein, and 0.5 μCi of γ-^{32}P-ATP ([ATP] ≪ K_m (ATP)) in a final volume of 30.2 μL. The reactions were incubated for 1 hour at rt and terminated by transferring 4.6 μL of the reaction mixture to a phosphocellulose membrane. The membranes were washed with 0.5% phosphoric acid (4×) and acetone (1×) and quantitated by phosphorimaging. The scanned membranes were quantified with ImageQuant and converted to percent inhibition. Data was analyzed using Prism Graphpad software and IC_{50} values were determined using non-linear regression analysis.

V. Protein Labeling and Enrichment with LTRs

A. In vitro labeling of proteins

Figure 4a: MK2 (400 nM), PAK5 (400 nM), and p38 (400 nM) were combined in PBS to a total volume of 50 μL. Competitor (**4**-**6**) (10μM) was added (or an equal volume of DMSO) and samples were incubated at rt for 10 min. LTR (**1**-**3**) (500 nM) was added and samples were incubated another 10 min at rt. Samples were placed under a handheld UV light at 365 nm, while on ice, for 30 min, followed by general click chemistry conditions (see below). After the gels were scanned, they were transferred to nitrocellulose and were subjected to Western blotting with α-His_6 antibody (Cell Signaling).

Figure 4c: MK2 (400 nM) and p38 (400 nM) were combined in PBS to a total volume of 50 μL. LTR (**1**) (500 nM) was added and samples were incubated another 10 min at rt. Samples were placed under a handheld UV light at 365 nm, while on ice, for up to 30 min, followed by general click chemistry conditions (see below).

Figure 5a: MK2 (400 nM) and p38 (400 nM) were combined in PBS to a total volume of 50 μL. Competitor (SB203580, Imatinib, Dasatinib, Erlotinib, **4,** or **5**) (10μM) was added (or an equal volume of DMSO) and samples were incubated at rt for 10 min. LTR **2** (500 nM) was added and samples were incubated another 10 min at rt. Samples were placed under a handheld UV light at 365 nm, while on ice, for 30 min, followed by general click chemistry conditions (see below).

Figure 5c: MK2 (200 nM), HeLa lysate (0.5 mg/mL), and a MAP kinase (p38, ERK2, or JNK3) (200 nM) were combined in PBS to a total volume of 50 μL. Competitor (**4** or **6**) (10μM) was added (or an equal volume of DMSO) and samples were incubated at rt for 10 min. LTR (**1** or **3**) (250 nM) was added and samples were incubated another 10 min at rt. Samples were placed under a handheld UV light at 365 nm, while on ice, for 30 min, followed by general click chemistry conditions (see below).

Figure 6a: AGT (800 nM), AGT-MK2 (800 nM), and p38 (200 nM) were combined in PBS to a total volume of 50 μL. Competitor **4** (10μM) was added (or an equal volume of DMSO) and samples were incubated at rt for 10 min. LTR **1** (250 nM) was added and samples were incubated another 10 min at rt. Samples were placed under a handheld UV light at 365 nm, while on ice, for 30 min, followed by general click chemistry conditions (see below).

Figure 6b: MKK6 (2 μM), p38 (400 nM), and HeLa lysate (0.5 mg/mL) were combined in PBS to a total volume of 50 μL. Competitor (**4** or **6**) (10μM) was added (or an equal volume of DMSO) and samples were incubated at rt for 10 min. LTR (**1** or **3**) (500 nM) was added and samples were incubated another 10 min at rt. Samples were placed under a handheld UV light at 365 nm, while on ice, for 30 min, followed by general click chemistry conditions (see below).

Figure 6c: DUSP10 (~400 nM), p38 (400 nM), and HEK293 lysate (0.1 mg/mL) were combined in PBS to a total volume of 50 μL. Competitor **4** (10μM) was added (or an equal volume of DMSO) and samples were incubated at rt for 5 min. LTR **1** (500 nM) was added and samples were incubated another 5 min at rt. Samples were placed under a handheld UV light at 365 nm, while on ice, for 30 min, followed by general click chemistry conditions, though without precipitation.

Figure 7: p38 (400 nM) and HEK293 lysate (0.2 mg/mL) were combined in PBS to a total volume of 50 μL. Competitor **4** (10μM) was added (or an equal volume of DMSO) and samples were incubated at rt for 5 min. LTR **1** or **8** (500 nM) was added and samples were incubated another 5 min at rt. Samples were placed under a handheld UV light at 365 nm, while on ice, for 30 min, followed by general click chemistry conditions, though without precipitation. After the gels were scanned, they were transferred to nitrocellulose and were subjected to Western blotting with α-His_6 antibody (Cell Signaling).

B. General Click Chemistry Conditions. 1.1 μL of 2.5 mM rhodamine-azide, 1.1 μL of fresh 50 mM TCEP in H_2O, 3.3 μL of 1.7 mM TBTA in 1:4 DMSO:tBuOH, and 1.1 μL fresh 50 mM

$CuSO_4$ in H_2O were added to each 50 μL reaction after irradiation. The reactions were incubated for 1 hour at rt, then precipitated to remove excess click chemistry reagents: 50 μg BSA was added to each reaction (if no HeLa lysate had been used), along with 600 μL MeOH, 150 μL $CHCl_3$, and 400 μL H_2O. The mixtures were vortexed briefly and spun down for 4 min at 16.1K × g. The upper layer was removed, and the remainder was vortexed with 450 μL MeOH and spun down again. The liquid was removed and the pellet was washed with another 450 μL MeOH. The pellet was left to dry for > 15 min. 30 μL of 1 × SDS loading buffer was added to each sample. The samples were vortexed briefly, then boiled for 5 min. 25 μL of each sample was loaded on a 10% SDS-PAGE gel. After electrophoresis, the gel was scanned on a Typhoon fluorescent scanner.

C. Labeling endogenous p38

HeLa cells from a mostly confluent 25-cm plate were scraped off the plate into 3 mL PBS, spun down, and resuspended in 400 μL PBS with Roche protease inhibitor cocktail and 1 mM PMSF. Cells were lysed by sonication, then spun down at 5 K × *g* for 10 min at 4° C to clear the lysate. Supernatant was removed and found to have 3.0 mg/mL protein by Bradford assay. This lysate was divided between two wells in a round-bottom 96-well plate. One well received 4 μL DMSO, and the other 4 μL 500 μM **4** (final concentration of 10 μM); this was incubated 10 min at rt. Both wells then received 4 μL 100 μM **1** (final concentration 2 μM) and were incubated at rt for another 10 min. The plate was placed under a UV lamp (365 nm) for 30 min while sitting on ice. At the end of irradiation, samples were transferred to microcentrifuge tubes and diluted with 100 μL PBS to a final concentration of 2 mg/mL protein, and 75 μL of SDS buffer (4% SDS, 150

mM TEA pH 7.4, 150 mM NaCl). Click chemistry reagents were added to the same concentrations as for general click chemistry conditions (see above), including precipitation, but with cleavable biotin-azide **10** as the azide. The protein pellets were resuspended in 200 μL of 1.2% SDS in PBS by sonication in a water bath for 10 min, followed by boiling for 5 min. Solubilized protein was diluted 6-fold with PBS to bring the SDS concentration down to 0.2%, then added to 40 uL of streptavidin-agarose beads washed with PBS, and twirled at RT for 1 hr. Streptavidin beads were washed 3 times with urea buffer (6M urea, 2 M thiourea, 10 mM HEPES pH 8.0) and then 4 times with 1% SDS in PBS; all washes were 500 μL in volume and twirled with samples for 1 min prior to removal. A fresh elution buffer (300 mM sodium dithionite solution in 1% SDS in PBS) was prepared, and 50 μL of it was added to each sample and twirled at rt for 30 min. This elution was removed, and added another 25 μL of elution buffer was briefly incubated with beads before removal as well. All samples received SDS loading buffer and proteins were resolved with SDS-PAGE. Gels were transferred and probed with anti-p38 Western blot.

D. IP/crosslinking

Four 10-cm plates of HEK293 cells were grown to 95% confluency and transfected with two plasmids, 5 μg of each, using standard FuGENE-HD protocol. Plate 1 received MK2-pDEST26-flag and eGFP-p38; plate 2 received MK2-pDEST26-flag and LifeAct-eGFP; plates 3 and 4 mirrored plates 1 and 2, but with MKK6 in place of MK2. Cells were grown ~ 24 hrs after transfection, then pushed off the plate and spun down. Cells were resuspended in 1 mL mammalian cell lysis buffer (20 mM Tris-HCl pH 7.4, 150 mM NaCl, 1 mM EDTA, 1 mM

EGTA, 1% Triton X-100, 2.5 mM sodium pyrophosphate, 1 mM sodium glycerophosphate, 1 mM PMSF, and protease inhibitor cocktail (Roche)) and lysed by sonication. Lysate was cleared by centrifugation (10 min at max speed at 4° C) and then added to 40 μL of anti-flag resin slurry (Sigma Aldrich) before being placed on an orbital shaker overnight at 4° C. Beads were then washed once with 500 μL PBS, and beads were transferred to a round-bottom 96-well plate. The beads from each lysate were split into two identical wells, such that the total volume (including beads) in each well was 50 μL. To one well, 0.5 μL of 1 mM inhibitor **4** was added to a final concentration of 10 μM, and an equal volume of DMSO was added to the other well. After 5 min, 1 μL of 100 μM LTR **1** was added to all wells and incubated at rt 15 min. The plate with samples was placed on ice, and a UV lamp (365 nm) was rested directly on it for 30 min, with plate agitations every 5 min to keep the beads in suspension. Beads were transferred to microcentrifuge tubes, received 50 μL 0.2 mg/mL flag peptide in PBS, and were twirled for 5 min at rt. Supernatant was removed, and beads were eluted with an additional 2 aliquots of 50 μL of 0.1 mg/mL flag peptide in PBS. The eluate then received 20% SDS (to final concentration 1.8%), rhodamine-azide **7** (to final concentration 50 μM), TCEP (to final concentration 1 mM), TBTA (to final concentration 0.1 mM), and $CuSO_4$ (to final concentration 1 mM); incubated at room temperature for 1 hr. Click chemistry reactions then received 50 μg of BSA each and were subjected to precipitation as described in General Click Chemistry Conditions (see above, with volumes appropriately adjusted). Dried protein pellets were resuspended by boiling in 60 μL SDS loading buffer for 5 min. Samples were run on SDS-PAGE gels, scanned for fluorescence, transferred to nitrocellulose, and subjected to anti-flag or anti-GFP Western analysis.

References

(1) Manning, G.; Whyte, D. B.; Martinez, R.; Hunter, T.; Sudarsanam, S. *Science* **2002**, *298*, 1912-34.

(2) Whitmarsh, A. J. *Biochem Soc Trans* **2006**, *34*, 828-32.

(3) Skroblin, P.; Grossmann, S.; Schafer, G.; Rosenthal, W.; Klussmann, E. *Int Rev Cell Mol Biol*, *283*, 235-330.

(4) Cuadrado, A.; Nebreda, A. R. *Biochem J*, *429*, 403-17.

(5) Ge, B.; Gram, H.; Di Padova, F.; Huang, B.; New, L.; Ulevitch, R. J.; Luo, Y.; Han, J. *Science* **2002**, *295*, 1291-4.

(6) Lu, G.; Kang, Y. J.; Han, J.; Herschman, H. R.; Stefani, E.; Wang, Y. *J Biol Chem* **2006**, *281*, 6087-95.

(7) Ferreiro, I.; Joaquin, M.; Islam, A.; Gomez-Lopez, G.; Barragan, M.; Lombardia, L.; Dominguez, O.; Pisano, D. G.; Lopez-Bigas, N.; Nebreda, A. R.; Posas, F. *BMC Genomics*, *11*, 144.

(8) Wu, R.; Kausar, H.; Johnson, P.; Montoya-Durango, D. E.; Merchant, M.; Rane, M. J. *J Biol Chem* **2007**, *282*, 21598-608.

(9) Dorman, G.; Prestwich, G. D. *Biochemistry* **1994**, *33*, 5661-73.

(10) Rostovtsev, V. V.; Green, L. G.; Fokin, V. V.; Sharpless, K. B. *Angew Chem Int Ed Engl* **2002**, *41*, 2596-9.

(11) Herberich, B.; Cao, G. Q.; Chakrabarti, P. P.; Falsey, J. R.; Pettus, L.; Rzasa, R. M.; Reed, A. B.; Reichelt, A.; Sham, K.; Thaman, M.; Wurz, R. P.; Xu, S.; Zhang, D.; Hsieh, F.; Lee, M. R.; Syed, R.; Li, V.; Grosfeld, D.; Plant, M. H.; Henkle, B.; Sherman, L.; Middleton, S.; Wong, L. M.; Tasker, A. S. *J Med Chem* **2008**, *51*, 6271-9.

(12) Sullivan, J. E.; Holdgate, G. A.; Campbell, D.; Timms, D.; Gerhardt, S.; Breed, J.; Breeze, A. L.; Bermingham, A.; Pauptit, R. A.; Norman, R. A.; Embrey, K. J.; Read, J.; VanScyoc, W. S.; Ward, W. H. *Biochemistry* **2005**, *44*, 16475-90.

(13) Karaman, M. W.; Herrgard, S.; Treiber, D. K.; Gallant, P.; Atteridge, C. E.; Campbell, B. T.; Chan, K. W.; Ciceri, P.; Davis, M. I.; Edeen, P. T.; Faraoni, R.; Floyd, M.;

Hunt, J. P.; Lockhart, D. J.; Milanov, Z. V.; Morrison, M. J.; Pallares, G.; Patel, H. K.; Pritchard, S.; Wodicka, L. M.; Zarrinkar, P. P. *Nat Biotechnol* **2008**, *26*, 127-32.

(14) ter Haar, E.; Prabhakar, P.; Liu, X.; Lepre, C. *J Biol Chem* **2007**, *282*, 9733-9.

(15) Theodosiou, A.; Smith, A.; Gillieron, C.; Arkinstall, S.; Ashworth, A. *Oncogene* **1999**, *18*, 6981-8.

(16) Zhang, Y. Y.; Wu, J. W.; Wang, Z. X. *Sci Signal* **2011**, *4*, ra88.

(17) Tanoue, T.; Moriguchi, T.; Nishida, E. *J Biol Chem* **1999**, *274*, 19949-56.

(18) Szychowski, J.; Mahdavi, A.; Hodas, J. J.; Bagert, J. D.; Ngo, J. T.; Landgraf, P.; Dieterich, D. C.; Schuman, E. M.; Tirrell, D. A. *J Am Chem Soc* **2010**, *132*, 18351-60.

(19) Tasker, A. Z., Dawei; Pettus, Liping H.; Rzasa, Robert M.; Sham, Kelvin K. C.; Xu, Shimin; Chakrabarti, Partha Pratim 2008; Vol. WO 2008030466 A1 20080313.

(20) Perera, B. G.; Maly, D. J. *Mol Biosyst* **2008**, *4*, 542-50.

(21) Hsu, T. L.; Hanson, S. R.; Kishikawa, K.; Wang, S. K.; Sawa, M.; Wong, C. H. *Proc Natl Acad Sci U S A* **2007**, *104*, 2614-9.

(22) Hintersteiner, M.; Kimmerlin, T.; Garavel, G.; Schindler, T.; Bauer, R.; Meisner, N. C.; Seifert, J. M.; Uhl, V.; Auer, M. *Chembiochem* **2009**, *10*, 994-8.

(23) Szafranska, A. E.; Luo, X.; Dalby, K. N. *Anal Biochem* **2005**, *336*, 1-10.

Chapter 2

Further Exploration of Kinase-Directed Label Transfer Reagents

Introduction

The work presented in chapter 1 represents the efforts in this doctoral work which were largely successful. In the progress of this work, we also explored several other avenues of research. We synthesized a variety of other LTRs in an attempt to improve their efficiency. The "label" portion of the LTR to was changed to other bioorthogonal labels such as hexylchloride, chloropyrimidine, and biotin, in order to avoid the click chemistry step. We also used a chemically activated crosslinking moiety, DOPA, in place of the benzophenone, and we varied the length of the linker between the kinase inhibitor and the crosslinker. While some of these LTRs achieved results similar to those reported in chapter 1, none improved the signal, and several had significant drawbacks.

We attempted to broaden the scope of the LTRs by attaching the linker/crosslinker/label moieties used for p38 to other kinase inhibitors. The first, based on a recently reported scaffold for a BMK1 inhibitor, did not succeed in labeling the kinase, but we were also unable to observe any activity from the kinase. The second was based on a bumped kinase inhibitor and was expected to bind only to proteins with small gatekeeper residues; however, we found the labeling by this probe to be quite non-specific.

Finally, we tried to use the LTRs described in chapter 1 to answer some specific biological questions. We found we were unable to detect any labeling of proteins when the LTR was used *in vivo* in spite of good cell permeability. When we attempted to use our LTRs to study the kinase complex formed by PKN, MLTK, MKK3/6, and p38, we also discovered that the extremely weak nature of this complex thwarted our attempts to use LTRs for studying it.

Results and Discussion

Attempts to improve the efficiency of LTRs

First, based on our work with click chemistry, we were aware than even under optimized conditions, a significant fraction of proteins modified with an alkyne would not be labeled with the azide of interest. Consequently, we synthesized a variety of label transfer reagents (LTRs) with the same phthalazine scaffold and different crosslinkers or labels (Scheme 1).

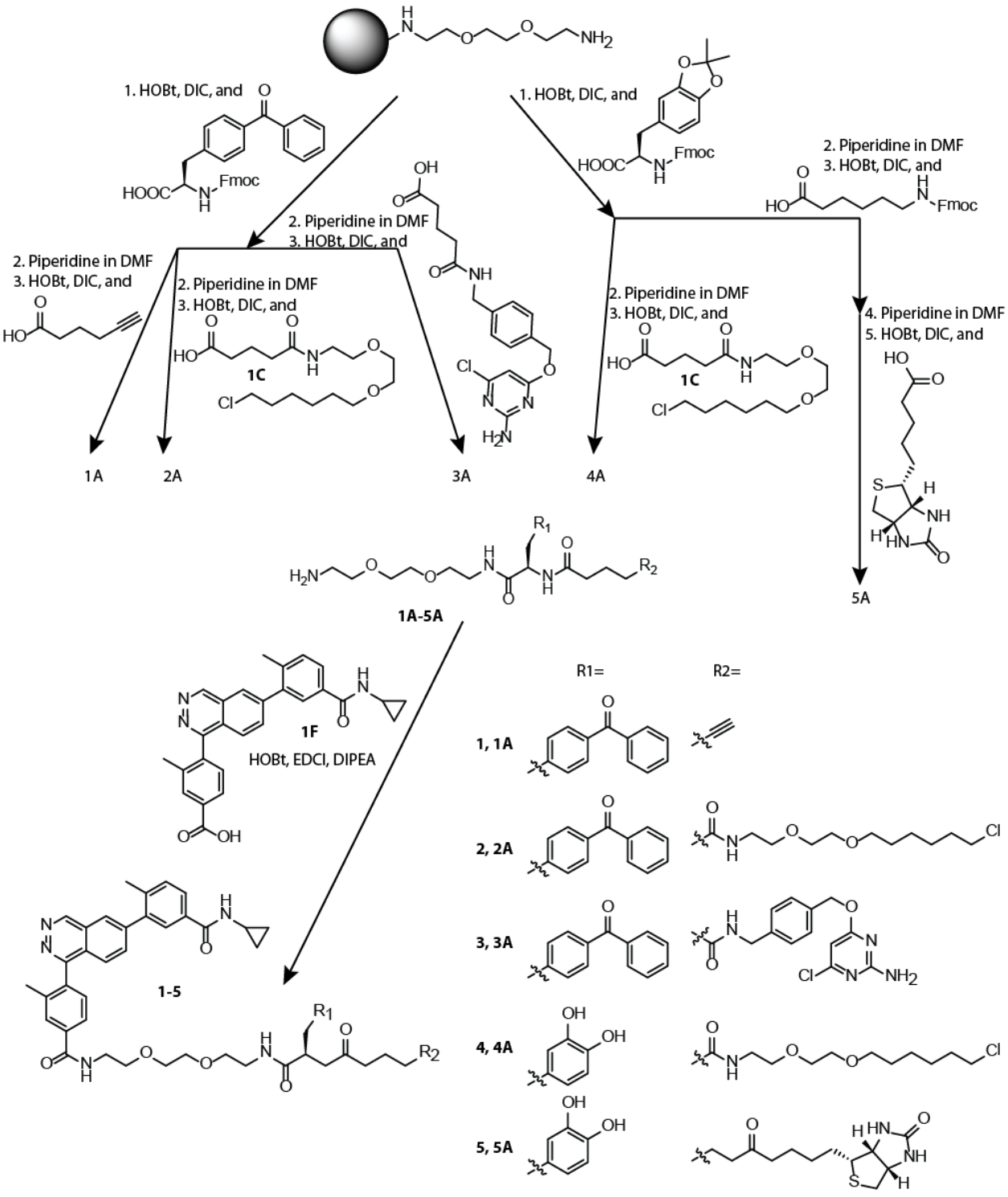

Scheme 1: Synthesis of LTRs **1-5** based on the phthalazine scaffold.

The alkyne was in many ways an ideal choice of a tag because its small size meant it had little effect on cell permeability. However, we concluded that replacement of the alkyne with a hexyl-chloride moiety would be a fairly conservative modification. The hexylchloride moiety is known to be an efficient target of the self-labeling protein Halo-tag (Figure 1a).[10] A hexylchloride-containing LTR could be used for both visualization of labeled proteins and for purification through the intermediate of the SNAP- and Halo-tag fusion protein ASH (Figure 1c,d).[11,46] SNAP-tag and Halo-tag are both modified enzymes which have been developed to covalently and irreversibly self-label with small molecules. SNAP-tag, based on the DNA repair protein AGT, will covalently attach itself to any small molecule bearing a benzyl-guanine or chloropyrimidine moiety (Figure 1b).[8,9] We have created a fusion in which these two proteins are connected by the protein SUMO, which we have called ASH (AGT-SUMO-Halo).[11] Since endogenous SUMO proteases efficiently cleaved our original design of this protein, it has been modified to be only cleavable by a mutated SUMO protease, Ulp1*. For visualization, labeled proteins can be incubated with the ASH protein, resulting in a covalent ASH-labeled protein complex that is higher in molecular weight. Western blot analysis of the protein mixture can reveal the ratio of ASH-tagged protein to non-ASH-tagged protein. For purification, the ASH protein can be preincubated with chloropyrimidine resin. The SNAP-tag portion of ASH covalently binds to this resin, while excess ASH can be washed away. Labeled proteins that are incubated with the ASH-containing resin can be selectively retained from complex mixtures. After extensive washes, selective elution can then be achieved by incubation with Ulp1*.

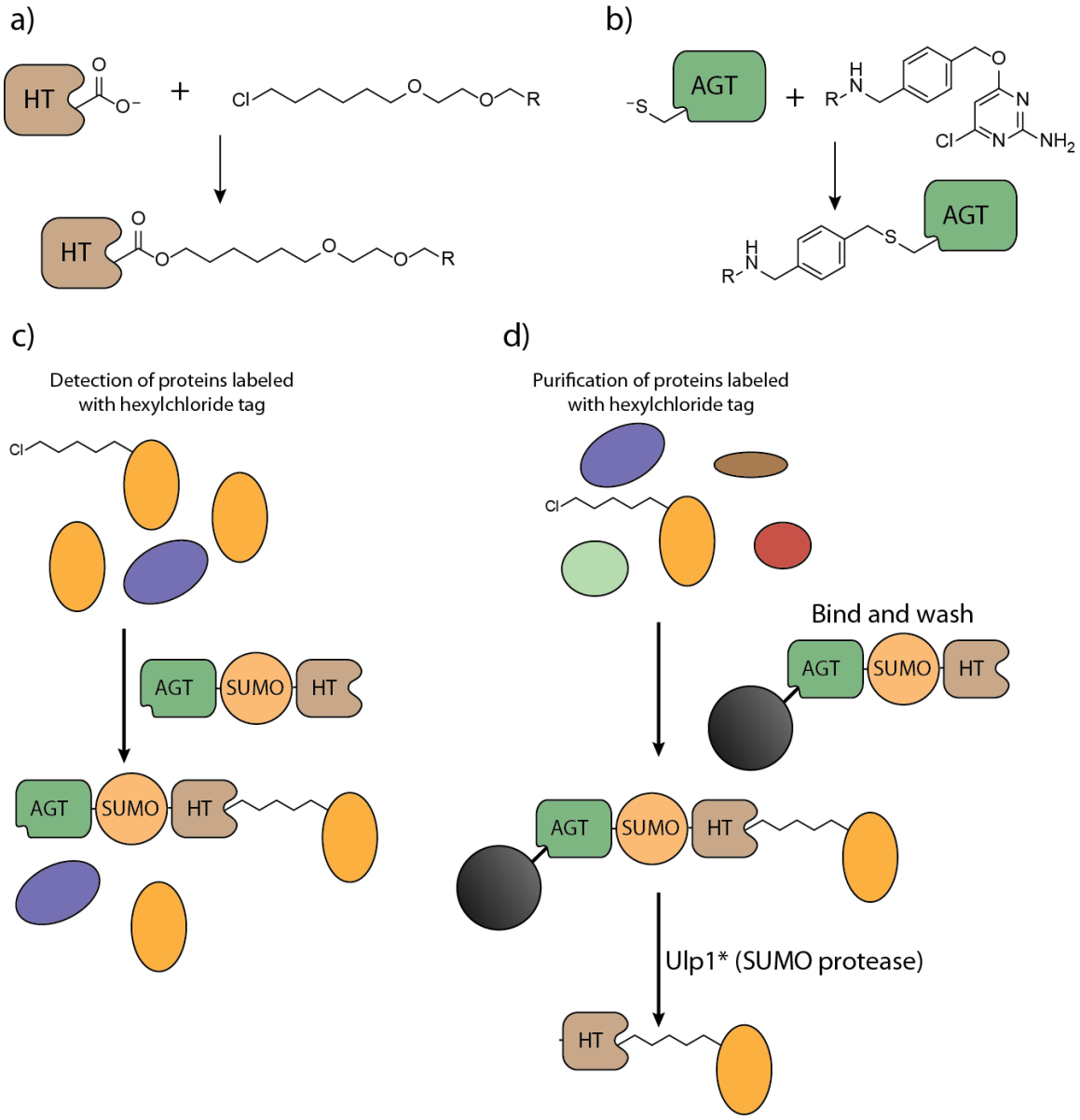

Figure 1. Detection and purification of hexylchloride labeled proteins. a) Halo-tag has an active site aspartate residue that selectively displaces alkyl chlorides like hexylchloride, forming a stable ester bond. b) SNAP-tag, a modified AGT protein, has an active site cysteine that attacks benzyl-modified chloropyrimidines or guanines, forming a stable thioether bond. c) In order to detect labeled proteins, the mixture is incubated with ASH, leading to covalently modified proteins. SDS-PAGE gels can then distinguish labeled and unlabeled proteins by size due to the increase in mass from ASH. d) Purification is accomplished by incubating labeled proteins with ASH immobilized on chloropyrimidine-derivatized beads, followed by cleavage with the SUMO protease Ulp1* to cleave off the protein of interest attached to Halo-tag.

LTR **1** had been reasonably effective (see chapter 1). We synthesized a probe equivalent to **1**, but with a hexylchloride replacing the alkyne (**2**, Figure 2a). After extensive optimization, it was found that **2** was capable of labeling p38 and that labeled protein could be selectively captured and eluted (Figure 2b). Following labeling of p38 with **2** under UV light, the protein was incubated with ASH preconjugated to chloropyrimidine beads. A small portion was incubated with free ASH and retained for loading on a gel, and shows that a new band appears in the anti-p38 western at a high molecular weight, representing the ASH-LTR-p38 complex. Elution with the Ulp1* shows release of the Halo-tag-LTR-p38 portion of the complex. While a significant amount of unlabeled protein was also eluted in these conditions, more extensive washing of the beads and the elimination of SDS in the elution buffer should prove more selective. Though it is encouraging that p38 is labeled and purified independent of high protein concentrations, the fraction of p38 that is labeled is quite small – well below 10%.

Similarly, **2** was used to show that p38 could be labeled and purified from lysate (Figure 2c). After lysing cells and subjecting them to cross-linking with **2**, a portion of the lysate was incubated with ASH and shown to contain labeled protein due to the presence of p38-LTR-ASH complex. Addition of ASH to the flow through (to probe for labeled but uncaptured p38) demonstrated that about one third of photocrosslinked protein failed to be captured by the ASH on resin. However, elution with Ulp1* demonstrated selective capture and release of some labeled protein. Regrettably, the fraction of p38 labeled in this case is even lower than with purified protein (Figure 2b). The p38 binding partner MK2, with a low nanomolar binding affinity for p38, is the most likely endogenous partner to be observed, but no MK2 labeling could be detected in these samples.

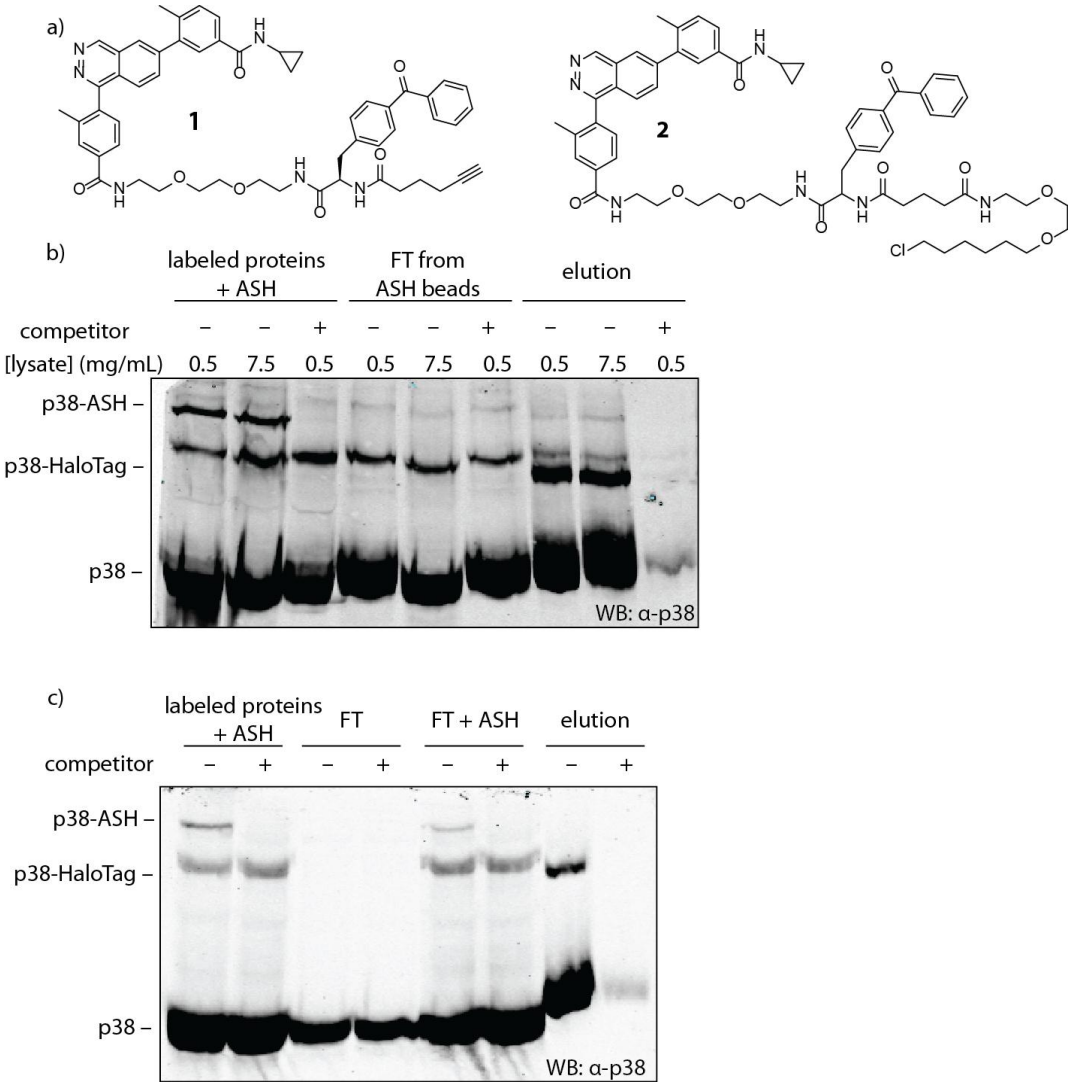

Figure 2.LTR **2**. a) Structures of LTRs **1** and **2**. b) Labeling and capture with purified p38. 400 nM p38 was cross-linked with **2** in either 0.5 or 7.5 mg/mL HeLa lysate, in the presence or absence of competitor. Samples of labeled protein were incubated with ASH for one hour to visualize labeling, and demonstrate that some p38 is selectively labeled by **2** and covalently attached to ASH. The remainder of the sample was incubated with ASH immobilized on resin, then washed, followed by cleavage of the ASH by the SUMO protease ULP1* to elute the p38-LTR-Halo-tag complex. Beads were also rinsed with 3x SDS loading buffer, which was added to the elution. c) Labeling and capture of endogenous p38 with **2**. 0.5 mL of 6.5 mg/mL lysate samples were crosslinked with **2** in either the presence or absence of a competitor. Labeled protein was loaded on beads conjugated with ASH, incubated, washed, and eluted as above. Samples of labeled lysate and flow-through (FT) were incubated with ASH to visualize the labeled p38 in the mixture.

Having observed a low efficiency for labeling and capture with hexylchloride-tagged LTR, we wondered if switching the ends of the ASH protein would be effective. We therefore synthesized LTR **3** (Figure 3a) which contains a chloropyrimidine moiety in place of the hexylchloride. While this is a substantially larger chemical group, it has been seen to be highly cell permeable.[47] **3** was capable of labeling p38, as shown by the appearance of a mass-shifted band after incubation with ASH (Figure 3b, lane 3). However, its efficiency is even lower than that of **2**, and was therefore not pursued further.

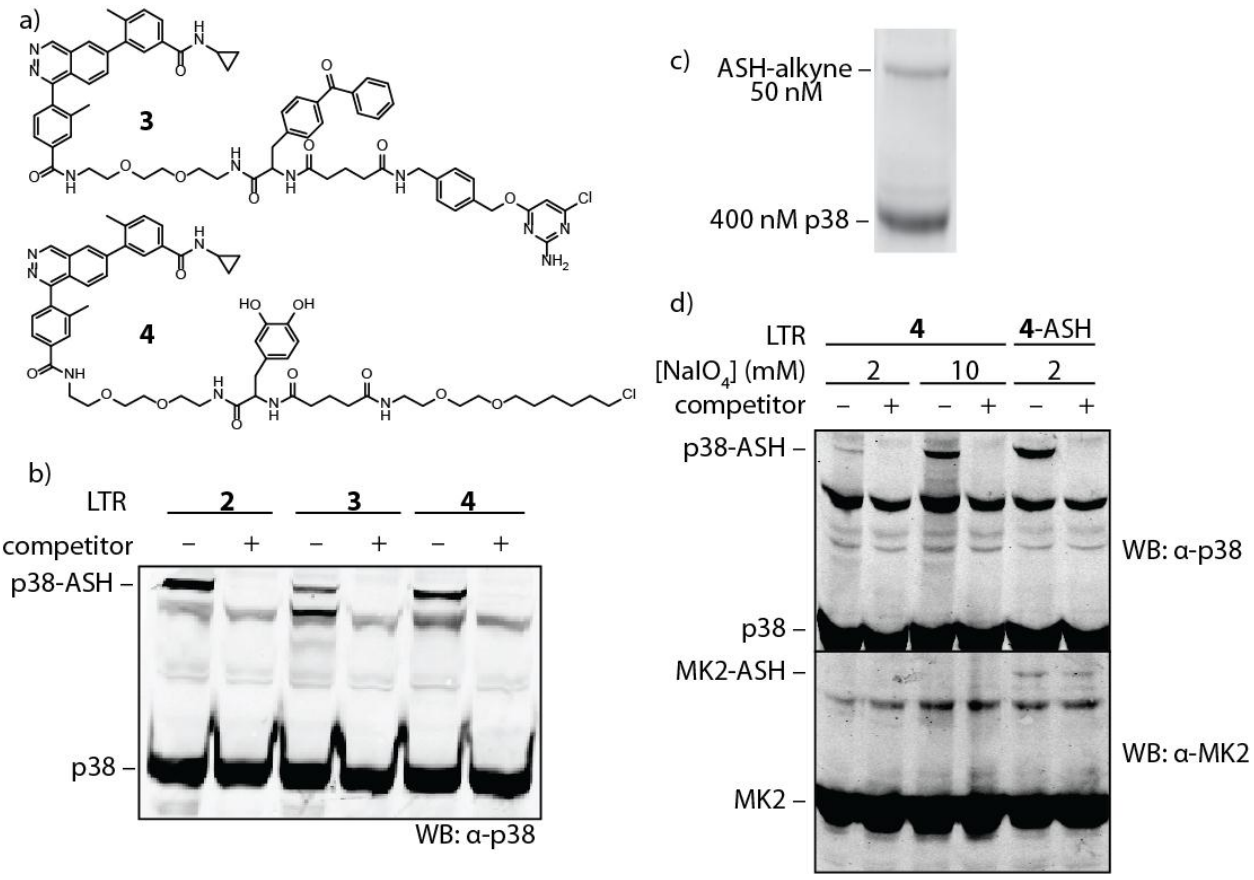

Figure 3. LTRs to improve labeling efficiency. a) Structures of LTRs **3** and **4** b) 400 nM p38 was crosslinked with **2, 3, or 4**. **2** and **3** labeling was done with 30 min UV irradiation; **4** crosslinking was accomplished with 1 mM $NaIO_4$ exposure for 2 min. After crosslinking, all samples were incubated with an excess of ASH to form complexes with labeled proteins. **c**) Fluorescence scan, comparing 400 nM p38 crosslinked with LTR **1** to 50 nM ASH-alkyne; the ratio reveals that around 50% of p38 is labeled. d) 400 nM each of p38 and MK2 were either crosslinked with **4** and then incubated with ASH (lanes 1-4) or crosslinked with **4** that had already been conjugated to ASH (lanes 5-6).

In the course of our work with benzophenone-containing LTRs, we desired to know the extent of protein being labeled by each LTR. To investigate this, we crosslinked our LTR with 400 nM p38 and then added 50 nM ASH that had been fully labeled with benzylguanine-alkyne (as used in chapter 3). By comparing the ratio of fluorescence in these two proteins obtained after click chemistry with rhodamine-azide, we discovered that even with purified proteins, less than 50%

of our p38 of was being labeled (Figure 3c). Consequently, we sought to use a different cross-linking moiety. Though we have done some synthetic work with diazirines and aryl azides, the most synthetically accessible crosslinker was DOPA (L-3,4-dihydroxyphenylalanine). When exposed to sodium periodate, DOPA becomes oxidized and will react with lysines and cysteines in its vicinity.[48] The protected DOPA amino acid was commercially available for inclusion in the synthesis of a new LTR. Since the sodium periodate would likely be incompatible with the reducing conditions needed for click chemistry, we used the hexylchloride moiety as the tag in the LTR, resulting in the synthesis of **4**. Following optimization of crosslinking, it was found to label p38 about as efficiently as probe **2**, based upon the equivalent amounts of ASH-LTR-p38 complex that was observed (Figure 3b, lane 5). Analysis of labeling of the p38-binding partner MK2, however, showed very poor efficiency of labeling (Figure 3d, lanes 1,3). Work by Ratika Krisnamurthy with a hexylchloride tagged probe had shown highest efficiency labeling when the crosslinker was pre-incubated with Halo-tag or ASH. We found labeling with the hexylchloride LTRs to also be increased if the LTR was preincubated with the Halo-tag before crosslinking. However, (Figure 3d, lane 5), labeling of MK2 was non-specific and faint.

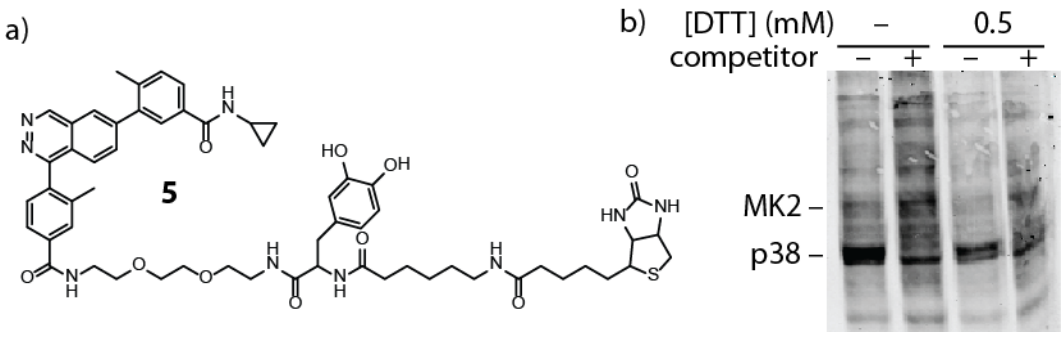

Figure 4. LTR **5**. a)Structure of LTR **5** b) p38 and GST-AGT-MK2 were combined in lysate and exposed to crosslinking with **5** in the presence or absence of a competitor or 0.5 mM DTT. Proteins were then separated on SDS-PAGE gel, transferred, and the blot was then probed with streptavidin-IRDye 800.

Just as we had used a LTR with biotin in place of alkyne with the benzophenone crosslinker (chapter 1, compound **8**), we also synthesized a DOPA-based crosslinker containing biotin as a tag, **5** (Figure 4a). This LTR was indeed effective at selectively biotinylating p38 (Figure 4b). Regrettably, there was significant background signal as well, such that biotinylation of MK2 was difficult to separate from the noise. This lack of specificity makes **5** unattractive as an LTR of further interest.

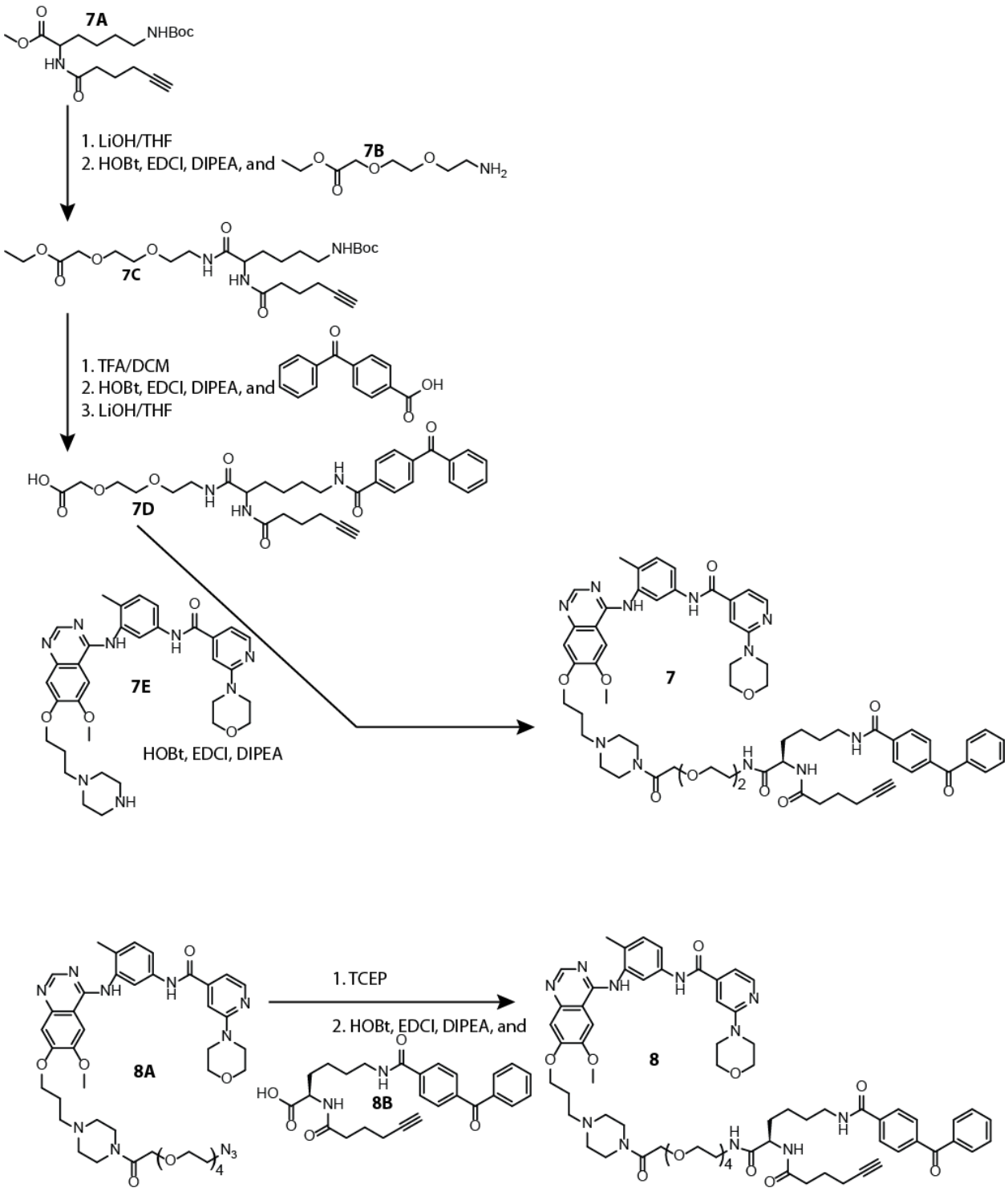

Scheme 2: Synthesis of LTRs **7** and **8** (synthesis of LTR **6** is described in chapter 1)

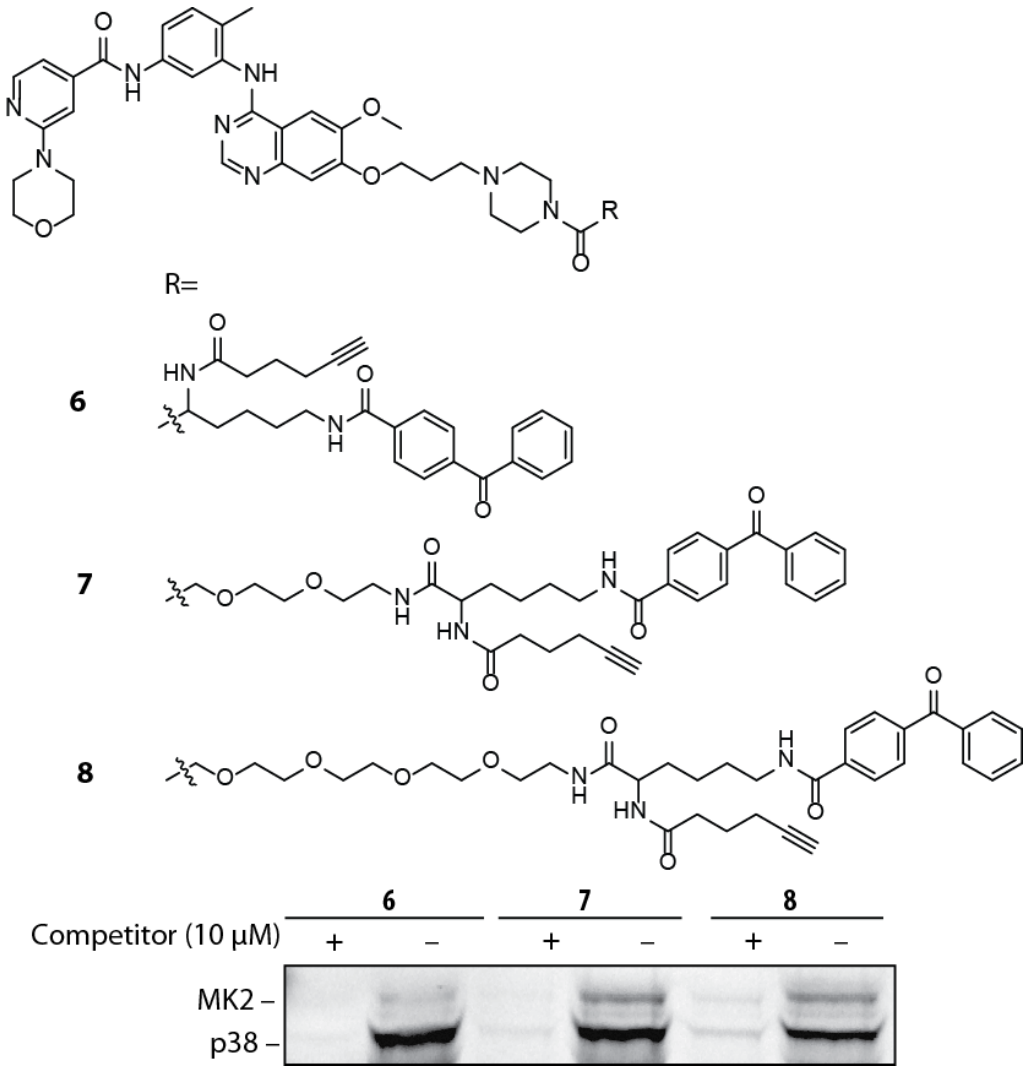

Figure 5. Linker length variation of LTR **6**. a) Structures of the three LTRs, showing that **8** and **7** were identical to **6** with the addition of a varied-length PEG linker to move the photocrosslinker farther from the active site. b) Fluorescence scan of *in vitro* crosslinking of p38 and MK2 (400 nM each) in the presence of each LTR.

We also synthesized LTRs **7** and **8**, which are identical to LTR **2** (described in chapter 1), but with longer linker lengths (Scheme 3). Although the ratio of binding partner to p38 labeling is higher with longer linker lengths, overall labeling is somewhat lower at very long lengths, which motivated a focus on the intermediate linker in these studies (Figure 5).

Attempts to broaden the scope of LTRs

The kinase p38, as a well characterized kinase with several selective and potent inhibitors described for it, was an ideal candidate for initial exploration of LTRs. However, we desired to expand this work, particularly for applications with kinases that are less well understood.

Among the MAPKs (mitogen-activated protein kinases), the ERK, JNK, and p38 families have been widely studied. A fourth MAPK family, however, contains only one member, BMK1 (big MAP kinase 1, also known as ERK5). BMK1 is activated by MEK5, and is involved in responses to growth factors.[49] However, relatively little is known about its binding partners. Since a recent publication reported a potent and selective inhibitor of BMK1, compound **9**,[50] we sought to make an LTR based on this inhibitor scaffold (Scheme 3). A straightforward synthesis produced inhibitor **10**, modified only in that it contains an ester at a site directed out of the ATP-binding site. De-esterification, followed by coupling with the same benzophenone/alkyne crosslinking portion used for LTR **1** produced BMK1-specific LTR **11**, which was characterized by mass spectrometry, NMR, and HPLC for identity and purity.

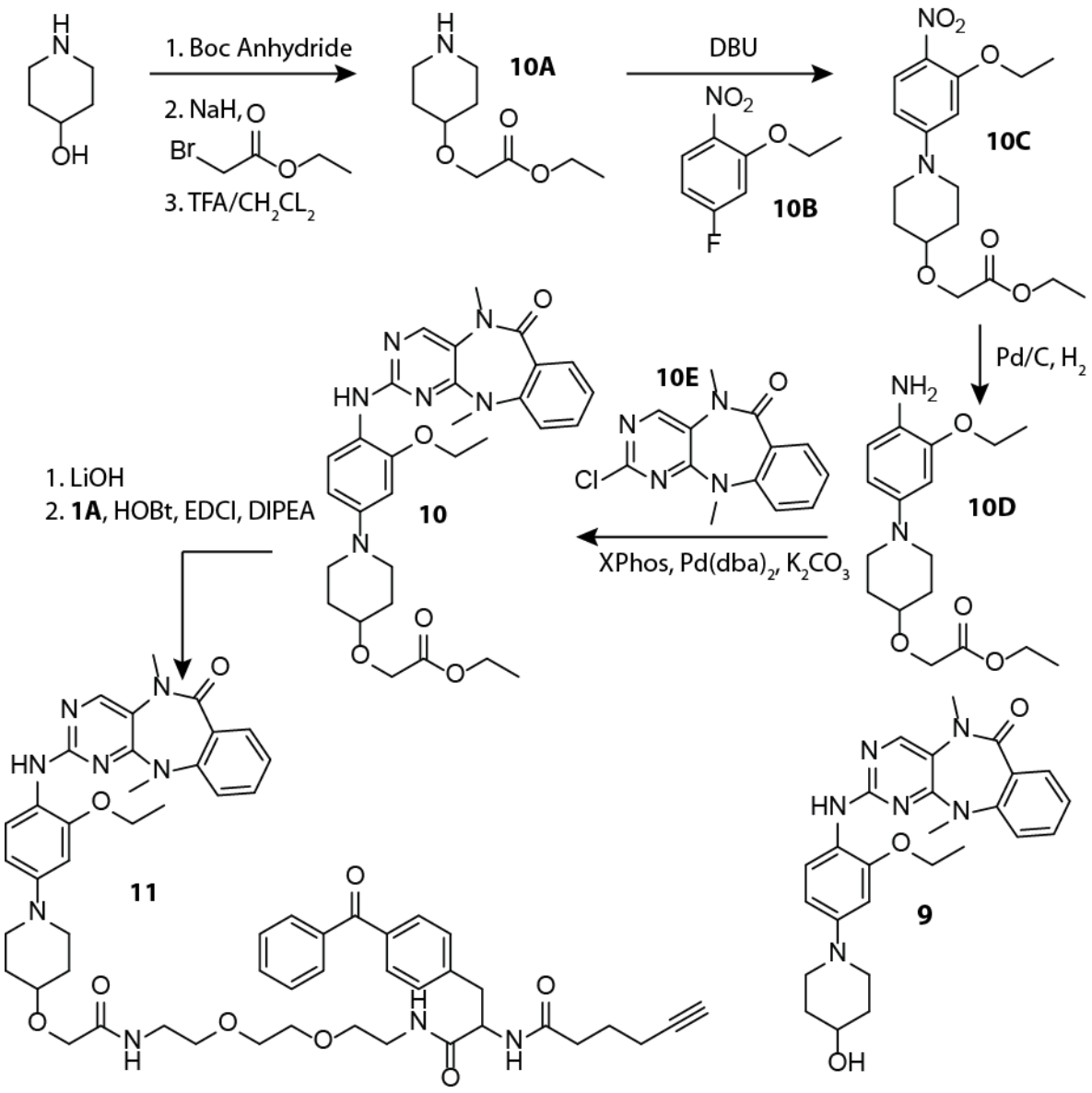

Scheme 3: Synthesis of BMK1-specific inhibitor **10** and its derivative LTR **11**.

Initially, we attempted to test this small molecule for its ability to inhibit the activity of BMK1. BMK1 activity has been tested by both immunoprecipitation of BMK1 from cells[51] or by observation of a phosphorylation-induced mobility shift in SDS-PAGE gels.[52] However, no

activity was observed under either assay. We also attempted to use **11** in an IP/crosslinking assay such as was used with LTR **1** to observe labeling of MK2 and MKK6 (Figure 6). Constitutively active MEK5 (caMEK5) and BMK1 or p38 were coexpressed as flag-tagged proteins in HEK293 cells. After anti-flag IP, crosslinking was carried out in the presence of 2 μM **11**, followed by elution and click chemistry with rhodamine-azide. Regrettably, this resulted in no apparent labeling of either BMK1 or its activator caMEK5, with only a slightly visible band from off-target labeling of p38 due to the high concentration of **11** used. caMEK5 expression was poor in this experiment, but labeling of BMK1 should have been robust regardless. It is far from clear exactly what the issue with this LTR is. The BMK1 and caMEK5 genes used for these studies were used as received (and recommended) by another laboratory, and the catalytic domain of BMK1 was sequenced and shown to match the reported sequence, but it is possible there is a mutation that abrogates the ability of BMK1 to bind or to be active. However, this was not pursued further given the challenges encountered with the p38-specific LTRs as well.

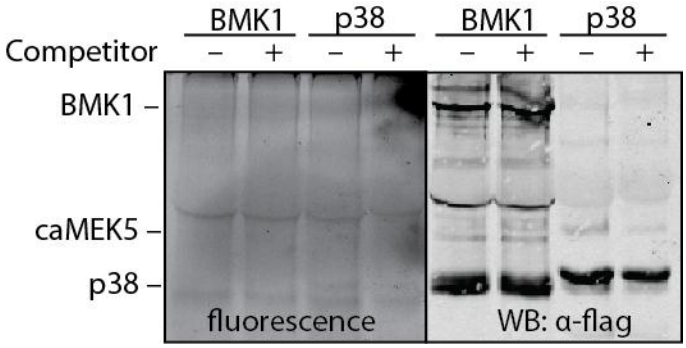

Figure 6. Results of IP/crosslinking experiment with **11**. BMK1 or p38 were co-expressed with caMEK5 as flag-tagged proteins in HEK293 cells. Following precipitation with anti-flag resin, beads were exposed to **11** in the presence of UV light, then eluted with flag peptide and subjected to click chemistry with rhodamine-azide. Resulting labeled proteins were run on a gel and scanned for fluorescence before being transferred and probed by an anti-flag western.

It would be desirable to make an LTR which would be both general and specific: that is, one which does not require the synthesis of a different LTR for each kinase of interest, and yet is specific for the kinase under consideration. To address this, we have employed the "bump-hole" approach of chemical genetics (Figure 7a).[53] Briefly, a residue (or multiple residues) in the ATP binding pocket of a kinase of interest is mutated to a glycine or alanine. This creates a "hole" in the kinase. Inhibitors are then used which have a "bump," a region which would sterically clash with wild-type kinases, but is accommodated by the mutated kinase. In this fashion, a selective kinase/inhibitor pair has been developed for a variety of kinases.[54-61] We employed the scaffold of the widely used **NA-PP1** inhibitor (Figure 7b), and modified it as with other LTRs with a benzophenone and alkyne (Figure 7c, **12**), though this necessitated a reasonably conservative change in the structure of the inhibitor.

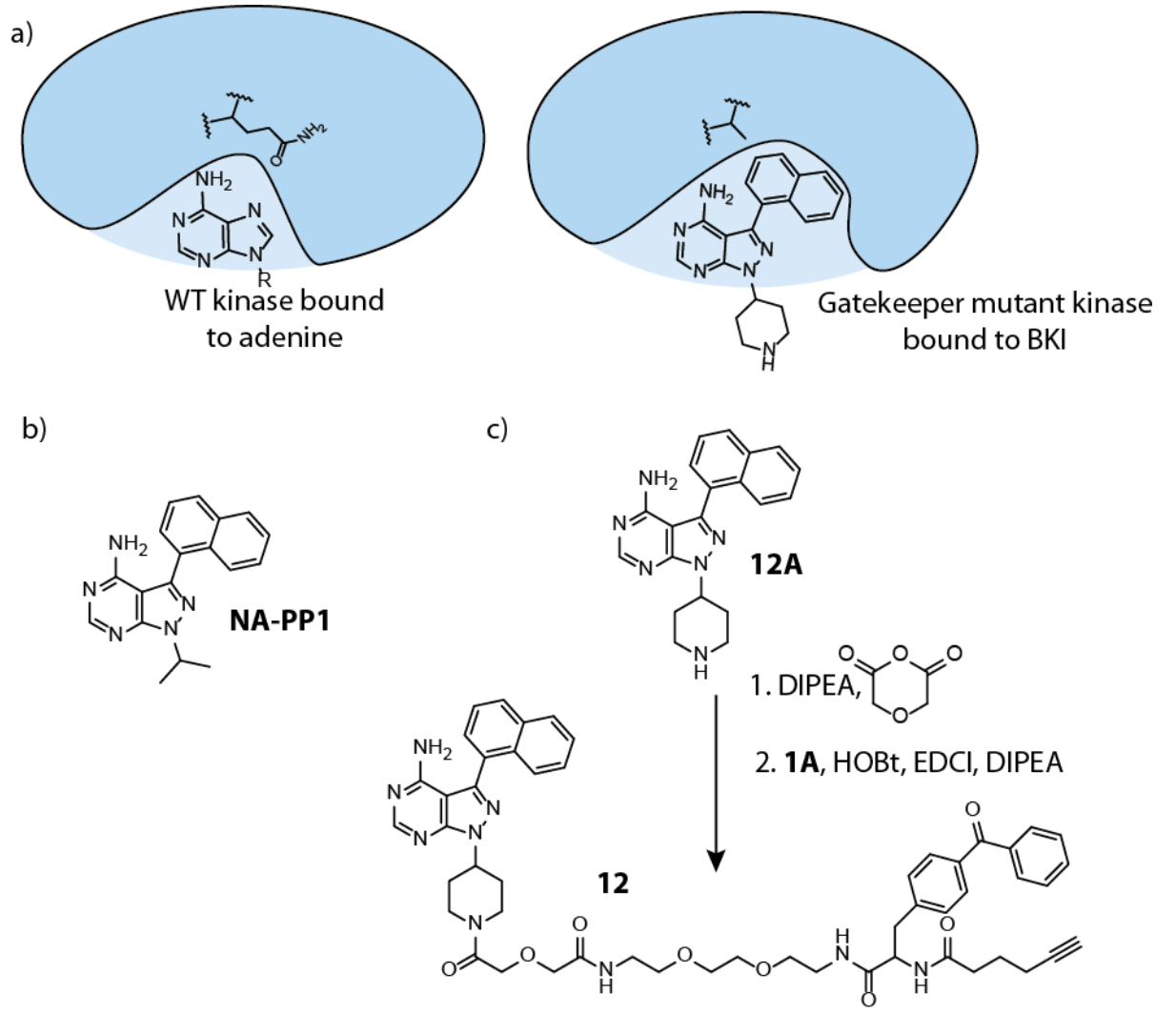

Figure 7. NA-PP1-based LTR. a) Diagram showing the bumped kinase inhibitor approach. In the wildtype kinase, the gatekeeper residue reduces the size of the adenine binding pocket. Mutation of the gatekeeper to a smaller side chain increases the size of the binding pocket, allowing "bumped" kinase inhibitors like NA-PP1 to bind. b) Structure of **NA-PP1** c) Synthesis and structure of the NA-PP1-based LTR **12**.

Initial work with ERK2 showed the expected result that wildtype ERK2 was not labeled by **12**, but that ERK2 Q103A was labeled by it in a selective fashion (Fig 7c). Surprisingly, however, **12**

also labeled wild-type MEK1 and MEK2, even in the absence of ERK2 Q103A. The inhibitor NA-PP1 has been reported to be quite selective for mutated kinases, and we have seen that the benzophenone/alkyne portion of **12** had no deleterious effects on the p38-directed LTRs. However, NA-PP1 has been reported to significantly inhibit p38, several tyrosine kinases, and MKK1 at 1 and 10 μM concentrations, so it is possible that it has significant affinity for the MEK2 as well.[62]

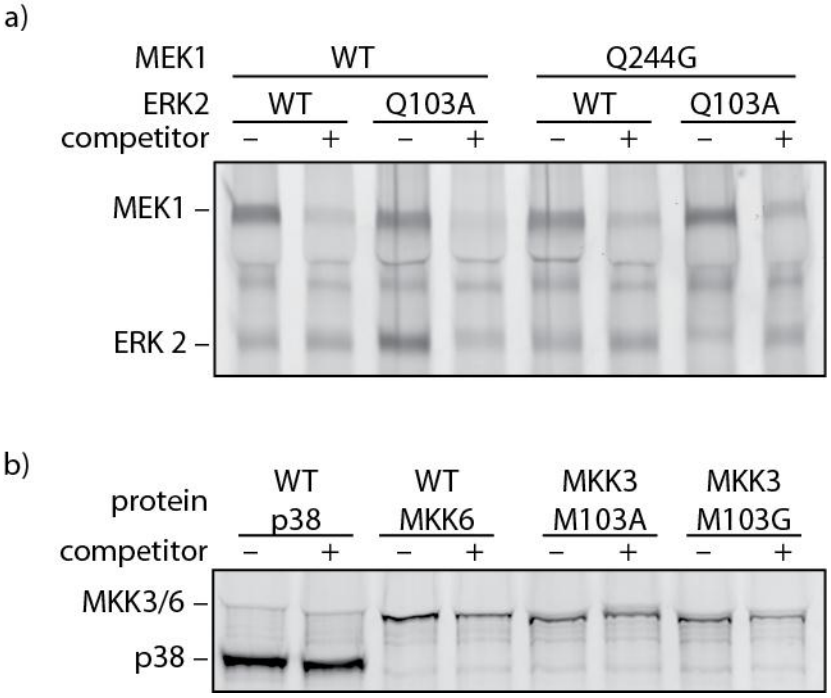

Figure 8: In vitro labeling of proteins with LTR **12**. The indicated kinases (WT or the indicated gatekeeper mutants) were exposed to **12** under UV light in the presence or absence of competitor **NA-PP1**, followed by click chemistry to attach rhodamine-azide to labeled molecules. .

We also sought to modify MKK3 so that it would bind to **12**. While MKK3 was indeed labeled by **12** when mutated, we found that wildtype p38 and MKK6 were equally well labeled (Figure

7d). Unlike with MEK1 and MEK2, p38, MKK3, and MKK6 signals were virtually unaffected by addition of competitor **NA-PP1**, suggesting that the interaction is a non-specific one. It is possible that the poor solubility of this compound is causing non-specific interactions, and it is possible that reduction of this particular bond to an amine would increase the solubility and reduce non-specific labeling. It is also possible that the piperidine ring contributes to non-specific interactions, and this could be altered to a variety of groups as well. This work is ongoing.

Biological Applications of LTR 1

In addition to the experiments described in the first chapter, we also attempted to use LTR **1** *in vivo*. In order to determine whether the LTRs are cell permeable, we took advantage of the property of LTR **1** and its cognate inhibitor **13** of preventing phosphorylation of p38 by its upstream activators. This has previously been reported only for inhibitors which induce the "DFG-out" inactive conformation to the kinase.[36] While a very close analog of **13** has been crystallized with p38 in the active conformation of the kinase, it is also true that **13** shares some features with classic DFG-out inhibitors: the presence of an amide donor/acceptor pair, as well as interactions near the DFG motif. Therefore, it is not entirely surprising that this inhibitor is able to block phosphorylation by the upstream MKK.

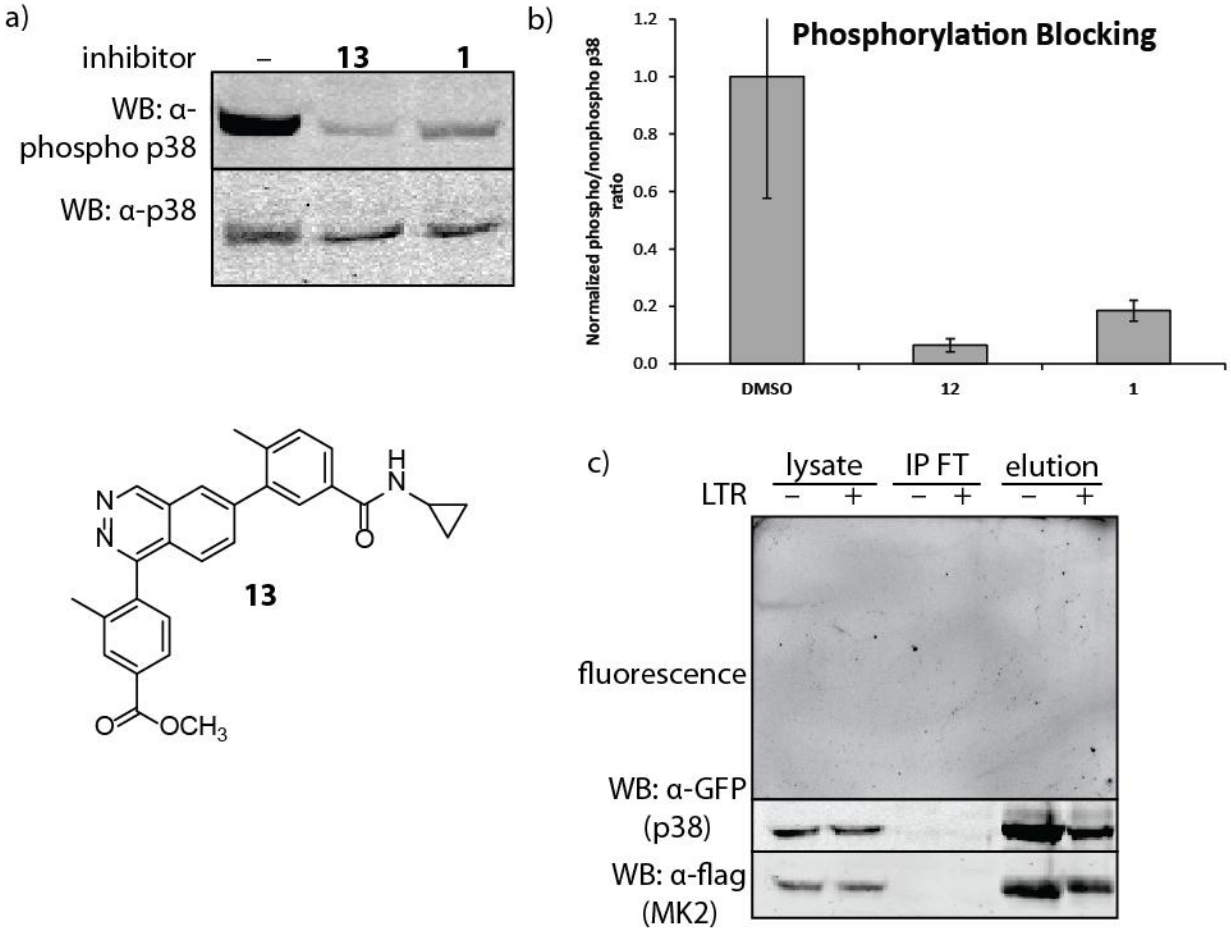

Figure 9. *In vivo* studies with LTRs. a) western blots showing blocking of phosphorylation of p38 by inhibitors and structure of inhibitor **13**. COS-7 cells in 12-well plates were preincubated with listed small molecules (or DMSO), then stimulated with NaCl. After 30 min, cells were harvested and subjected to western blot analysis for both total p38 and phopho-p38. b) Quantitation of results in part a, conducted in triplicate. c) GFP-p38 and flag-MK2 were coexpressed in HEK293 cells, and LTR **1** was introduced prior to crosslinking under a UV lamp for 10 min at 37°C. Cells were lysed, and subjected to anti-flag IP, followed by elution and click chemistry with rhodamine-azide. Proteins were separated on SDS-PAGE gel and scanned for fluorescence before being subject to western Blot.

The cell permeability of these inhibitors can be analyzed by preincubation of cells with the LTR, followed by stimulation of the p38 pathway and western blot to determine the extent phosphorylation of p38 is inhibited by the LTR (Figure 9a,b). We found that p38

phosphorylation was almost entirely blocked by 2 μM of LTR or parent inhibitor **13**, demonstrating that these molecules are at least sufficiently cell permeable to occupy most or all of the p38 binding sites in the cell. We then attempted to use LTR **1** in live cells by incubating the cells with the LTR, then exposing the cells to UV light for 10 min. While similar experiments were effective for different crosslinkers used in our laboratory, we could not detect any signal for labeled p38 or MK2, even when these proteins were overexpressed (Figure 9c).

We desired to apply **1** to the study of a p38 protein kinase complex of interest. Protein kinase N (PKN) has been demonstrated to bind p38α as well as its upstream activator MKK3 and one of its activators, MLTK.[63] We were therefore interested in coexpressing these proteins and doing an IP and crosslinking experiment to determine which of these proteins is actually proximal to p38 when the complex forms. Co-expression of these proteins was complicated by the poor expression of MLTK, and thus we tested multiple vectors and labeling tags, but found that even under the best conditions, MLTK expression was consistently lower than the other complex members. We attempted to pull down HA-tagged p38α, MKK3, and MLTK with flag-PKN, but almost no HA-tagged proteins were detectable in the elution from the pull-down, making it unsurprising that there were no fluorescently labeled bands (Fig 10a**)**. We attempted a similar pull-down with flag-p38 and HA-tagged MKK6, MLTK, and PKN, and found again that the only fluorescent band was for p38 itself, which was unsurprising given that the pull-down failed to retain many HA-tagged proteins, despite the gentleness of the washing conditions (one wash with PBS, 10b). While we have shown that **1** can work for weak binding interactions, it is necessary to have relatively high concentrations, especially of the target protein.

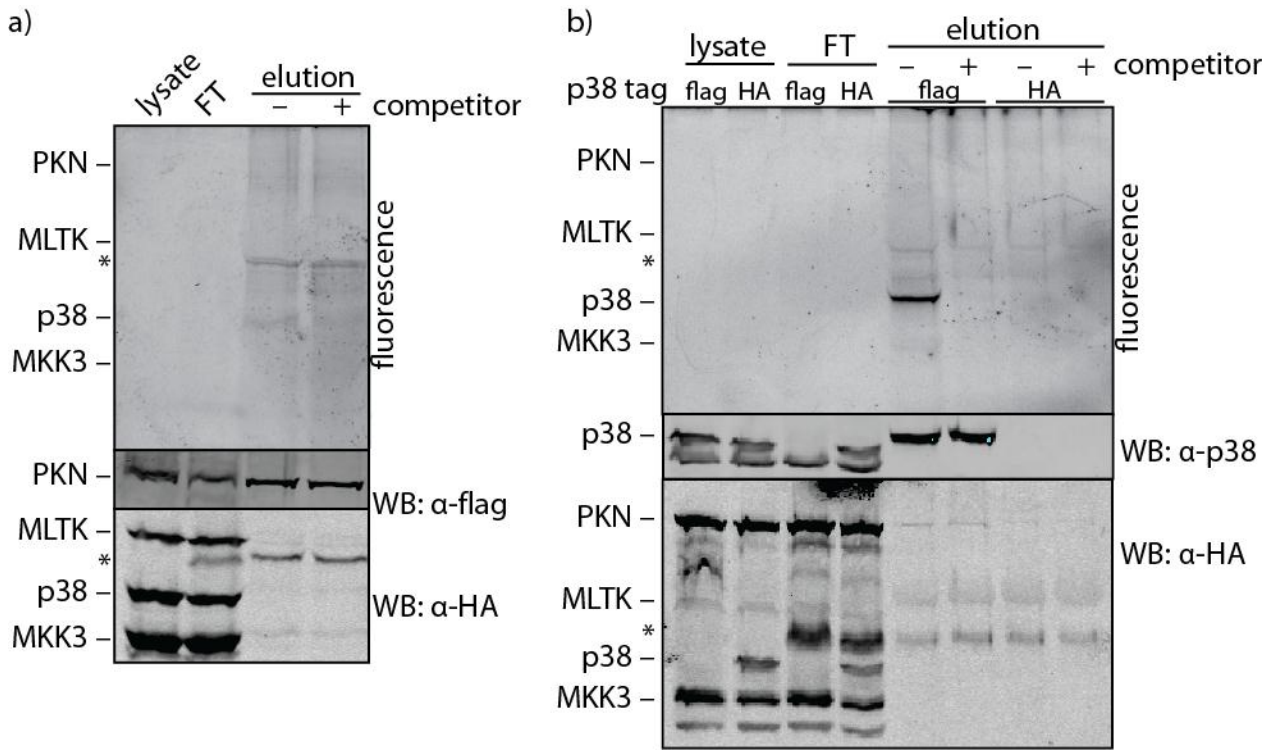

Figure 10. Attempts at labeling the PKN complex. a) Failure to fluorescently label any proteins in the PKN complex. Flag-PKN was coexpressed with HA-tagged p38, MKK3, and MLTK, then subjected to an α-flag IP. UV light was shined on the beads after incubation with LTR **1**, followed by elution and click chemistry with rhodamine-azide. b) A similar experiment to part a, in which flag-p38 or HA-p38 was co-expressed with HA-tagged PKN, MKK3, and MLTK and subjected to the IP/crosslinking conditions as before. Asterisk indicates anti-flag antibody from anti-flag resin used in IP.

Conclusion

We have described here a variety of attempts to improve the efficiency or scope of usefulness of label transfer reagents. While a variety of LTRs was explored, including very different labeling and purification schemes, we were unable to find labeling efficiency that surpassed that found by LTR **1**, described in depth in chapter 1. To date, we have not succeeded in demonstrating that the

LTR strategy can be applied to other kinases. However, our attempts to create LTRs for other kinases have only been preliminary, and we expect that this strategy will be broadly useful. Our attempts to use LTRs to answer biologically important questions have thus far also been hampered by the very weak nature of the interactions we have probed. We are currently collaborating with another lab to use our LTRs to probe the interactions between p38 and its non-cannonical activator TAB-1.

Methods

A. Synthesis

Unless otherwise noted, all reagents were obtained from commercial suppliers and used without further purification. ^{1}H-NMR spectra were obtained on a Bruker DRX-499 or AV500 instrument at room temperature. Chemical shifts are reported in ppm, and coupling constants are reported in Hz. Mass spectrometry was performed on a Bruker Esquire Ion Trap MS instrument.

General HPLC Purification Conditions: Preparatory reverse-phase C18 column (250 x 21 mm), Acetonitrile/Water–0.1% CF_3CO_2H gradient: 1:99 to 100:0 over 60 min; 8 mL/min; 254 nm detection for 65 min.

General Analytical HPLC Conditions: C18 column (250 x 4.6 mm), Acetonitrile/Water-0.1%

CF_3CO_2H gradient: 1:99 to 100:0 over 40 min. Methanol/Water–0.1% CF_3CO_2H gradient: 1:99 to 100:0 over 30 or 40 min. Flow rate = 1 mL/min; 220 and 254 nM detection for 45 min.

General Information: See General Information section of methods for chapter 1.

[1A-5A]: 0.08 mmol of *O*-Bis(aminoethyl)ethylene glycol trityl resin was swelled in ~ 1 mL CH_2Cl_2, and washed with CH_2Cl_2 and DMF. A solution of Fmoc-benzoylphenylalanine (98 mg, 0.2 mmol) or Fmoc-DOPA(acetonide)-OH (91.9 mg, 0.2 mmol), HOBt (31 mg, 0.2 mmol), and DIC (31 μL, 0.2 mmol) was added to the filtered resin. The reaction mixture was twirled ~24h. The Fmoc group was removed (2 treatements with 25% piperidine in DMF for 25 min each), and the resin was filtered and washed with DMF. Next, a solution of HOBt (31 mg, 0.2 mmol), DIC (31 μL, 0.2 mmol), and either 5-hexynoic acid (22 μL, 0.2 mmol), hexylchloride acid **1C** (68 mg, 0.2 mmol), chloropyrimidine acid **1D** (75 mg, 0.2 mmol), or Fmoc-Ahx-OH (70.7 mg, 0.2 mmol) in DMF was added to the resin. The reaction mixture was twirled for ~24 hrs. (In the case of **5A**, the Fmoc group was then removed (2 treatements with 25% piperidine in DMF for 25 min each), and the resin was filtered and washed with DMF. Next, a solution of HOBt (31 mg, 0.2 mmol), DIC (31 μL, 0.2 mmol), and biotin (49 mg, 0.2 mmol) was added to the resin and twirled for ~24 hrs, then treated as the other reactions). The reactions were drained and washed sequentially with DMF, CH_2Cl_2, MeOH, and CH_2Cl_2. 1 mL of cleavage cocktail (95% TFA, 2.5 % H_2O, 2.5% TIS) was added and incubated for 1 hr. The resin was then drained, washed with CH_2Cl_2, and resubjected to cleavage cocktail for 10 min, then washed with CH_2Cl_2. Elutions were

concentrated and purified by HPLC, using General HPLC Purification (see above). Compound data: **1A:** See methods section of chapter 1. **2A:** obtained 11.3 mg (20% yield) of pure product. Calc'd for $C_{37}H_{35}ClN_4O_8$ ($M+H^+$): 719.4; found 719.5. **3A:** obtained 49.5 mg (92% yield) product, verified by MS. **4A:** Obtained product, 27.3 mg (45% yield). Calc'd for $C_{30}H_{51}ClN_4O_9$ ($M+H^+$): 646.3; found 647. **5A:** verified identity by MS.

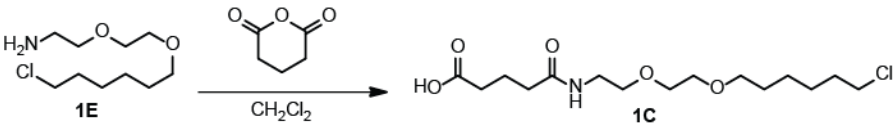

[1B]: 1E was synthesized as previously reported.[10] **1E** (754 mg, 2.23 mmol) and DIPEA (1.2 mL, 6.69 mmol) were added to 12 mL of CH_2Cl_2. Glutaric anhydride (254 mg, 2.23 mmol) was then added and the mixture was stirred overnight at room temperature. Subsequently, more DIPEA (776 μL, 4.46 mmol) and glutaric anhydride (50.9 mg, 0.446 mmol) were added and the mixture was stirred overnight. The reaction was concentrated *in vacuo*, dissolved in EtOAc/1 M HCl, and washed with 1 M HCl (3×) and brine (1×) before being dried over Na_2SO_4. Solvent was evaporated to give 754 mg of pure product (100% yield). ^{1}H NMR (500 MHz, $CDCl_3$) δ 3.65 (s, 4H), 3.60 – 3.47 (m, 8H), 2.46 (dt, *J* = 12.3, 7.0 Hz, 4H), 2.01 (p, *J* = 7.0 Hz, 2H), 1.82 – 1.74 (m, 2H), 1.68 – 1.60 (m, 2H), 1.51 – 1.43 (m, 2H), 1.42 – 1.34 (m, 2H). Calc'd for $C_{15}H_{29}ClNO_5$ $(M+H)^+$: 338.2; found 338.4.

[1D]: 1D was synthesized as previously described.[47]

[1]: 1 is described in chapter 1 (see compound **1**).

[2]: 1F (5 mg, 0.011mmol), **2A** (10.4 mg, 0.013 mmol), DIPEA (8 µL, 0.046 mmol), HOBt (2.0 mg, 0.013 mmol), and EDCI (2.4 mg, 0.013 mmol) were combined in 57 µL of DMF and stirred at room temperature for ~48 hrs. The crude reaction was taken up in MeOH/H_2O and purified using General HPLC Purification (see above), providing 1.04 mg of pure product. ^{1}H NMR (500 MHz, MeOD) δ 9.72 (s, 1H), 8.27 (s, 1H), 7.98 (s, 1H), 7.94 (s, 1H), 7.90 – 7.86 (m, 1H), 7.80 (s, 2H), 7.72 – 7.64 (m, 5H), 7.64 – 7.59 (m, 1H), 7.50 (t, *J* = 7.3 Hz, 4H), 7.40 (d, *J* = 8.2 Hz, 2H), 4.71 – 4.66 (m, 1H), 3.77 – 3.59 (m, 16H), 3.58 – 3.48 (m, 8H), 3.46 – 3.41 (m, 2H), 3.17 (s, 1H), 2.99 – 2.95 (m, 1H), 2.85 – 2.82 (m, 1H), 2.35 (s,3H), 2.21 – 2.13 (m, 5H), 2.08 (td, *J* = 7.2, 2.4 Hz, 2H), 1.80 – 1.68 (m, 4H), 1.49 (m, 4H), 0.80 (m, 2H), 0.63 (m, 2H). Calc'd for $C_{55}H_{57}N_6O_7$ ($M+H^+$): 1138.5; found 1138.8.

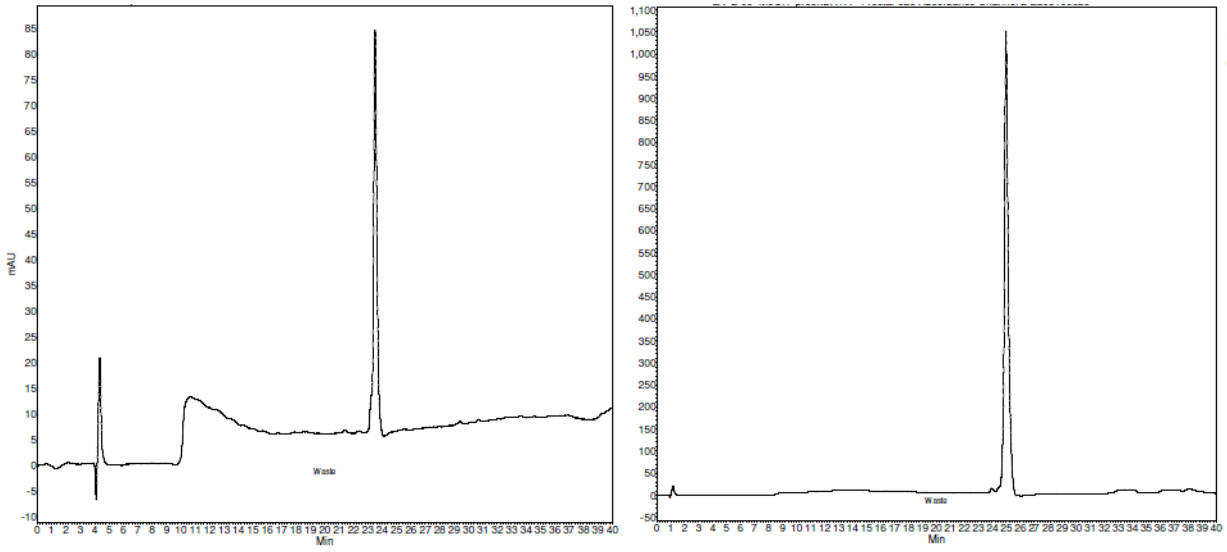

Figure 11: Analytical HPLC traces for **2**. (Acetonitrile – Right; MeOH – Left)

[3]: 1F (6.0 mg, 0.014mmol), **3A** (10.0 mg, 0.011 mmol), DIPEA (8 µL, 0.046 mmol), HOBt (2.3 mg, 0.015 mmol), and EDCI (2.8 mg, 0.015 mmol) were combined in 57 µL of DMF and stirred at room temperature for ~48 hrs. The crude reaction was taken up in MeOH/H_2O and purified using General HPLC Purification (see above), providing ~1 mg of pure product. ^{1}H NMR (500 MHz, Methanol-d4) δ 9.76 (s, 1H), 8.31 (s, 1H), 8.16 (t, *J* = 5.8 Hz, 1H), 8.02 (dd, *J* = 8.5, 1.7 Hz, 1H), 7.97 (s, 1H), 7.91 (d, *J* = 9.2 Hz, 1H), 7.85 – 7.81 (m, 2H), 7.74 – 7.66 (m, 5H), 7.63 (t, *J* = 7.5 Hz, 1H), 7.55 – 7.47 (m, 4H), 7.39 (dd, *J* = 22.1, 8.1 Hz, 4H), 7.26 (d, *J* = 8.0 Hz, 2H), 6.07 (s, 1H), 5.32 (s, 2H), 4.74 – 4.67 (m, 1H), 4.33 (s, 2H), 3.77 – 3.70 (m, 2H), 3.70 – 3.60 (m, 6H), 3.22 (dd, *J* = 14.1, 6.1 Hz, 1H), 2.99 (dd, *J* = 13.7, 9.2 Hz, 1H), 2.92 – 2.85 (m, 1H), 2.38 (s, 3H), 2.23 (t, *J* = 7.6 Hz, 2H), 2.18 (s, 3H), 2.15 (t, *J* = 7.5 Hz, 2H), 1.82 (p, *J* = 7.3 Hz, 2H), 0.83 (q, *J* = 7.0 Hz, 2H), 0.70 – 0.62 (m, 2H), 3.57 – 3.45 (m, 4H). Calc'd for $C_{66}H_{68}ClN_{10}O_9$ ($M+H^+$): 1179.5; found 1179.7.

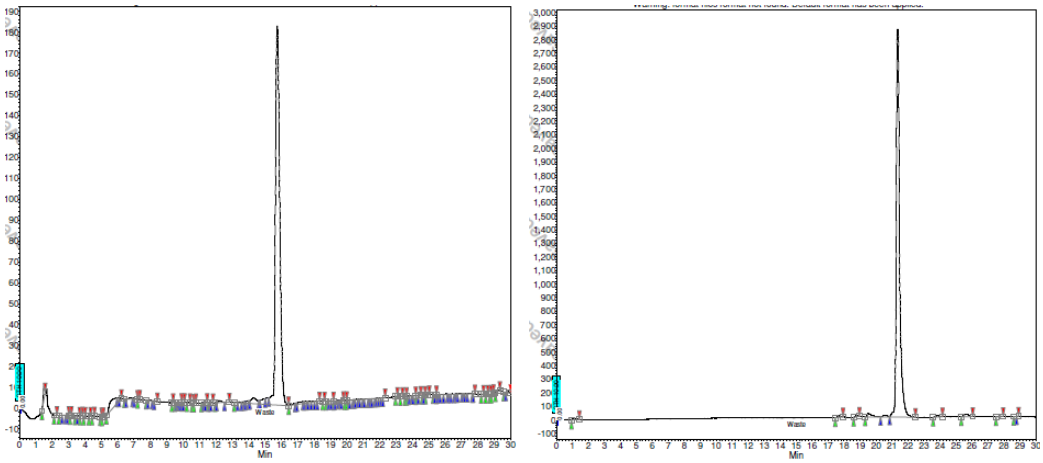

Figure 12: Analytical HPLC traces for **3**. (Acetonitrile – Right; MeOH – Left)

[4]: 1F (5.0 mg, 0.014mmol), **4A** (6.7 mg, 0.0088 mmol), DIPEA (6.1 μL, 0.035 mmol), HOBt (1.8 mg, 0.011 mmol), and EDCI (2.2 mg, 0.011 mmol) were combined in 57 μL of DMF and stirred at room temperature for 3 days. The crude reaction was taken up in MeOH/H_2O and purified using General HPLC Purification (see above), providing 2.82 mg of pure product. ^{1}H NMR (500 MHz, Methanol-d4) δ 9.98 (s, 1H), 8.51 (s, 1H), 8.23 (dd, *J* = 8.5, 1.6 Hz, 1H), 8.02 (s, 1H), 7.94 (dd, *J* = 17.3, 8.2 Hz, 2H), 7.88 – 7.82 (m, 2H), 7.63 (d, *J* = 8.0 Hz, 1H), 7.51 (d, *J* = 7.7 Hz, 1H), 6.68 – 6.63 (m, 2H), 6.54 (dd, *J* = 8.1, 2.0 Hz, 1H), 4.53 – 4.48 (m, 1H), 3.74 (t, *J* = 5.4 Hz, 2H), 3.68 (d, *J* = 4.1 Hz, 4H), 3.64 – 3.52 (m, 10H), 3.52 – 3.36 (m, 5H), 3.30 – 3.21 (m, 1H), 2.97 – 2.85 (m, 2H), 2.75 (dd, *J* = 13.7, 8.3 Hz, 1H), 2.40 (s, 3H), 2.25 (s, 5H), 2.20 (t, *J* = 7.4 Hz, 2H), 2.14 – 2.06 (m, 2H), 1.77 (ddd, *J* = 28.2, 14.6, 7.0 Hz, 4H), 1.58 (p, *J* = 14.4, 6.7 Hz, 2H), 1.42 (dt, *J* = 31.2, 7.9 Hz, 4H), 0.82 (dd, *J* = 7.1, 5.1 Hz, 2H), 0.69 – 0.63 (m, 2H). Calc'd for $C_{57}H_{73}ClN_7O_{11}$ ($M+H^+$): 1066.5; found 1067.0.

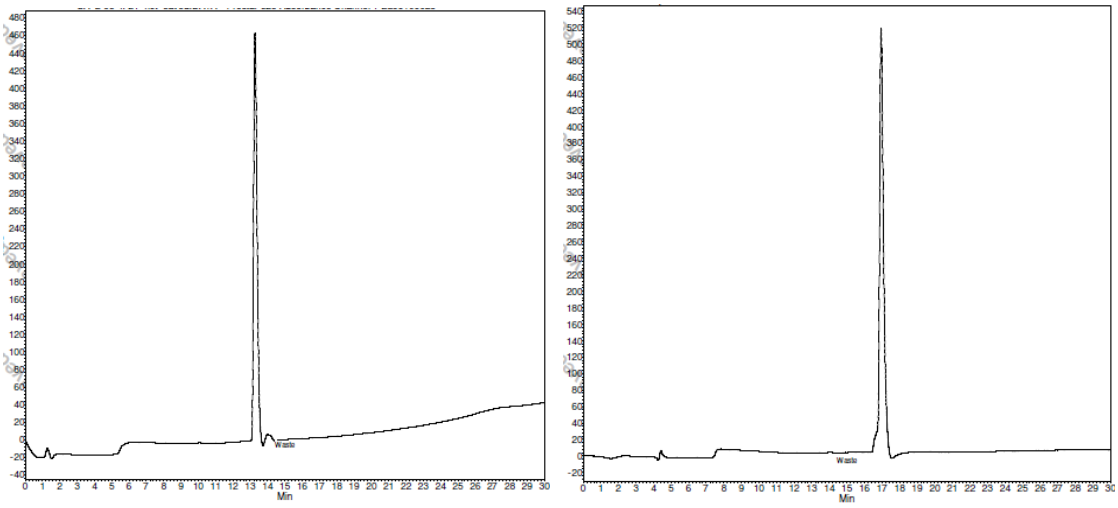

Figure 13: Analytical HPLC traces for **4**. (Acetonitrile – Right; MeOH – Left)

[5]: **1F** (6.8 mg, 0.014mmol), **5A** (7.6 mg, 0.011 mmol), DIPEA (8 µL, 0.046 mmol), HOBt (2.3 mg, 0.015 mmol), and EDCI (2.8 mg, 0.015 mmol) were combined in 57 µL of DMF and stirred at room temperature for 3 days. The crude reaction was taken up in MeOH/H_2O and purified using General HPLC Purification (see above), providing 0.41 mg of pure product. ^{1}H NMR (500 MHz, Methanol-d4) δ 9.76 (s, 1H), 8.31 (s, 1H), 8.16 (t, *J* = 5.8 Hz, 1H), 8.02 (dd, *J* = 8.5, 1.7 Hz, 1H), 7.97 (s, 1H), 7.91 (d, *J* = 9.2 Hz, 1H), 7.85 – 7.81 (m, 2H), 7.74 – 7.66 (m, 5H), 7.63 (t, *J* = 7.5 Hz, 1H), 7.55 – 7.47 (m, 4H), 7.39 (dd, *J* = 22.1, 8.1 Hz, 4H), 7.26 (d, *J* = 8.0 Hz, 2H), 6.07 (s, 1H), 5.32 (s, 2H), 4.74 – 4.67 (m, 1H), 4.33 (s, 2H), 3.77 – 3.70 (m, 2H), 3.70 – 3.60 (m, 6H), 3.22 (dd, *J* = 14.1, 6.1 Hz, 1H), 2.99 (dd, *J* = 13.7, 9.2 Hz, 1H), 2.92 – 2.85 (m, 1H), 2.38 (s, 3H), 2.23 (t, *J* = 7.6 Hz, 2H), 2.18 (s, 3H), 2.15 (t, *J* = 7.5 Hz, 2H), 1.82 (p, *J* = 7.3 Hz, 2H), 0.83 (q, *J* = 7.0 Hz, 2H), 0.70 – 0.62 (m, 2H), 3.57 – 3.45 (m, 4H). Calc'd for $C_{58}H_{72}N_9O_{10}S$ ($M+H^+$): 1086.5; found 1086.7.

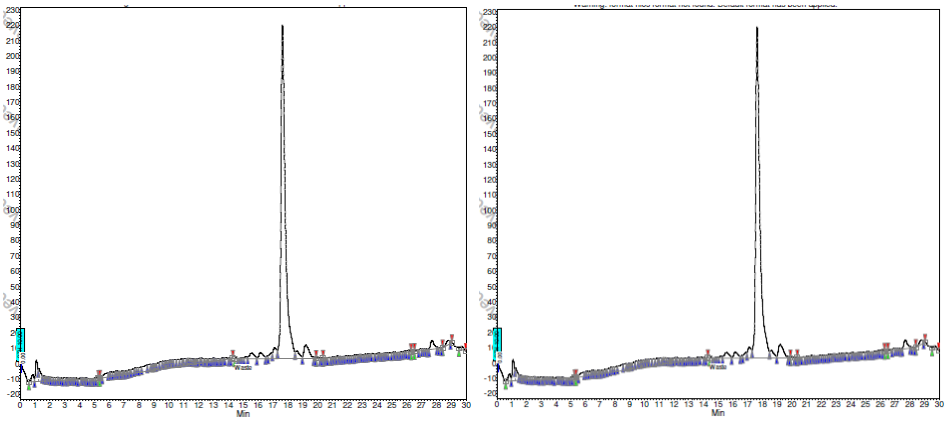

Figure 14: Analytical HPLC traces for **5**. (Acetonitrile – Right; MeOH – Left)

[6]: see methods section of chapter 1 (compound **2**)

[7A]: see methods section of chapter 1 (compound **2A**)

[7B]: was received from another lab member (Gayani Perera).

[7C]: 7A (237 mg, 0.669 mmol) was dissolved in 1.6 mL of a 1:1 THF:H_2O mixture, and received lithium hydroxide monohydrate (84.3 mg, 2.01 mmol) before being stirred overnight at room temperature. The THF was evaporated, and the remainder was acidified with HCl. The aqueous layer was extracted 3 times with EtOAc, then the organic layer was washed once with brine before being dried over Na_2SO_4 and evaporated to give ~100% yield. Deprotected **7A** (106 mg, 0.310 mmol), **7B** (84.5 mg, 0.280 mmol), DIPEA (244 μL, 1.40 mmol), HOBt (55.4 mg, 0.355 mmol), and EDCI (71.5 mg, 0.375 mmol) were combined in 1.4 mL of DMF and stirred at room temperature for 3 days. The reaction was taken up in EtOAc, and washed twice with saturated Na_2CO_3, twice with saturated NH_4Cl, and twice with brine before being dried over Na_2SO_4 and evaporated to give 119 mg of crude product.

[7D]: 7C (119 mg, 0.231 mmol) was diluted in 2.31 mL of 30% TFA in CH_2Cl_2 and stirred at room temperature for 3 hrs. Solvent was evaporated *in vacuo*. The product was then taken up in 300 μL DMF with DIPEA (108 μL, 0.619 mmol) and was mixed with 4-carboxybenzophenone (24.3 mg, 0.107 mmol), HOBt (16.7 mg, 0.107 mmol), and EDCI (20.5 mg, 0.107 mmol) for 4 days at room temperature. The reaction was taken up in EtOAc, and washed twice with saturated Na_2CO_3, twice with saturated NH_4Cl, and twice with brine before being dried over Na_2SO_4 and evaporated to give 46.0 mg of crude product. This was purified by flash chromatography (12g silica column, 5 min of 100% DCM, 5 min gradient to 1:99 MeOH:DCM, and a 20 min gradient

to 10:90 MeOH:DCM) to give 23.1 mg of pure product. This product was then taken up in 400 μL of 1:1 THF:H_2O with two drops of EtOH and received lithium hydroxide monohydrate (6 mg, 0.14 mmol) and was stirred overnight at room temperature. The reaction was then diluted with EtOAc, H_2O, and NaOH. The layers were separated, and the organic layer was extracted 4 times with 1 M NaOH. The aqueous layer was acidified with 5 M HCl, and then extracted 3 times with EtOAc. The combined organic layer was washed once with 10% citric acid, and once with brine before being dried over Na_2SO_4 and evaporated to give a crude solid. A large amount of citric acid was present, so the product was taken up in EtOAc and washed three times with NH_4Cl, dried over Na_2SO_4, and evaporated to give 15 mg of pure product.

[7E]: See methods section of chapter 1 (compound **2C**)

[7]: 7E (5.8 mg, 0.008 mmol), **7D** (7.1 mg, 0.012 mmol), DIPEA (7.0 μL, 0.040 mmol), HOBt (1.9 mg, 0.012 mmol), and EDCI (2.3 mg, 0.012 mmol) were combined in 80 μL of DMF and stirred at room temperature for 3 days. The crude reaction was taken up in MeOH/H_2O and purified using General HPLC Purification (see above), obtaining 1.27 mg of pure product. ^{1}H NMR (500 MHz, DMSO) δ 10.34 (s, 1H), 8.65 (s, 1H), 8.28 (d, *J* = 5.1 Hz, 1H), 7.98 (d, *J* = 8.4 Hz, 2H), 7.96 – 7.90 (m, 2H), 7.79 (m, 3H), 7.76 – 7.72 (m, 2H), 7.69 (d, *J* = 7.3 Hz, 1H), 7.57 (t, *J* = 7.6 Hz, 3H), 7.31 (d, *J* = 8.1 Hz, 1H), 7.21 (d, *J* = 21.2 Hz, 3H), 7.13 – 7.08 (m, 1H), 6.66 (s, 1H), 6.53 (s, 1H), 4.32 – 4.09 (m, 5H), 3.94 (s, 3H), 3.72 (m, 4H), 3.65 – 3.40 (m, 20H), 2.25 – 2.17 (m, 3H), 2.17 – 2.13 (m, 4H), 2.11 (dd, *J* = 6.6, 3.1 Hz, 2H), 1.70 – 1.58 (m, 4H), 1.57 – 1.40 (m, 4H), 1.40 – 1.30 (m, 2H). Calc'd for $C_{65}H_{79}N_{11}O_{11}$ ((M+2H$^+$)/2): 594.8; found 595.2.

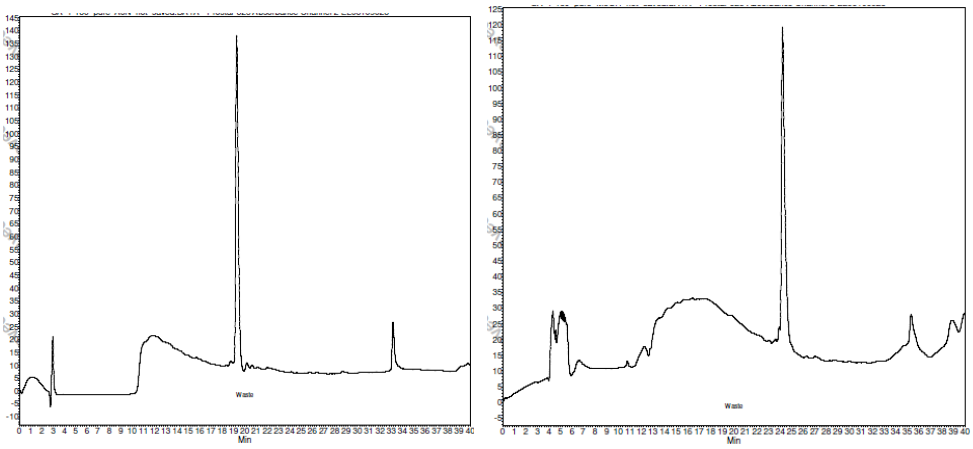

Figure 15: Analytical HPLC traces for **7**. (Acetonitrile – Right; MeOH – Left)

[8A]: The synthesis of **8A** has been reported previously.[43]

[8B]: See methods section of chapter 1 (compound **2B**)

[8]: 8A (5.9 mg, 0.007 mmol), **8B** (4.1 mg, 0.009 mmol), DIPEA (3.6 μL, 0.021 mmol), HOBt (1.4 mg, 0.009 mmol), and EDCI (1.7 mg, 0.009 mmol) were combined in 500 μL of DMF and stirred at room temperature overnight. The crude reaction was taken up in acetonitrile/H_2O and purified using General HPLC Purification (see above), obtaining 0.35 mg of pure product. ^{1}H NMR (300 MHz, MeOD) δ 8.35 (s, 1H), 8.25 (d, *J* = 5.5 Hz, 1H), 7.93 (d, *J* = 8.4 Hz, 2H), 7.88 (s, 1H), 7.84 – 7.73 (m, 5H), 7.67 – 7.62 (m, 2H), 7.60 – 7.49 (m, 3H), 7.36 (d, *J* = 8.5 Hz, 1H), 7.24 (s, 1H), 7.23 – 7.18 (m, 1H), 7.11 (d, *J* = 5.1 Hz, 1H), 4.80 (m, 1H), 4.32 (s, 2H), 4.03 (s, 3H), 3.84 – 3.77 (m, 4H), 3.71 – 3.50 (m, 20H), 3.37 (d, *J* = 4.9 Hz, 12H), 2.39 – 2.31 (m, 2H), 2.28 – 2.23 (m, 3H), 2.21 – 2.13 (m, 3H), 1.84 – 1.55 (m, 10H). Calc'd for $C_{69}H_{86}N_{11}O_{13}$ ((M+2H$^+$)/2): 638.9; found 639.1

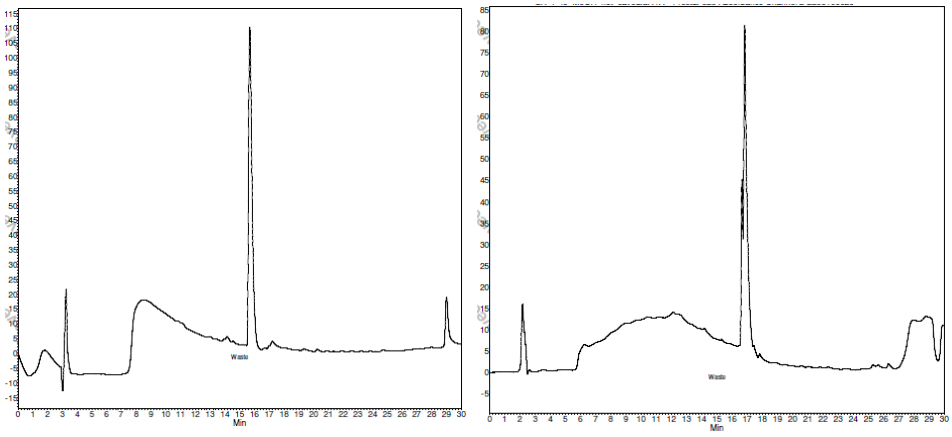

Figure 16: Analytical HPLC traces for **8**. (Acetonitrile – Right; MeOH – Left)

[10A]: 4-hydroxypiperidine (1.00 g, 9.89 mmol) was dissolved in 14 mL CH_2Cl_2. Di-tertbutyl-dicarbonate (boc anhydride, 2.16 g, 10.9 mmol) was added and the reaction was stirred at room temperature before concentration *in vacuo* to give 1.9 g (95% yield) of crude product. The product (1.00 g, 5.00 mmol) was transferred to a roundbottom flask and flushed with N_2. This then received 1.8 dry dioxane and NaH (98% pure, 167 mg, 5.70 mmol). After stirring the mixture for 1 hr at room temperature, the reaction was cooled to 0° C and 2-bromoacetate, ethyl ester (775 µL, 5.70 mmol) was added slowly. After stirring for 20 min on ice, the reaction was poured over ice and mixed with EtOAc and H_2O. The aqueous layer was removed and the organic layer was washed twice with H_2O, and once with brine before being dried over Na_2SO_4 and evaporated to give 1.3 g crude product. This was purified by flash chromatography (40g, silica, 100% hexanes to 100% EtOAc gradient over 15 min, then 100% EtOAc for 10 min), providing 184.6 mg of crude product. This product was then taken up in 14.2 mL of 30% TFA in CH_2Cl_2 and stirred at room temperature for 1.5 hrs before evaporation of solvent.

[10B]: Compound **10B** was synthesized as previously published.[64]

[10C]: 9A (381 mg, 2.03 mmol) was dissolved in 3.8 mL of acetonitrile and combined with **10B** (381 mg, 2.06 mmol) and DBU (910 μL, 6.08 mmol). The mixture was stirred at room temperature under N_2 for 3 days, then the solvent was evaporated. The reaction was taken up in EtOAc and H_2O, and the layers were separated. The aqueous layer was washed twice with EtOAc. The combined organic layer was washed twice with saturated NH_4Cl and once with brine before being dried over Na_2SO_4 and evaporated. Crude product was purified by flash chromatography (Silica, 100% hexanes to 100% EtOAc gradient) to give 363 mg (45% yield) of pure product.

[10D]: 10C (363 mg, 1.03 mmol) was dissolved in 30 mL of EtOH and flushed with H_2. Pd/C (103 mg, 10% (g/mmol)) was added and the flask was flushed with H_2 again; the reaction was stirred under H_2 overnight at room temperature. The reaction was filtered through celite, washing with MeOH. Crude product was purified by flash chromatography (40 g Silica, gradient from 100% hexanes to 100% EtOAc) to give 41.8 mg (12% yield) of pure product. ^{1}H NMR (300 MHz, Chloroform-d) δ 6.64 (d, *J* = 8.3 Hz, 1H), 6.52 (d, *J* = 2.4 Hz, 1H), 6.42 (dd, *J* = 8.4, 2.5 Hz, 1H), 4.23 (q, *J* = 7.1 Hz, 2H), 4.15 (s, 2H), 4.05 (q, *J* = 7.0 Hz, 2H), 3.63 – 3.46 (m, 2H), 3.42 – 3.30 (m, 2H), 2.84 – 2.70 (m, 2H), 2.10 – 1.97 (m, 2H), 1.88 – 1.74 (m, 2H), 1.43 (t, *J* = 7.0 Hz, 3H), 1.30 (t, *J* = 7.1 Hz, 3H). Calc'd for $C_{17}H_{26}N_2O_4$ ($M+H^+$): 323.2; found 323.5.

[10E]: 10E was synthesized as previously described.[52]

[**10]: 10D** (41.8 mg, 0.150 mmol), **10E** (41.0 mg, 0.150 mmol), X-Phos (4.7 mg, 0.010 mmol), $Pd_2(dba)_3$ (9.0 mg, 0.010 mmol), and K_2CO_3 (63 mg, 0.49 mmol) were combined in 1.5 mL of tBuOH and heated to 100° C for 4 hrs. The reaction was cooled and filtered through celite, washing with CH_2Cl_2, and the filtrate was evaporated to give 129 mg of crude product. This was purified first by flash chromatography (40g silica, 45 min gradient from 100% CH_2Cl_2 to 95% CH_2Cl_2, 3.75% MeOH, 1.25% Et_3N), then by HPLC using General HPLC Purification (see above), providing 17.7 mg (21% yield) of pure prodcut. ^{1}H NMR (500 MHz, Methanol-d4) δ 8.58 (d, *J* = 5.7 Hz, 1H), 8.34 (s, 1H), 7.76 (dd, *J* = 7.9, 1.8 Hz, 1H), 7.53 (ddd, *J* = 8.4, 7.3, 1.8 Hz, 1H), 7.26 (d, *J* = 8.6 Hz, 1H), 7.23 – 7.16 (m, 3H), 4.34 – 4.16 (m, 6H), 3.98 – 3.80 (m, 3H), 3.58 – 3.52 (m, 2H), 3.50 (s, 3H), 3.46 (s, 3H), 2.30 – 2.08 (m, 4H), 1.52 (t, *J* = 7.0 Hz, 3H), 1.30 (t, *J* = 7.1 Hz, 3H). Calc'd for $C_{30}H_{36}N_6O_5$ ($M+H^+$): 561.3; found 561.5.

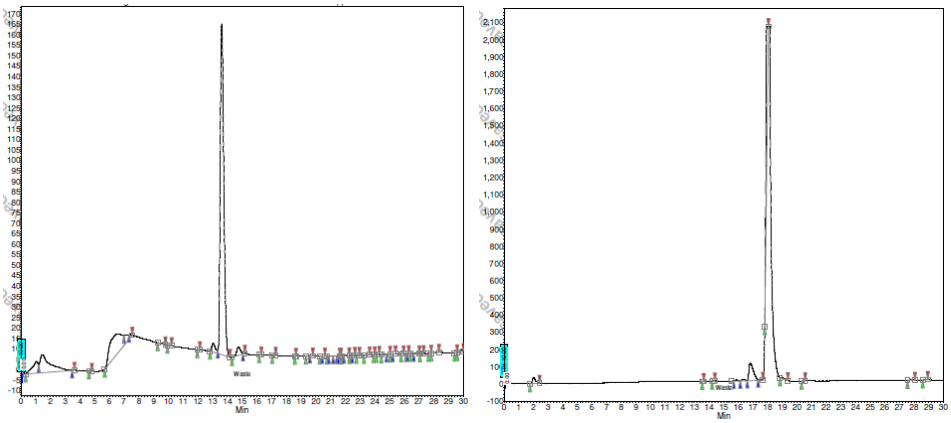

Figure 17: Analytical HPLC traces for **10**. (Acetonitrile – Right; MeOH – Left)

[11]: 10 (15.6 mg, 0.023 mmol) was dissolved in 230 µL of 1:1 THF:H_2O, and then received 3.2 mg of lithium hydroxide monohydrate. The reaction was stirred at room temperature for 3 hrs.

The reaction was evaporated and then purified by HPLC using General HPLC Purification (see above), obtaining 2.5 mg (20% yield) of pure product. This was taken up in 47 µL of DMF and combined with **1A** (4.2 mg, 0.007 mmol), DIPEA (3.3 µL, 0.019 mmol), HOBt (0.95 mg, 0.006 mmol), and EDCI (1.17 mg, 0.006 mmol). The reaction was stirred at room temperature for 3 days, then the crude reaction was taken up in acetonitrile/H_2O and purified using General HPLC Purification (see above), obtaining 1.27 mg (24.4% yield) of pure product. ^{1}H NMR (500 MHz, Methanol-d4) δ 8.25 (s, 1H), 8.13 (d, *J* = 8.1 Hz, 1H), 7.81 – 7.62 (m, 4H), 7.59 – 7.50 (m, 5H), 7.48 – 7.39 (m, 3H), 7.27 – 7.16 (m, 3H), 4.77 – 4.68 (m, 1H), 4.13 (q, *J* = 7.0 Hz, 2H), 4.05 (s, 2H), 3.73 – 3.55 (m, 11H), 3.55 – 3.39 (m, 12H), 3.27 – 3.22 (m, 1H), 3.06 – 2.91 (m, 1H), 2.38 – 2.28 (m, 2H), 2.27 – 2.20 (m, 3H), 2.12 – 2.02 (m, 4H), 1.75 – 1.68 (m, 2H), 1.45 (t, *J* = 7.0 Hz, 3H). Calc'd for $C_{56}H_{66}N_9O_9$ ($M+H^+$): 1008.5; found 1008.5.

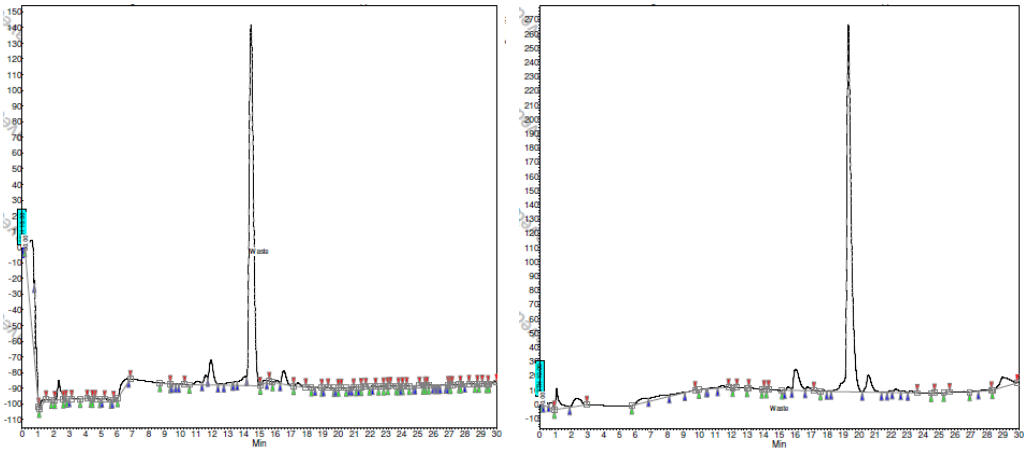

Figure 18: Analytical HPLC traces for **11**. (Acetonitrile – Right; MeOH – Left)

[12A]: Compound **12A** was received from a colleague (Ryan Murphy).

[12]: 12A (40 mg, 0.116 mmol) was mixed with diglycolic anhydride (16.2 mg, 0.139 mmol) and DIPEA (101 μL, 0.581 mmol) in 1.16 mL of CH_2Cl_2 and stirred 2 days at room temperature. The reaction was partitioned between CH_2Cl_2 and saturated Na_2CO_3. The aqueous layer was made acidic and extracted with CH_2Cl_2 before evaporation of the organic layer. This provided 33 mg (66% yield) of product. 11 μg (0.024 mmol) of this product was then combined with **1A** (17.4 mg, 0.029 mmol), DIPEA (12.5 μL, 0.072 mmol), HOBt (4.84 mg, 0.031 mmol), and EDCI (5.96 mg, 0.031 mmol) in 65 μL of DMF and stirred at room temperature for 3 days. The reaction was taken up in MeOH/H_2O and purified with General HPLC Procedure (see above). Found 0.70 mg of pure product. ^{1}H NMR (500 MHz, Methanol-d4) δ 8.32 (s, 1H), 8.10 (dd, *J* = 6.8, 2.5 Hz, 1H), 8.04 (d, *J* = 7.9 Hz, 1H), 7.84 (d, *J* = 7.7 Hz, 1H), 7.81 – 7.64 (m, 6H), 7.62 – 7.58 (m, 1H), 7.58 – 7.50 (m, 4H), 7.50 – 7.39 (m, 2H), 4.77 – 4.67 (m, 1H), 4.53 – 4.38 (m, 2H), 4.09 (s, 2H), 3.76 – 3.41 (m, 15H), 3.25 (d, *J* = 6.5 Hz, 1H), 3.15 (s, 0H), 3.07 – 2.95 (m, 3H), 2.40 – 2.28 (m, 2H), 2.28 – 2.17 (m, 5H), 2.15 – 2.02 (m, 2H), 1.76 – 1.68 (m, 2H). Calc'd for $C_{52}H_{58}N_9O_8$ ($M+H^+$): 936.4; found 936.7.

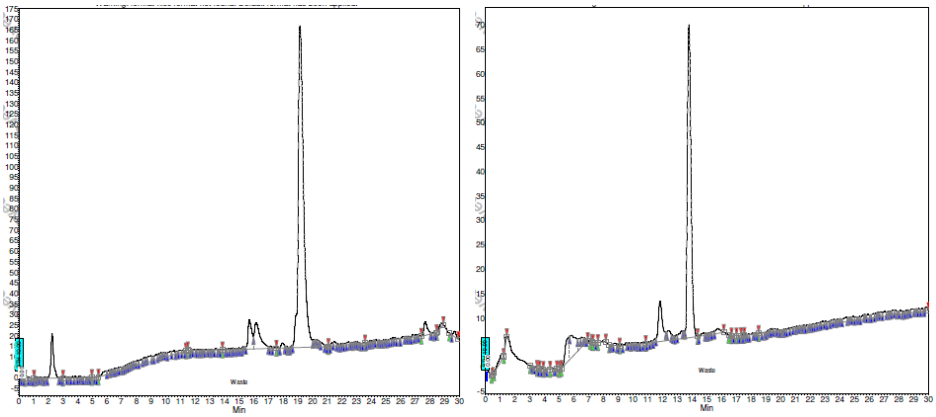

Figure 19: Analytical HPLC traces for **11**. (Acetonitrile – Right; MeOH – Left)

NA-PP1 was synthesized as previously published.[65]

[13]: See methods section of chapter 1 (compound **4**)

[14]: See compound **1** of chapter 3. Synthesis has been previously described.[43]

[15]: See compound **9**, chapter 1.

[16]: See compound **7**, chapter 1.

2. Biological Experiments

General Click Chemistry Conditions. 1.1 μL of 2.5 mM azide, 1.1 μL of fresh 50 mM TCEP in H_2O, 3.3 μL of 1.7 mM TBTA in 1:4 DMSO:tBuOH, and 1.1 μL fresh 50 mM $CuSO_4$ in H_2O were added to each 50 μL reaction after irradiation. The reactions were incubated for 1 hr at room temperature.

Fig 2a: p38 (400 nM final) was diluted in PBS and HeLa lysate (0.5 or 7.5 mg/mL final, total volume 100 μL) with either competitor **13** (10 μM final) or an equivalent volume of DMSO and incubated for 5 min at room temperature. All reactions then received **2** (2 μM final) and incubated at room temperature another 5 min before being placed on ice under a UV lamp (365 nm) for 30 min. 20 μL of each reaction was removed and incubated with ASH (0.37 mg/mL final) for 1 hr at room temperature. Meanwhile, ASH beads were prepared: 65 μL of

chloropyrimidine beads[11] were incubated for 1 hr at room temperature with a solution of 0.6 mg/mL ASH, 1 mM DTT before being washed with four 5-min washes of PBST. The remainder of each reaction was added to the ASH beads and twirled at room temperature 1 hr. Beads were then washed with 4 5-minute washes of PBS, and then eluted with 41 μL of elution buffer (30 μL of PBS, 10 μL of 10 units/ μL ULP1* protease, and 1 μL of 100 mM DTT), twirled at 30° C for 1 hr. The elution was supplemented by washing the beads with 40 μL of 3× SDS loading buffer. Samples were separated on 10% SDS-PAGE gels, transferred, and probed by anti-p38 western.

Fig 2c: HeLa cells from four 25-cm plates were collected and resuspended in 1 mL PBS before being sonicated and spun down (15 min, max speed, 4° C) to clear the lysate. By Bradford assay, the lysate was 6.5 mg/mL. This was split into two tubes; one received competitor **13** (10 μM final), and the other an equal volume of DMSO; these were twirled at room temperature for 10 min. Each received **2** (2 μM final) and was twirled for another 10 min at room temperature before being aliquoted at 100 μL/well into a round-bottom 96-well plate. The plate was place on ice, directly under a UV lamp (365 nm) for 30 min. ASH beads were prepared as above (4 μg ASH per μL chloropyrimidine beads, 1 mM DTT) and washed to remove excess ASH. After UV irradiation, samples were passed through PD-10 desalting columns, and fractions with high protein concentrations were combined. 25 μL of combined fractions were incubated with 5 μL of 1.6 mg/mL ASH for 1 hr to determine the extent of labeling; the remainder was and added to 40 μL of ASH beads. These were twirled at room temperature for 1 hr. 25 μL of each flow-through was collected and incubated with ASH (as above), and the beads were then washed with PBST (three 5-min washes, 0.5 mL each), high salt buffer (50 mM HEPES pH 7.4, 1 M NaCl, 0.1% Tween-20, two 5- min washes, once with 1 mL, once with 0.5 mL), and PBS (one 5-min wash,

0.5 mL). Elution was accomplished with 40 μL of elution buffer (31 μL PBS, 8 μL ULP1* protease (10 units/ μL), 2 mM DTT) incubating for 1 hr at 30° C, with occasional gentle mixing. The elution was supplemented by a 20 μL wash with 3× SDS loading buffer. Samples were separated on 10% SDS-PAGE, transferred, and probed by anti-p38 western.

Fig 3b: A solution of p38 (400 nM) and GST-AGT-MK2(370-400) (1 μM) with 1 mg/mL HEK293 lysate in PBS (total vol: 50 μL) received either competitor **13** (10 μM) or an equal volume of DMSO and was incubated at room temperature for 5 min. **2**, **3**, or **4** (1 μM) was added to each sample and incubated at room temperature for 5 min. Samples with benzophenone moieties were placed on ice under a UV lamp (365 nM) for 30 min. Samples with DOPA moieties were incubated with 1 mM sodium periodate for 5 min before quenching with 100 mM DTT. All reactions received ASH to 10 μM and were twirled at room temperature for 1 hr. Samples were run out on an SDS-PAGE gel, transferred, and probed by anti-p38 western.

Fig 3c: p38 (400 nM) and HEK293 lysate (0.2 mg/mL) were combined in PBS to a total volume of 50 μL. LTR **1** (500 nM) was added and samples were incubated another 5 min at room temperature. Samples were placed under a handheld UV light at 365 nm, while on ice, for 30 min. Meanwhile, ASH (1 μM) was incubated in ASH-labeling buffer (50 mM Tris buffer, pH 7.5, 100 mM NaCl, 0.1%

Tween 20 and 1 mM DTT) with benzylguanine-alkyne **14** for 1 hr at room temperature to produce ASH-alkyne. ASH-alkyne was added to the crosslinked sample to a final 50 nM concentration followed by general click chemistry conditions (see above) with biotin-azide **15**.

After the gels were scanned, they were transferred to nitrocellulose and probed with IRDye800-labeled streptavidin.

Fig 3d: ASH (2 μM, from 265 μM stock) and **4** (2 μM, from 100 μM stock) were incubated together for 1 hr at room temperature. Meanwhile, p38 (200 nM), MK2 (200 nM), HEK293 lysate (4.2 mg/mL) in PBS (final volume, 50 μL) received either **13** (10 μM) or an equal volume of DMSO and incubated at room temperature 10 min. **4** or the **4**-ASH (300 nM) combination prepared above was added to the samples and incubated at room temperature 10 min. Sodium periodate was then added to the indicated concentrations and incubated at room temperature for 5 min, and the reaction were stopped by addition of DTT to 100 mM. Reactions without preconjugated **4** received ASH to 1.5 μM and were incubated at room temperature for 1 hr. All samples were separated on 10% SDS-PAGE gels, transferred, and probed by anti-p38 or anti-MK2 western.

Fig 4b: Solutions of p38 (400 nM) and GST-AGT-MK2(370-400) (1 μM) with 1 mg/mL HEK293 lysate in PBS (total vol: 50 μL), with or without DTT (0.5 mM) received either competitor **13** (10 μM) or an equal volume of DMSO and were incubated at room temperature for 5 min. 1 μM of **5** was added to each sample and the samples were incubated at room temperature for 5 min. Samples were then incubated with 1 mM sodium periodate for 5 min before the reaction was quenched with 100 mM DTT. All reactions received ASH to 10 μM and were twirled at room temperature for 1 hr. Samples were run out on an SDS-PAGE gel, transferred, and probed by IRDye800-labeled streptavidin.

Figure 5: p38 (400 nM) and MK2 (400 nM) in PBS (50 μL final) were incubated with competitor **8A** (10 μM) or an equal volume of DMSO for 10 min. Indicated LTRs were added (to 2 μM) and samples were incubated for another 10 min. Samples were placed on ice under a UV lamp (365 nM) for 30 min, then subjected to general click chemistry conditions (see above) with rhodamine-azide **16**. After addition of loading buffer, samples were separated on a 10% SDS-PAGE gel.

Figure 6: Two 10-cm plates of HEK293 cells were grown to 95% confluency and transfected with two plasmids, 5 μg of each, using standard FuGENE-HD protocol. Plate 1 received flag-BMK1-pcDNA3.2 and flag-caMEK5-pcDNA3.2; plate 2 received p38-pDEST26-flag and flag-caMEK5-pcDNA3.2. Cells were grown for ~24 hrs after transfection, then pushed off the plate and spun down. Cells were resuspended in 1 mL mammalian cell lysis buffer (20 mM Tris-HCl pH 7.4, 150 mM NaCl, 1 mM EDTA, 1 mM EGTA, 1% Triton X-100, 2.5 mM sodium pyrophosphate, 1 mM sodium glycerophosphate, 1 mM PMSF, and protease inhibitor cocktail (Roche)) and lysed by sonication. Lysate was cleared by centrifugation (10 min at max speed at 4° C) and then added to 40 μL of anti-flag resin slurry (Sigma Aldrich) before being placed on an orbital shaker overnight at 4° C. Beads were then washed once with 500 μL PBS, and beads were transferred to a round-bottom 96-well plate. The beads from each lysate were split into two identical wells, such that the total volume (including beads) in each well was 50 μL. To one well, 0.5 μL of 1 mM inhibitor **10** was added to a final concentration of 10 μM, and an equal volume of DMSO was added to the other well. After 5 min, 1 μL of 100 μM LTR **11** was added to all wells and incubated at room temperature 15 min. The plate with samples was placed on ice, and a UV lamp (365 nm) was rested directly on it for 30 min, with plate agitations every 5 min to

keep the beads in suspension. Beads were transferred to microcentrifuge tubes, received 50 μL 0.2 mg/mL flag peptide in PBS, and were twirled for 5 min at room temperature. Supernatant was removed, and beads were eluted with an additional 2 aliquots of 50 μL of 0.1 mg/mL flag peptide in PBS (each also incubated for 5 min at room temperature). The eluate then received 20% SDS (to final concentration 1.8%), rhodamine-azide **16** (to final concentration 50 μM), TCEP (to final concentration 1 mM), TBTA (to final concentration 0.1 mM), and $CuSO_4$ (to final concentration 1 mM); the reaction was then incubated at room temperature for 1 hr. Click chemistry reactions then received 50 μg of BSA each and were subjected to MeOH/CHCl3 precipitation. Dried protein pellets were resuspended by boiling in 60 μL SDS loading buffer for 5 min. Samples were run on SDS-PAGE gels, scanned for fluorescence, transferred to nitrocellulose, and subjected to anti-flag western analysis.

Fig 8a: Indicated kinases (400 nM) and HeLa lysate (0.2 mg/mL) in PBS (50 μL final) were incubated with competitor **NA-PP1** (10 μM) or an equal volume of DMSO for 5 min. LTR **12** was added (to 500 nM) and samples were incubated for another 10 min. Samples were placed on ice under a UV lamp (365 nM) for 30 min, then subjected to general click chemistry conditions (see above) with rhodamine-azide **16**. After addition of loading buffer, samples were separated on a 10% SDS-PAGE gel.

Fig 8b: p38 (400 nM), or indicated MKKs (2 μM) with 0.2 mg/mL HeLa lysate in PBS (50 μL total volume) were incubated with competitor **NA-PP1** (10 μM) or an equal volume of DMSO for 5 min. LTR **12** was added (to 500 nM) and samples were incubated another 10 min. Samples were placed on ice under a UV lamp (365 nM) for 30 min, then subjected to general click

chemistry conditions (see above) with rhodamine-azide **16**. After addition of loading buffer, samples were separated on a 10% SDS-PAGE gel.

Fig 9a,b: COS-7 cells were grown in a 12-well plate in high-glucose DMEM with 10% FBS and streptomycin/penicillin to confluency. Cells were washed once with PBS, then incubated in 500 μL PBS, to which was added 2 μM compounds or an equal volume of DMSO before incubation at 37° C for 10 min. 100 μL of 5 M NaCl (500 mM final) were added to each well and the cells were incubated at 37° C for 30 min. PBS was aspirated, and cells were taken up in 60 μL of SDS loading buffer, boiled 10 min, and separated on SDS-PAGE gels, transferred, and probed with either anti-p38 or anti-phospho-p38 antibodies.

Figure 9c: Two 6-cm plates of HEK293 cells were grown to 95% confluency and transfected equally with two plasmids: eGFP-p38 and MK2-pDEST26flag, 1.5 μg of each, using standard FuGENE-HD protocol. Cells were grown ~24 hrs after transfection, and the medium was replaced with 1 mL fresh high-glucose DMEM with 10% FBS. Competitor **13** (10 μM) was added to one plate, and an equal volume of DMSO to the other, and the cells incubated at 37° C for 5 min. LTR **1** (2 μM) was added to both plates and they were again incubated at 37° C for 5 min. The plates were uncovered and placed in a 37° C incubator, with a UV lamp directly over them (365 nm) for 10 min. Cells were pushed off the plate and harvested, lysing in PBS with sonication. Cleared lysate then added to 40 μL of anti-flag resin slurry (Sigma Aldrich) before being placed on an orbital shaker overnight at 4° C. Beads were washed once with 500 μL of PBS, then eluted by with three 50 μL aliquots of 0.1 mg/mL flag peptide in PBS (5 min each aliquot). The eluate was then subjected to general click chemistry conditions with rhodamine-

azide **16**, followed by MeOH/$CHCl_3$ precipitation; the protein pellet was taken up in SDS loading buffer and separated on 10% SDS-PAGE gel, followed by transfer and an anti-GFP and anti-flag western.

Figure 10a: A 10-cm plates of HEK293 cells were grown to 95% confluency and transfected with 4 plasmids, with a 1:2:1:1 ratio of PKN1-pDEST26flag : MLTK-pcDNA3.2HA : MKK3-pDEST26HA : p38-DEST26HA. A total of 10 μg of DNA was used, diluted to 500 μL with Opti-MEM, and mixed with 20 μL of FuGENE-HD transfection reagent. After incubation at room temperature for 15 min, the mixture was added to the cells with fresh high-glucose DMEM with 10% FBS, and the cells were allowed to grow for another 24 hrs. Cells were resuspended in 1 mL mammalian cell lysis buffer (20 mM Tris-HCl pH 7.4, 150 mM NaCl, 1 mM EDTA, 1 mM EGTA, 1% Triton X-100, 2.5 mM sodium pyrophosphate, 1 mM sodium glycerophosphate, 1 mM PMSF, and protease inhibitor cocktail (Roche)) and lysed by sonication. Lysate was cleared by centrifugation (10 min at max speed at 4° C) and then added to 40 μL of anti-flag resin slurry (Sigma Aldrich) before being placed on an orbital shaker overnight at 4° C. Beads were then washed once with 500 μL PBS, and beads were transferred to a round-bottom 96-well plate. The beads from each lysate were split into two identical wells, such that the total volume (including beads) in each well was 50 μL. To one well, 0.5 μL of 1 mM inhibitor **13** was added to a final concentration of 10 μM, and an equal volume of DMSO was added to the other well. After 5 min, 1 μL of 100 μM LTR **1** was added to all wells and incubated at room temperature 15 min. The plate with samples was placed on ice, and a UV lamp (365 nm) was rested directly on it for 30 min, with plate agitations every 5 min to keep the beads in suspension. Beads were transferred to microcentrifuge tubes, then received 50 μL 0.2 mg/mL flag peptide in PBS, and were twirled

for 5 min at room temperature. Supernatant was removed, and beads were eluted with an additional 2 aliquots of 50 μL of 0.1 mg/mL flag peptide in PBS. The eluate then received 20% SDS (to final concentration 1.8%), rhodamine-azide **16** (to final concentration 50 μM), TCEP (to final concentration 1 mM), TBTA (to final concentration 0.1 mM), and $CuSO_4$ (to final concentration 1 mM) and was incubated at room temperature for 1 hr. Click chemistry reactions then received 50 μg of BSA each and were subjected to MeOH/$CHCl_3$ precipitation. Dried protein pellets were resuspended by boiling in 60 μL SDS loading buffer for 5 min. Samples were run on SDS-PAGE gels, scanned for fluorescence, transferred to nitrocellulose, and subjected to anti-flag or anti-HA western analysis.

Fig 9b: Experiment was identical to Fig 9a, but with the transfection was of two plates with the following plasmids: a 1:2:1:1 ratio of PKN:MLTK:MKK6:p38, using PKN-pDEST26HA, MLTK-pcDNA3.2HA, MKK6-pDEST26HA, and p38-pDEST26flag or p38-pDEST26HA.

References

1. Manning, G., Whyte, D. B., Martinez, R., Hunter, T., and Sudarsanam, S. (2002) The protein kinase complement of the human genome, *Science 298*, 1912-1934.

2. Whitmarsh, A. J. (2006) The JIP family of MAPK scaffold proteins, *Biochem Soc Trans 34*, 828-832.

3. Skroblin, P., Grossmann, S., Schafer, G., Rosenthal, W., and Klussmann, E. Mechanisms of protein kinase a anchoring, *Int Rev Cell Mol Biol 283*, 235-330.

4. Cuadrado, A., and Nebreda, A. R. Mechanisms and functions of p38 MAPK signalling, *Biochem J 429*, 403-417.

5. Ge, B., Gram, H., Di Padova, F., Huang, B., New, L., Ulevitch, R. J., Luo, Y., and Han, J. (2002) MAPKK-independent activation of p38alpha mediated by TAB1-dependent autophosphorylation of p38alpha, *Science 295*, 1291-1294.

6. Lu, G., Kang, Y. J., Han, J., Herschman, H. R., Stefani, E., and Wang, Y. (2006) TAB-1 modulates intracellular localization of p38 MAP kinase and downstream signaling, *J Biol Chem 281*, 6087-6095.

7. Ferreiro, I., Joaquin, M., Islam, A., Gomez-Lopez, G., Barragan, M., Lombardia, L., Dominguez, O., Pisano, D. G., Lopez-Bigas, N., Nebreda, A. R., and Posas, F. Whole genome analysis of p38 SAPK-mediated gene expression upon stress, *BMC Genomics 11*, 144.

8. Wu, R., Kausar, H., Johnson, P., Montoya-Durango, D. E., Merchant, M., and Rane, M. J. (2007) Hsp27 regulates Akt activation and polymorphonuclear leukocyte apoptosis by scaffolding MK2 to Akt signal complex, *J Biol Chem 282*, 21598-21608.

9. Dorman, G., and Prestwich, G. D. (1994) Benzophenone photophores in biochemistry, *Biochemistry 33*, 5661-5673.

10. Rostovtsev, V. V., Green, L. G., Fokin, V. V., and Sharpless, K. B. (2002) A stepwise huisgen cycloaddition process: copper(I)-catalyzed regioselective "ligation" of azides and terminal alkynes, *Angew Chem Int Ed Engl 41*, 2596-2599.

11. Herberich, B., Cao, G. Q., Chakrabarti, P. P., Falsey, J. R., Pettus, L., Rzasa, R. M., Reed, A. B., Reichelt, A., Sham, K., Thaman, M., Wurz, R. P., Xu, S., Zhang, D., Hsieh, F., Lee, M. R., Syed, R., Li, V., Grosfeld, D., Plant, M. H., Henkle, B., Sherman, L., Middleton, S., Wong, L. M., and Tasker, A. S. (2008) Discovery of highly selective and potent p38 inhibitors based on a phthalazine scaffold, *J Med Chem 51*, 6271-6279.

12. Sullivan, J. E., Holdgate, G. A., Campbell, D., Timms, D., Gerhardt, S., Breed, J., Breeze, A. L., Bermingham, A., Pauptit, R. A., Norman, R. A., Embrey, K. J., Read, J., VanScyoc, W. S., and Ward, W. H. (2005) Prevention of MKK6-dependent activation by binding to p38alpha MAP kinase, *Biochemistry 44*, 16475-16490.

13. Karaman, M. W., Herrgard, S., Treiber, D. K., Gallant, P., Atteridge, C. E., Campbell, B. T., Chan, K. W., Ciceri, P., Davis, M. I., Edeen, P. T., Faraoni, R., Floyd, M., Hunt, J. P., Lockhart, D. J., Milanov, Z. V., Morrison, M. J., Pallares, G., Patel, H. K., Pritchard, S., Wodicka, L. M., and Zarrinkar, P. P. (2008) A quantitative analysis of kinase inhibitor selectivity, *Nat Biotechnol 26*, 127-132.

14. ter Haar, E., Prabhakar, P., Liu, X., and Lepre, C. (2007) Crystal structure of the p38 alpha-MAPKAP kinase 2 heterodimer, *J Biol Chem 282*, 9733-9739.

15. Theodosiou, A., Smith, A., Gillieron, C., Arkinstall, S., and Ashworth, A. (1999) MKP5, a new member of the MAP kinase phosphatase family, which selectively dephosphorylates stress-activated kinases, *Oncogene 18*, 6981-6988.

16. Zhang, Y. Y., Wu, J. W., and Wang, Z. X. (2011) A distinct interaction mode revealed by the crystal structure of the kinase p38alpha with the MAPK binding domain of the phosphatase MKP5, *Sci Signal 4*, ra88.

17. Tanoue, T., Moriguchi, T., and Nishida, E. (1999) Molecular cloning and characterization of a novel dual specificity phosphatase, MKP-5, *J Biol Chem 274*, 19949-19956.

18. Szychowski, J., Mahdavi, A., Hodas, J. J., Bagert, J. D., Ngo, J. T., Landgraf, P., Dieterich, D. C., Schuman, E. M., and Tirrell, D. A. (2010) Cleavable biotin probes for labeling of biomolecules via azide-alkyne cycloaddition, *J Am Chem Soc 132*, 18351-18360.

19. Tasker, A. Z., Dawei; Pettus, Liping H.; Rzasa, Robert M.; Sham, Kelvin K. C.; Xu, Shimin; Chakrabarti, Partha Pratim (2008) Phthalazine, aza- and diaza-phthalazine compounds as protein kinase inhibitors and their preparation, pharmaceutical compositions and use in the treatment of protein kinase-mediated diseases.

20. Perera, B. G., and Maly, D. J. (2008) Design, synthesis and characterization of "clickable" 4-anilinoquinazoline kinase inhibitors, *Mol Biosyst 4*, 542-550.

21. Hsu, T. L., Hanson, S. R., Kishikawa, K., Wang, S. K., Sawa, M., and Wong, C. H. (2007) Alkynyl sugar analogs for the labeling and visualization of glycoconjugates in cells, *Proc Natl Acad Sci U S A 104*, 2614-2619.

22. Hintersteiner, M., Kimmerlin, T., Garavel, G., Schindler, T., Bauer, R., Meisner, N. C., Seifert, J. M., Uhl, V., and Auer, M. (2009) A highly potent and cellularly active beta-peptidic inhibitor of the p53/hDM2 interaction, *Chembiochem 10*, 994-998.

23. Szafranska, A. E., Luo, X., and Dalby, K. N. (2005) Following in vitro activation of mitogen-activated protein kinases by mass spectrometry and tryptic peptide analysis: purifying fully activated p38 mitogen-activated protein kinase alpha, *Anal Biochem 336*, 1-10.

24. Los, G. V., Encell, L. P., McDougall, M. G., Hartzell, D. D., Karassina, N., Zimprich, C., Wood, M. G., Learish, R., Ohana, R. F., Urh, M., Simpson, D., Mendez, J., Zimmerman, K., Otto, P., Vidugiris, G., Zhu, J., Darzins, A., Klaubert, D. H., Bulleit, R. F., and Wood, K. V. (2008) HaloTag: a novel protein labeling technology for cell imaging and protein analysis, *ACS Chem Biol 3*, 373-382.

25. Chidley, C., Mosiewicz, K., and Johnsson, K. (2008) A Designed Protein for the Specific and Covalent Heteroconjugation of Biomolecules, *Bioconjugate Chemistry 19*, 1753-1756.

26. Brigham, J., Perera, G., Maly, D. *Manuscript in preparation*.

27. Gronemeyer, T., Chidley, C., Juillerat, A., Heinis, C., and Johnsson, K. (2006) Directed evolution of O6-alkylguanine-DNA alkyltransferase for applications in protein labeling, pp 309-316.

28. Juillerat, A., Gronemeyer, T., Keppler, A., Gendreizig, S., Pick, H., Vogel, H., and Johnsson, K. (2003) Directed Evolution of O6-Alkylguanine-DNA Alkyltransferase for Efficient Labeling of Fusion Proteins with Small Molecules In Vivo, *Chemistry & biology 10*, 313-317.

29. Hill, Z. B., Perera, B. G., Andrews, S. S., and Maly, D. J. (2012) Targeting diverse signaling interaction sites allows the rapid generation of bivalent kinase inhibitors, *ACS Chem Biol 7*, 487-495.

30. Liu, B., Burdine, L., and Kodadek, T. (2006) Chemistry of periodate-mediated cross-linking of 3,4-dihydroxylphenylalanine-containing molecules to proteins, *J Am Chem Soc 128*, 15228-15235.

31. Hayashi, M., and Lee, J. D. (2004) Role of the BMK1/ERK5 signaling pathway: lessons from knockout mice, *J Mol Med (Berl) 82*, 800-808.

32. Yang, Q., Deng, X., Lu, B., Cameron, M., Fearns, C., Patricelli, M. P., Yates, J. R., 3rd, Gray, N. S., and Lee, J. D. (2010) Pharmacological inhibition of BMK1 suppresses tumor growth through promyelocytic leukemia protein, *Cancer Cell 18*, 258-267.

33. Cameron, S. J., Abe, J., Malik, S., Che, W., and Yang, J. (2004) Differential role of MEK5alpha and MEK5beta in BMK1/ERK5 activation, *J Biol Chem 279*, 1506-1512.

34. Deng, X., Yang, Q., Kwiatkowski, N., Sim, T., McDermott, U., Settleman, J. E., Lee, J. D., and Gray, N. S. (2011) Discovery of a benzo[e]pyrimido-[5,4-b][1,4]diazepin-6(11H)-one as a Potent and Selective Inhibitor of Big MAP Kinase 1, *ACS Med Chem Lett 2*, 195-200.

35. Bishop, A. C., Ubersax, J. A., Petsch, D. T., Matheos, D. P., Gray, N. S., Blethrow, J., Shimizu, E., Tsien, J. Z., Schultz, P. G., Rose, M. D., Wood, J. L., Morgan, D. O., and Shokat, K. M. (2000) A chemical switch for inhibitor-sensitive alleles of any protein kinase, *Nature 407*, 395-401.

36. Bishop, A. C., Buzko, O., and Shokat, K. M. (2001) Magic bullets for protein kinases, *Trends Cell Biol 11*, 167-172.

37. Carroll, A. S., Bishop, A. C., DeRisi, J. L., Shokat, K. M., and O'Shea, E. K. (2001) Chemical inhibition of the Pho85 cyclin-dependent kinase reveals a role in the environmental stress response, *Proc Natl Acad Sci U S A 98*, 12578-12583.

38. Fan, Q. W., Specht, K. M., Zhang, C., Goldenberg, D. D., Shokat, K. M., and Weiss, W. A. (2003) Combinatorial efficacy achieved through two-point blockade within a signaling pathway-a chemical genetic approach, *Cancer Res 63*, 8930-8938.

39. Fan, Q. W., Zhang, C., Shokat, K. M., and Weiss, W. A. (2002) Chemical genetic blockade of transformation reveals dependence on aberrant oncogenic signaling, *Curr Biol 12*, 1386-1394.

40. Niswender, C. M., Ishihara, R. W., Judge, L. M., Zhang, C., Shokat, K. M., and McKnight, G. S. (2002) Protein engineering of protein kinase A catalytic subunits results in the acquisition of novel inhibitor sensitivity, *J Biol Chem 277*, 28916-28922.

41. Hindley, A. D., Park, S., Wang, L., Shah, K., Wang, Y., Hu, X., Shokat, K. M., Kolch, W., Sedivy, J. M., and Yeung, K. C. (2004) Engineering the serine/threonine protein kinase Raf-1 to utilise an orthogonal analogue of ATP substituted at the N6 position, *FEBS Lett 556*, 26-34.

42. Endo, S., Satoh, Y., Shah, K., and Takishima, K. (2006) A single amino-acid change in ERK1/2 makes the enzyme susceptible to PP1 derivatives, *Biochem Biophys Res Commun 341*, 261-265.

43. Ventura, J. J., Hubner, A., Zhang, C., Flavell, R. A., Shokat, K. M., and Davis, R. J. (2006) Chemical genetic analysis of the time course of signal transduction by JNK, *Mol Cell 21*, 701-710.

44. Bain, J., Plater, L., Elliott, M., Shpiro, N., Hastie, C. J., McLauchlan, H., Klevernic, I., Arthur, J. S., Alessi, D. R., and Cohen, P. (2007) The selectivity of protein kinase inhibitors: a further update, *Biochem J 408*, 297-315.

45. Cariolato, L., Cavin, S., and Diviani, D. A-kinase anchoring protein (AKAP)-Lbc anchors a PKN-based signaling complex involved in alpha1-adrenergic receptor-induced p38 activation, *J Biol Chem 286*, 7925-7937.

46. Baum, E. W., Emmittee, K.A., Kuntz, K.W., Mook, R.A., Nailor, K.E., Salovich, J.M., Shotwell, J.B., Smith, S.C., Stevens, K.L., Uehling, D.E., Waterson, A.G., Cheung, M., Moorthy, G.S., Wilson, B.J. (2010) Imidazopyridine Kinase Inhibitors, (Office, U. P., Ed.), GlaxoSmithKline LLC, USA.

47. Bishop, A. C., Kung, C., Shah, K., Witucki, L., Shokat, K., Liu, Y. (1999) Generation of Monospecific Nanomolar Tyrosine Kinase Inhibitors via a Chemical Genetic Approach, *J Am Chem Soc 121*, 627-631.

Chapter 3

Click chemistry optimization for protein labeling and recovery

Introduction

The desirability of bio-orthogonal conjugation reactions that are efficient in aqueous buffers at low concentrations has led to the development of various forms of "click chemistry" reactions.[1] In particular, copper (I)-mediated Huisgen cycloaddition reactions between alkynes and azides (or CuAAC for Cu-catalyzed azide-alkyne cycloaddition) has become popular due to its high efficiency, simplicity, and ease of synthesis of the necessary reagents.[2] The cycloaddition is catalyzed by Cu(I), which is usually generated *in situ* from Cu(II) by a reducing agent, such as sodium ascorbate or *tris*(2-carboxyethyl)phosphine (TCEP). This reaction has been used for labeling azide- and alkyne-containing proteins and other biomolecules, and has been suggested to be the best form of click chemistry when no live cells or organisms are involved.[3] The instability of copper in the reduced state in aqueous solution, as well as its propensity to create radicals which damage biomolecules, leads to a requirement for a suitable ligand to coordinate the copper. This ligand stabilizes the reduced copper and may also prevent the formation of oxidizing species.[4]

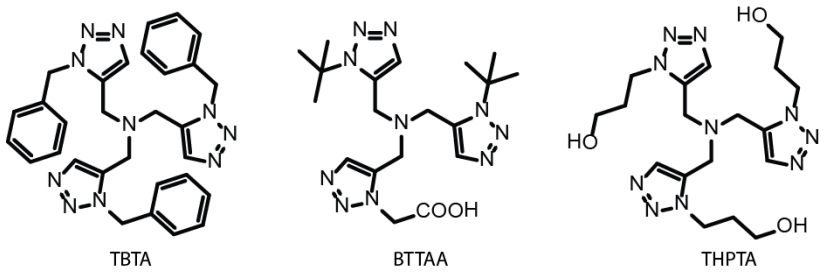

***Figure 1*:** Structures of the copper ligands discussed in this chapter.

The most commonly used ligand is tribenzyl triazole (TBTA) (Fig 1A).[5] This ligand has generally been observed to provide high efficiency under most conditions and is commercially available. However, it is only poorly soluble in water and therefore must be used at low concentrations (usually 0.1 mM, in the presence of 1 mM $CuSO_4$). The consequence of this is that proteins often precipitate during the click chemistry reaction as a result of the oxidizing species formed.[6] This is obviously undesirable for applications that require folded proteins or in live cells. Additionally, there is some question as to whether the precipitated proteins are thus removed from solution before they have a chance to be labeled. THPTA and BTTAA are two of the ligands have been developed to date to circumvent this problem. THPTA (Fig 1), originally reported by Hong *et al*,[4] replaces the benzyl groups with propanol, yielding a water-soluble ligand reported to be highly efficient in click chemistry compared to TBTA, and does not cause protein precipitation. BTTAA (Fig 1), reported more recently by Besanceney-Webler *et al*,[7] contains a single carboxylic acid that provides an additional coordination site to the copper and imparts water solubility. This ligand also prevents protein precipitation, and has been used on live cells and even in live zebrafish embryos. It is not entirely clear why the water solubility of THPTA and BTTAA prevent protein precipitation, but it is probable that this simply enables the use of these ligands at much higher concentrations, usually at a 1:5 to 1:2 copper:ligand ratios. Thus, unlike with TBTA, water-soluble ligands can bind all the Cu (I) present. This permits the use of lower copper concentrations due to the higher stability of the Cu(I), and also act as an ever-present object for its reductive potential, soaking up reactive oxygen species.

In our investigations of label transfer reagents bearing alkyne tags, we sought to maximize the recovery of labeled proteins by click chemistry with a cleavable biotin-azide tag and streptavidin bead purification. Having observed that the presence of SDS in the click chemistry reaction with TBTA increased our recovery of labeled proteins, we were interested to see if water-soluble ligands that prevent protein precipitation would similarly increase yield. However, published work with THPTA and BTTAA focus on live-cell applications, and therefore are conducted at minimal $CuSO_4$ concentrations and under conditions that are less efficient for TBTA. Consequently, we desired to compare these three ligands under conditions in which they are maximally efficient for proteomic applications. Some kinetic work has been done with these click chemistry ligands, but these studies employ an azide- or alkyne-conjugated coumarin, a substantially different substrate from the alkynylated biological molecules of interest. Published work with labeling of proteins usually relies on incorporation of non-natural amino acids or sugars. Consequently, the precise fraction of protein that is alkyne- or azide-labeled is difficult to determine, and rates of reaction are generally relative. This makes it challenging to quantitate the fraction of alkyne- or azide-labeled proteins that are labeled under a given condition, or what fraction of labeled proteins is recovered from purification.

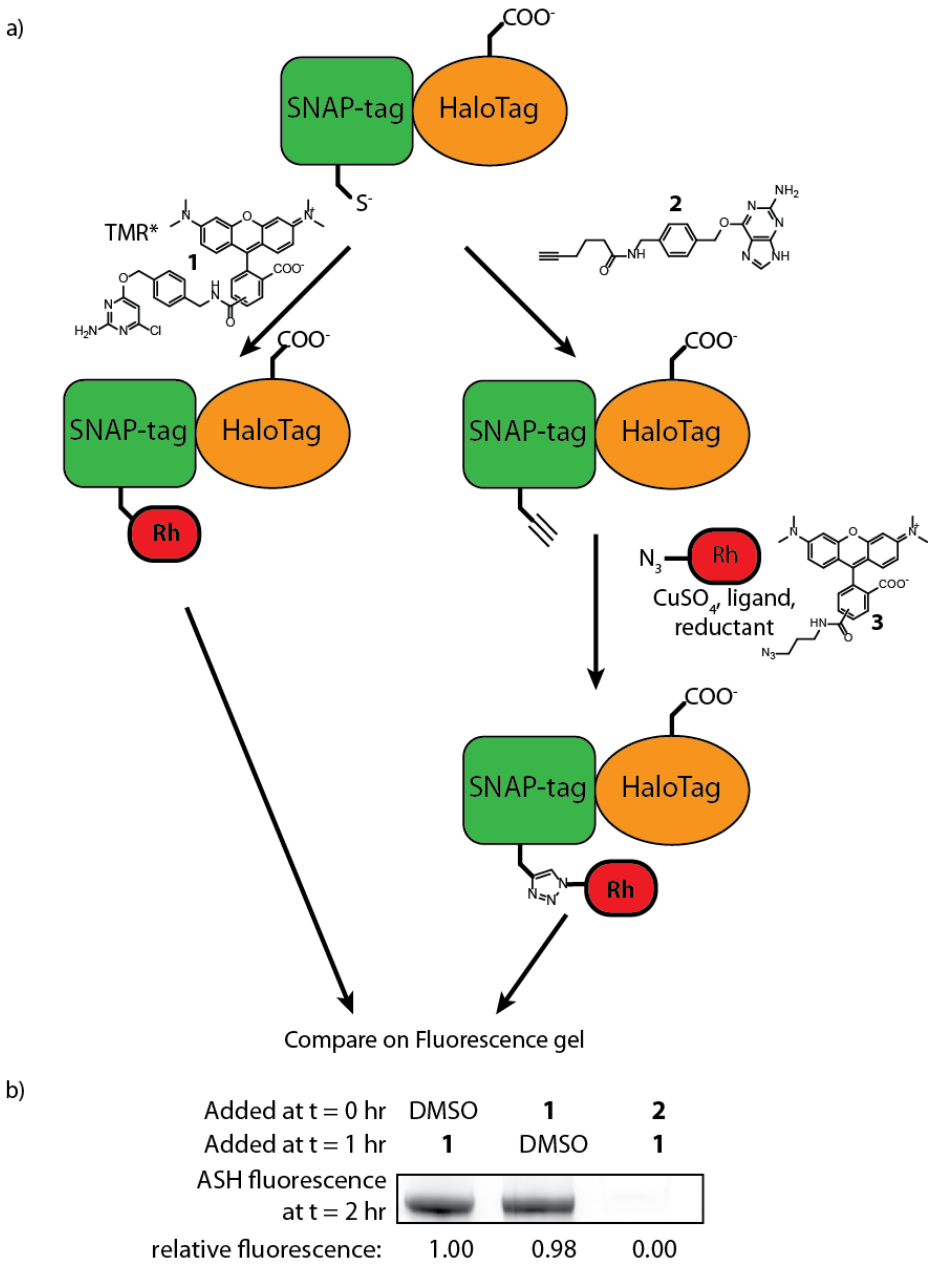

***Figure 2*:** Quantitation method. a) The SNAP-tag-Halo-tag fusion protein ASH can be incubated with benzylguanine-alkyne **2** to provide fully alkynylated protein; this can then be subjected to CuAAC with rhodamine-azide **3**. TMR* (compound **1**) incubated with ASH separately provides a signal for maximal labeling; comparison to rhodamine fluorescence from click chemistry permits calculation of the percentage of protein that is labeled under click chemistry conditions. b) The SNAP-tag site of ASH is fully occupied. ASH was incubated with DMSO, **1**, or **2** for one hour, then received an aliquot of DMSO or **1** and was incubated for another hour before being separated on a gel and scanned for fluorescence.

In order to obtain absolute quantitative data, rather than just relative rates, we have developed an assay based on self-labeling proteins (Fig 2). SNAP-tag and Halo-tag are two modified enzymes that have been developed to covalently and irreversibly self-label with small molecules. SNAP-tag, based on the DNA repair protein AGT, will covalently attach itself to any small molecule bearing a benzylguanine or chloropyrimidine moiety.[8,9] Similarly, Halo-tag self-labels with small molecules that contain a hexylchloride chain.[10] We have created a fusion in which these two proteins are connected by the protein SUMO, which we have called ASH (AGT-SUMO-Halo).[11] Both of these proteins can be labeled to greater than 99% when exposed to appropriately modified small molecules. By labeling ASH with **1**, we can observe the amount of fluorescence expected for 100% fluorophore-conjugated ASH. ASH can alternately labeled with benzylguanine-alkyne **2**. Alkyne-labeled ASH can then be tested under a variety of click chemistry conditions with rhodamine-azide **3**, and the percentage of the protein labeled by the click chemistry can be obtained by comparison to the **1**-labeled ASH. To confirm complete labeling of the SNAP-tag portion with alkyne, a portion of alkyne-labeled protein is set aside and then incubated with **1** (TMR*) (Figure 1b). Incubation of ASH with **2** fully occupies the active site of the SNAP-tag portion of ASH, preventing labeling by **1** when it is added subsequently.

Results and Discussion

We first carried out this quantitative analysis by varying the conditions used for TBTA (Fig 3). Given that a great deal of click chemistry on biological molecules is done in complex mixtures, where the protein of interest is a relatively small component of all biomolecules present, we have carried out our optimization in HEK293 lysate, with ASH-alkyne at only 38 nM. The most

common condition reported for CuAAC with TBTA (especially when it is to be subsequently used with streptavidin beads) includes 1% SDS in addition to the 1mM TCEP, 0.1 mM TBTA, and 1 mM $CuSO_4$. While we found the labeling efficiency was moderate under these conditions (39%, condition T1), omitting SDS gave substantially higher signal (66%, T4); a similar value was obtained by using 1% Triton X-100 in place of the SDS. While SDS in the click chemistry step has been reported to be important,[12,13] this has not generally been through a direct observation of the efficiency of biotinylation, but rather recovery from avidin/streptavidin beads after labeling. This suggests that the increased recovery of proteins seen with SDS in the click chemistry reaction is not due to an increase in labeling, and that Triton X-100 may be a better alternative to SDS if a detergent is required. Increasing the concentration of mammalian lysate in the reaction to 0.5 mg/mL had little effect on the efficiency of click chemistry with TBTA (T2); however, at 1 mg/mL, labeling efficiency was approximately halved (T3). This greatly impacts much work done on alkyne- or azide-tagged proteins in lysate, and suggests greater dilution than usual would improve CuAAC yield. While TCEP is the standard reducing agent used with TBTA, we sought to use sodium ascorbate instead, as it is reported to be preferred for BTTAA and THPTA. However, the labeling efficiency with TBTA in the presence of sodium ascorbate was much lower (T6), consistent with previous reports.[12] The usual order of addition of click chemistry reagents with TBTA is to add the reducing reagent and ligand to the alkyne/azide mixture first, and to add $CuSO_4$ last. THPTA and BTTAA, however, are usually premixed with $CuSO_4$ before addition to the alkyne/azide mixture, and the reducing agent is added last. We attempted, therefore, to premix the TBTA and $CuSO_4$, adding TCEP last; this resulted in equivalent signal, demonstrating the order of addition is of little consequence here (T7).

Unsurprisingly, we note that in the absence of a ligand, TBTA conditions give inefficient labeling (T8). BTTAA and THPTA have been used at much higher ligand:Cu ratios than for TBTA, but attempts to use these concentrations of TBTA resulted in a visible precipitate due to the insolubility of the ligand. Use of 2- or 4-fold higher concentrations of TBTA (0.2 and 0.4 mM) showed no visible precipitation of the ligand; however, they also did not increase labeling (T9-10). Aminoguanidine has been suggested as an additive for click chemistry to soak up reactive species, thus decreasing protein oxidation.[14] Its inclusion in TBTA click chemistry had little effect, and provided no visible decrease in protein precipitation. Consequently, it would appear that our original conditions used for TBTA (T1 or T4) provide the highest level of click chemistry labeling in the course of an hour.

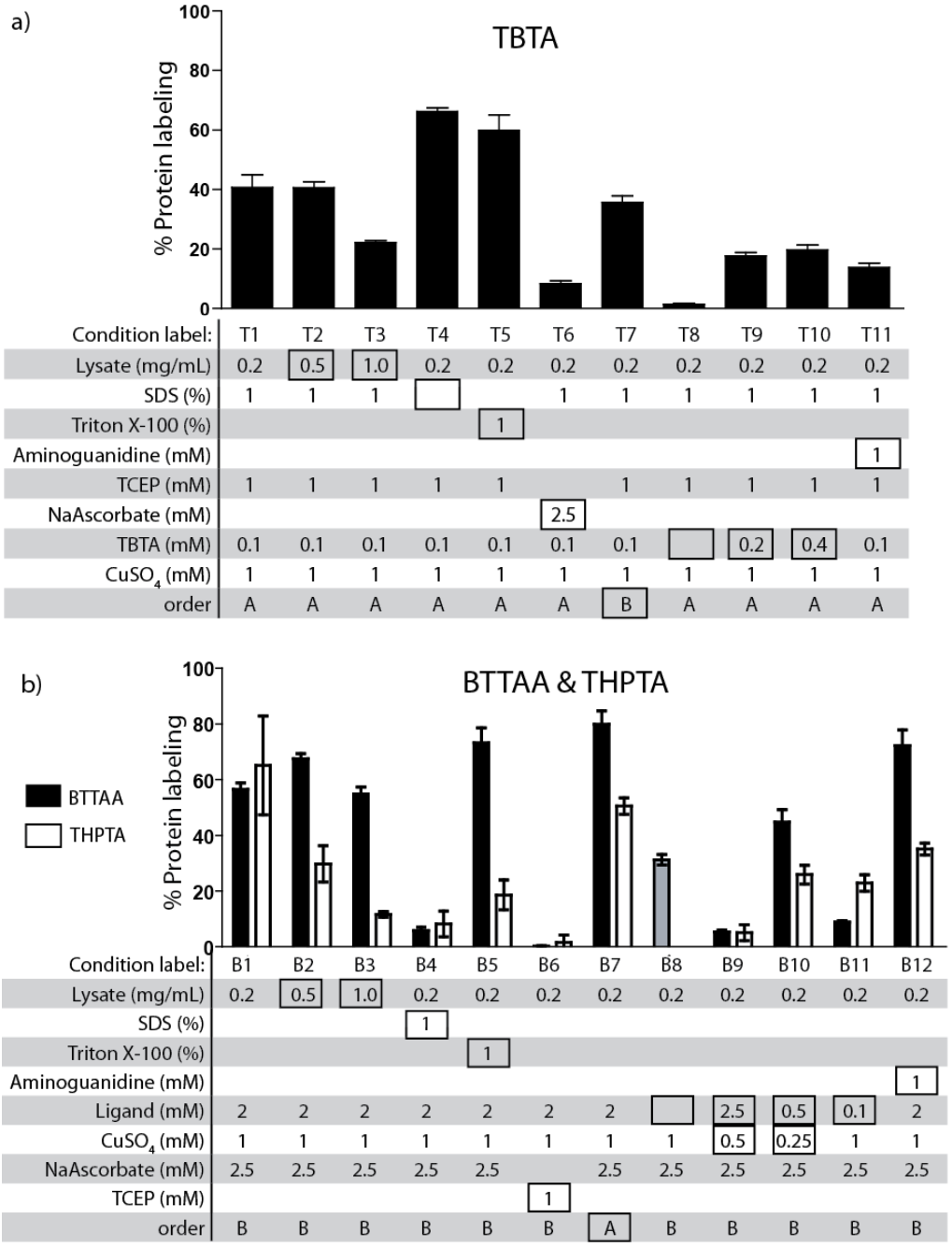

Condition label:	T1	T2	T3	T4	T5	T6	T7	T8	T9	T10	T11
Lysate (mg/mL)	0.2	0.5	1.0	0.2	0.2	0.2	0.2	0.2	0.2	0.2	0.2
SDS (%)	1	1	1			1	1	1	1	1	1
Triton X-100 (%)					1						
Aminoguanidine (mM)											1
TCEP (mM)	1	1	1	1	1		1	1	1	1	1
NaAscorbate (mM)						2.5					
TBTA (mM)	0.1	0.1	0.1	0.1	0.1	0.1	0.1		0.2	0.4	0.1
$CuSO_4$ (mM)	1	1	1	1	1	1	1	1	1	1	1
order	A	A	A	A	A	A	B	A	A	A	A

Condition label:	B1	B2	B3	B4	B5	B6	B7	B8	B9	B10	B11	B12
Lysate (mg/mL)	0.2	0.5	1.0	0.2	0.2	0.2	0.2	0.2	0.2	0.2	0.2	0.2
SDS (%)				1								
Triton X-100 (%)					1							
Aminoguanidine (mM)												1
Ligand (mM)	2	2	2	2	2	2	2		2.5	0.5	0.1	2
$CuSO_4$ (mM)	1	1	1	1	1	1	1	1	0.5	0.25	1	1
NaAscorbate (mM)	2.5	2.5	2.5	2.5	2.5		2.5	2.5	2.5	2.5	2.5	2.5
TCEP (mM)						1						
order	B	B	B	B	B	B	A	B	B	B	B	B

***Figure 3*:** Quantitation of click chemistry efficiency. TBTA (a) or BTTAA and THPTA (b) were used under a variety of conditions to label ASH-alkyne with **3** and compared to ASH-rhodamine as described for Figure 2. Order A: sequential addition of alkyne, azide, reductant, ligand, and copper; order B: ligand and copper are premixed, then added to azide/alkyne mixture, followed by addition of reductant.

BTTAA and THPTA have been used under a variety of ligand:Cu ratios and $CuSO_4$ concentrations, and generally in contexts that attempted to minimize cell damage.[4,14,15] As we do not need live cells for this experiment, we attempted to increase labeling by increasing the $CuSO_4$ concentration and maintaining constant ligand:Cu ratios. After initial optimization, we determined these ligands were most effective at 2.5 mM sodium ascorbate, 1 mM $CuSO_4$, and 2 mM ligand, which we have used as our "standard" condition. We also used the recommended order of addition, in which $CuSO_4$ and ligand are premixed before addition to the alkyne/azide mixture, and the reducing agent is added last to initiate the reaction.

Both BTTAA and THPTA gave maximum efficiencies at around 70-80%, comparable to the maximum achievable labeling with TBTA (B1, B7). Notably, reactions performed with THPTA often looked streaky after being subjected to SDS-PAGE and in-gel fluorescence scanning, with a number of fluorescent non-ASH bands (Fig 4a), indicating labeling of non-alkynylated proteins. Addition of SDS to BTTAA or THPTA reactions severely reduced labeling (B4); a similar trend was observed with Triton X-100 for THPTA, though BTTAA was insensitive to its presence (B5). Increasing concentrations of lysate protein had little to no effect on click chemistry with BTTAA up to 1 mg/mL, whereas it severely impacted THPTA-mediated labeling (B2-3). Curiously, while TBTA works substantially better with TCEP than with sodium ascorbate, the opposite trend is observed with water-soluble ligands, consistent with previous observations for THPTA (B6).[4] BTTAA and THPTA were also used with the same order of addition as for TBTA (order B, B7). This resulted in equivalent or higher labeling than what was observed for the previously reported order of addition, indicating these ligands are insensitive to

the order of addition, as was also true for TBTA. BTTAA and THPTA were also both tested at the highest reported $CuSO_4$ concentrations for each. While the reported BTTAA condition of 0.25 mM $CuSO_4$ and 2:1 ligand:Cu ratio was moderately effective for both ligands (B9), use of the reported THPTA conditions (0.50 mM $CuSO_4$ and a 5:1 ligand:Cu ratio) were inefficient for both ligands (B10), suggesting that at high ligand:Cu ratios, the ligands can be inhibitory. Use of these ligands at the concentrations used for TBTA also resulted in very little labeling (B11). Aminoguanidine had no effect or was detrimental to the signal when added (B12).

These data suggest that, while total labeling with ligand THPTA can achieve the same level as BTTAA and TBTA, its strong dependence on protein concentration and the non-specific bands observed with it make it a less desirable ligand overall when pursuing maximal labeling. The use of the conditions T1, T5, or T7 represent the maximal signal for CuAAC with BTTAA; since condition T7 is the simplest, it will be used for subsequent experiments with both BTTAA and THPTA.

In summary, we have identified optimized conditions for TBTA (50 μM azide, 1 mM TCEP, 0.1 mM TBTA, and 1 mM $CuSO_4$), THPTA, and BTTAA (50 μM azide, 2.5 mM sodium ascorbate, 2 mM ligand, and 1 mM $CuSO_4$). While use of triton X-100 was considered for standard conditions, it was not found to reduce visible protein precipitation when TBTA was used, indicating it fails to solubilize the proteins (in contrast to SDS). Optimized conditions were then tested with some other conditions that had been reported. Specifically, Kaschani *et al*[13] report the

use of ligand-free click chemistry with 0.4 mM DTT as a reductant, 1 mM $CuSO_4$, 50 mM sodium acetate buffer (pH 6.0) and only 10 μM of the azide tag. As these conditions were attractive for conservation of resources and for simplicity, we tested each of these variations separately, and together (Figure 2b). While click chemistry with TBTA and THPTA could tolerate substitution of the sodium acetate buffer for PBS, and CuAAC with TBTA accepted DTT as a replacement for TCEP, we did not find that any other modifications, alone or in combination, could provide similar labeling as our optimized conditions for each ligand.

As it is often desirable to perform click chemistry on cell lysate, we investigated the effect of a variety of lysis buffers on click chemistry. PBS and PBS with 1% Triton X-100 both gave robust click chemistry with TBTA, as did RIPA buffer (50 mM Tris pH 7.4, 150 mM NaCl, 1% Triton X-100, 0.5% deoxycholate, 0.1% SDS). Mammalian lysis buffer (20 mM Tris-HCl pH 7.4, 150 mM NaCl, 1 mM EDTA, 1 mM EGTA, 1% Triton X-100, 2.5 mM sodium pyrophosphate, 1 mM sodium glycerophosphate, 1 mM PMSF, and EDTA-free protease inhibitor cocktail (Roche)) inhibited click chemistry quite potently, even when prepared without EDTA or EGTA.

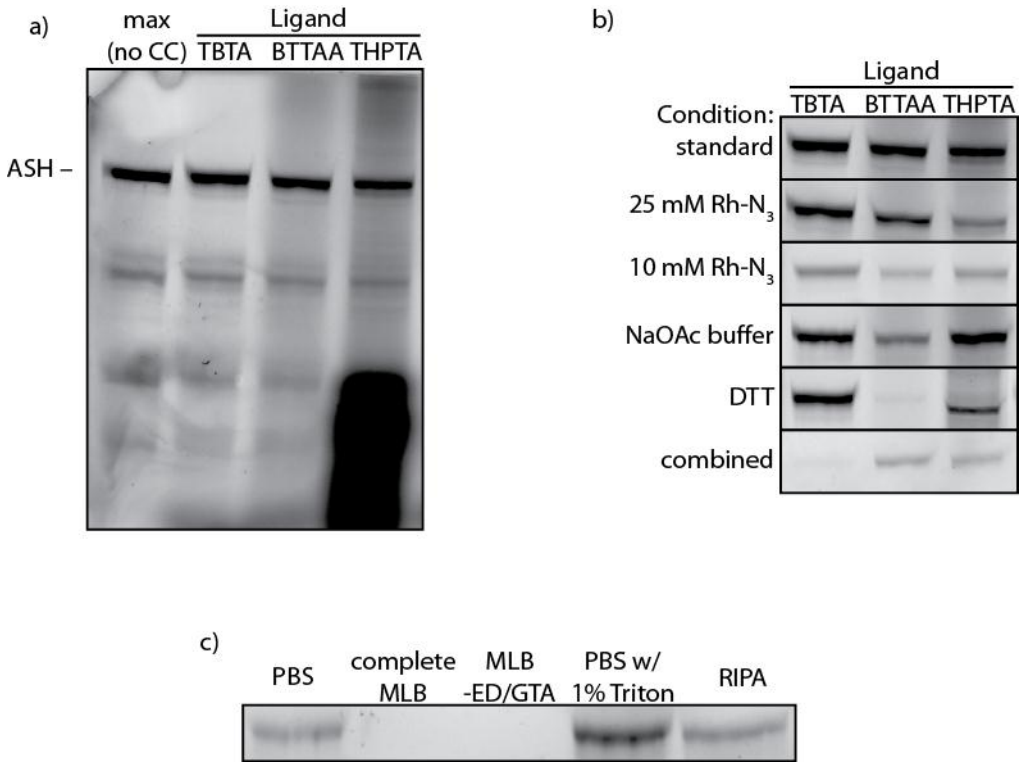

***Figure 4*:** Additional click chemistry optimization. a) Full fluorescent gel scan of optimized conditions for each ligand. b) Fluorescent gel scan of a diversity of other conditions. Optimized conditions for each ligand were used, with the indicated modifications. c) Optimized TBTA click chemistry in a variety of buffer solutions.

We then sought to compare these ligands with respect to their ability to biotinylate proteins and allow their capture and recovery from streptavidin beads. We therefore employed the cleavable biotin-azide **5** (see Figure 6) published by Szychowski *et al.*[16,17] This can be efficiently cleaved by 300 mM sodium dithionite ($Na_2S_2O_4$) in 1% SDS. In order to quantitatively analyze the fate of the alkynylated protein, we utilized both labeling sites of ASH. In addition to the benzylguanine-alkyne to label the SNAP-tag portion, ASH was simultaneously incubated with hexylchloride-fluorescein to label the Halo-tag domain, creating doubly labeled ASH (dl-ASH). Fluorescence gels comparing samples taken at various points in the labeling and recovery process allow for quantitative tracking of the dl-ASH protein at each step (Figure 5). After the

CuAAC reaction, a step to remove excess biotin is necessary, or the amount of streptavidin beads needed to account for all the biotin is prohibitive. This step has generally been accomplished by precipitating the protein and washing it with a polar organic solvent, followed by resolubilization with an SDS or urea solution, then dilution before incubation with streptavidin beads. The extremely tight interaction between biotin and streptavidin permits extensive washes (including 1% SDS and a 6M urea, 2M thiourea buffer), and cleavage with sodium dithionite permits selective and complete elution of biotinylated proteins. As a control to show elution of only our biotinylated proteins, click chemistry can alternately be done with biotin-PEG-azide **6**, which cannot be cleaved by sodium dithionite.

In order to show that the ASH protein can be fully labeled at both active sites, it was incubated with hexylchloride-fluorescein **4** and/or benzylguanine-fluorescein **7** (Figure 6b). Exposure to both **4** and **7** provides an increase of fluorescence similar to the sum of labeling with only one or the other. Preincubation of ASH with benzylguanine-alkyne **2** before addition of **7** leads to the expected blocking of labeling. It is somewhat surprising that the fluorescence from labeling with **7** is not equivalent to labeling with **4**, as both contain the same fluorophore moiety. If the lower fluorescence from **7** labeling is due to differences in fluorophore properties, then this may still indicate that the SNAP-tag binding site can be fully labeled. If the lower fluorescence is due to a lower efficiency of **7** as a substrate of SNAP-tag, this would give us little information about the occupation of the SNAP-tag active site. This is unlikely to be the problem, however, given the excess of **7** relative to ASH. Finally, it is possible that some fraction of the ASH protein has an active Halo-tag enzyme but an inactive SNAP-tag enzyme. This would imply that a certain

fraction (around 40%) of ASH would be labeled at the Halo-tag site but not the SNAP-tag site. Consequently, it is difficult to be confident that the ASH can be fully labeled at both active sites. However, it is clear that the SNAP-tag site can be fully blocked by binding to benzylguanine alkyne **2**, and the alkynylated protein can be tracked reasonably well through the experiment.

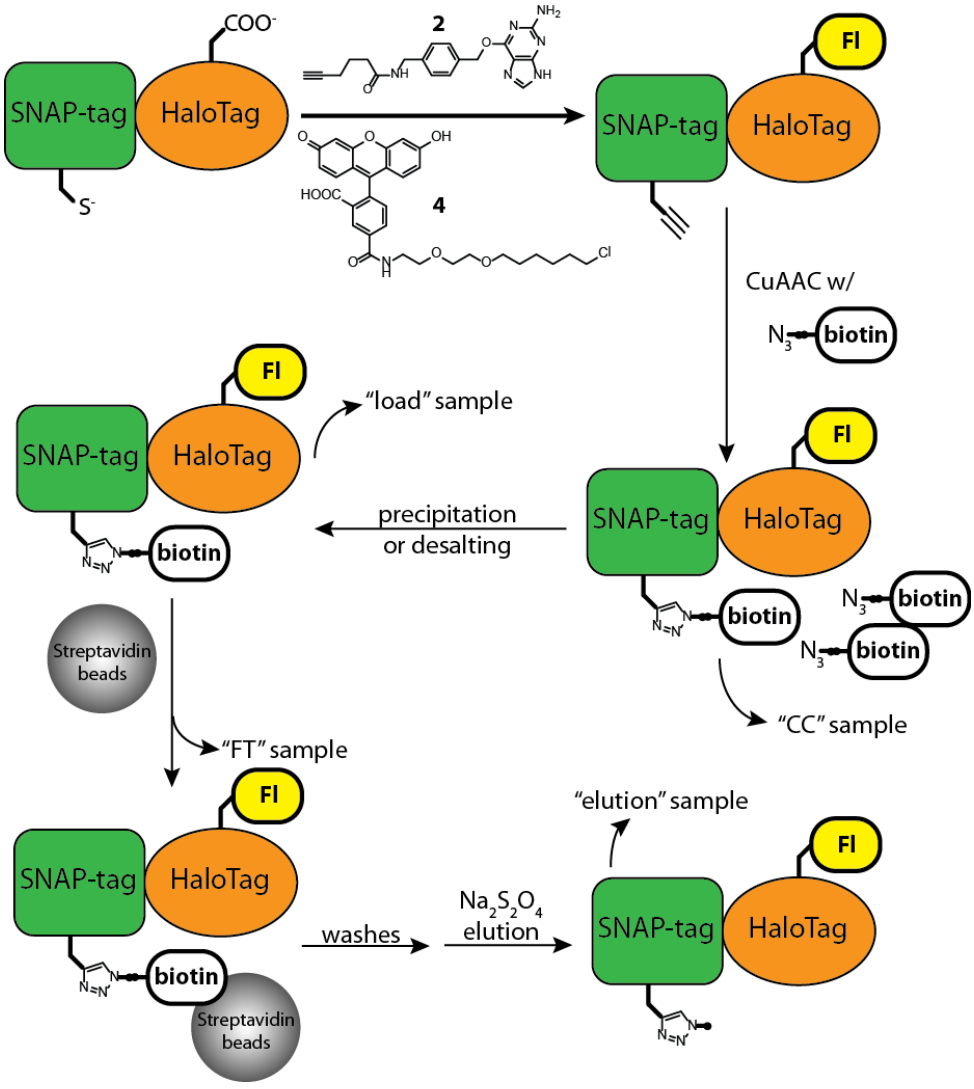

***Figure 5*:** Method for quantitation of recovery of alkynylated proteins. ASH is exposed to both **2** and **4**, leading to formation of ASH-alkyne-fluorescein. This is then subjected to click chemistry, the excess biotin is removed by precipitation or desalting, and the protein is then incubated with streptavidin beads. After extensive washes, incubation with sodium dithionite cleaves the linker in **5**, providing an elution with only proteins that were biotinylated through click chemistry.

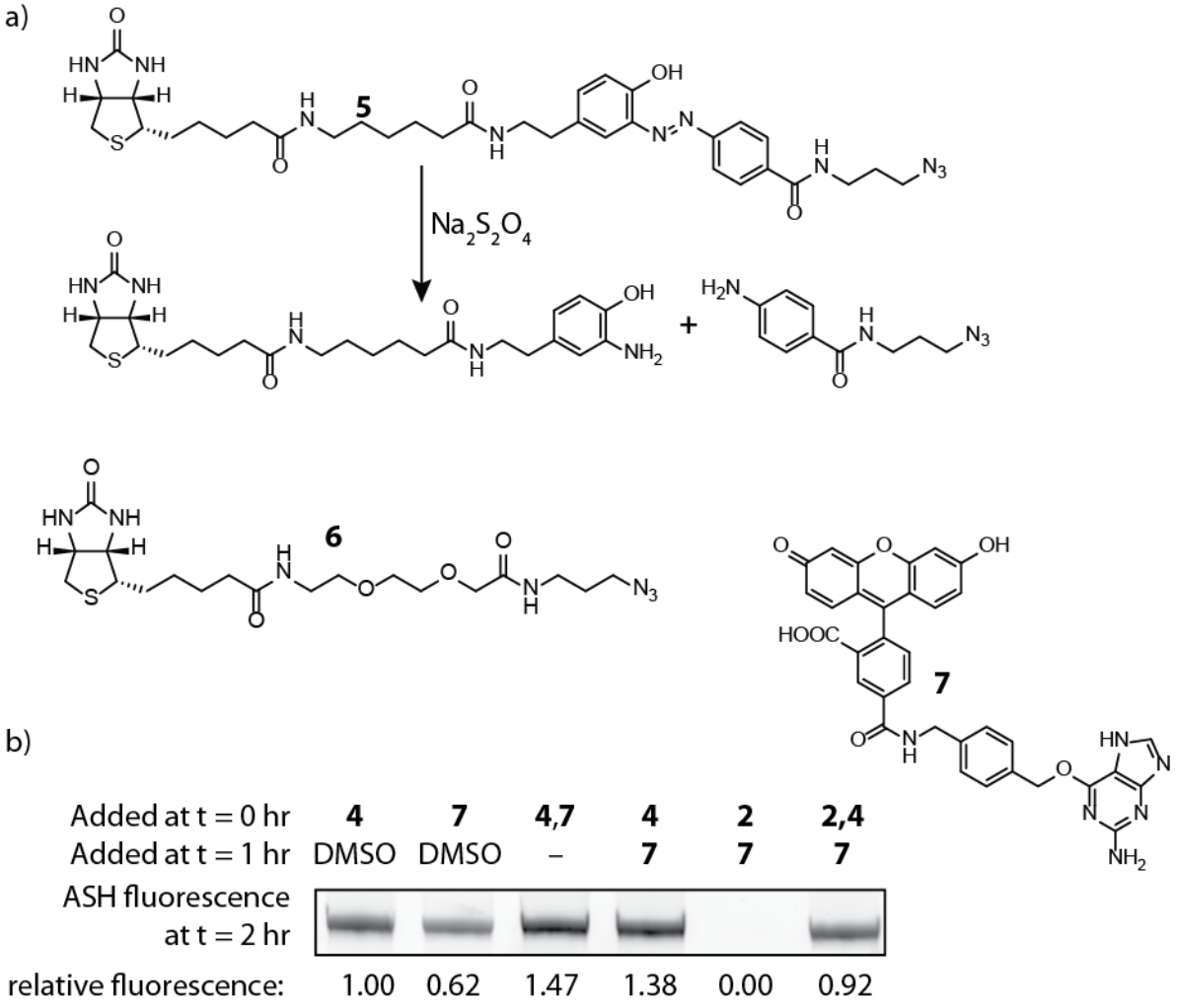

***Figure 6*:** a) Additional chemicals used in protein purification. Cleavable (**5**) and non-cleavable (**6**) biotin-azides. b) Incubation with benzylguanine and hexylchloride derivatives of fluorescein shows labeling of both active sites in ASH; labeling by **7** can be fully blocked by incubation with **2**, showing the active site is fully alkynylated.

Initial experiments with recovery from streptavidin beads showed that the precipitation step to remove excess biotin also led to substantial loss of protein, consistent with previous reports.[6] We first explored multiple precipitation protocols, and found a modest improvement by switching

from MeOH/$CHCl_3$ precipitation to TCA-based precipitation methods (Figure 7a). Having observed that some protein was not resolubilized by 1.2% SDS, we explored other resolubilization buffers (2.5% SDS and urea buffer (6 M urea, 2M thioura, 10 mM HEPES pH 8.0)), but found no improvement in protein recovery (data not shown). When these methods are applied to recover ASH (38 nM) from 0.5 mg/mL lysate, we find that the maximal achievable recovery is 6-7% of the dl-ASH protein after elution with dithionite. Use of non-cleavable biotin **6** in the click chemistry step yields no fluorescent protein in the elution, as expected. When SDS is added during click chemistry, about the same recovery of dl-ASH is observed as when no SDS is used. We also attempted to add SDS after click chemistry, before precipitation. While SDS addition indeed caused all protein precipitated during click chemistry to become soluble (*i.e.*, the solution went from cloudy to clear), it still reduced recovery from streptavidin beads. Recovery from click chemistry with BTTAA was similar to that of reactions employing TBTA, as long as no SDS was added after click chemistry.

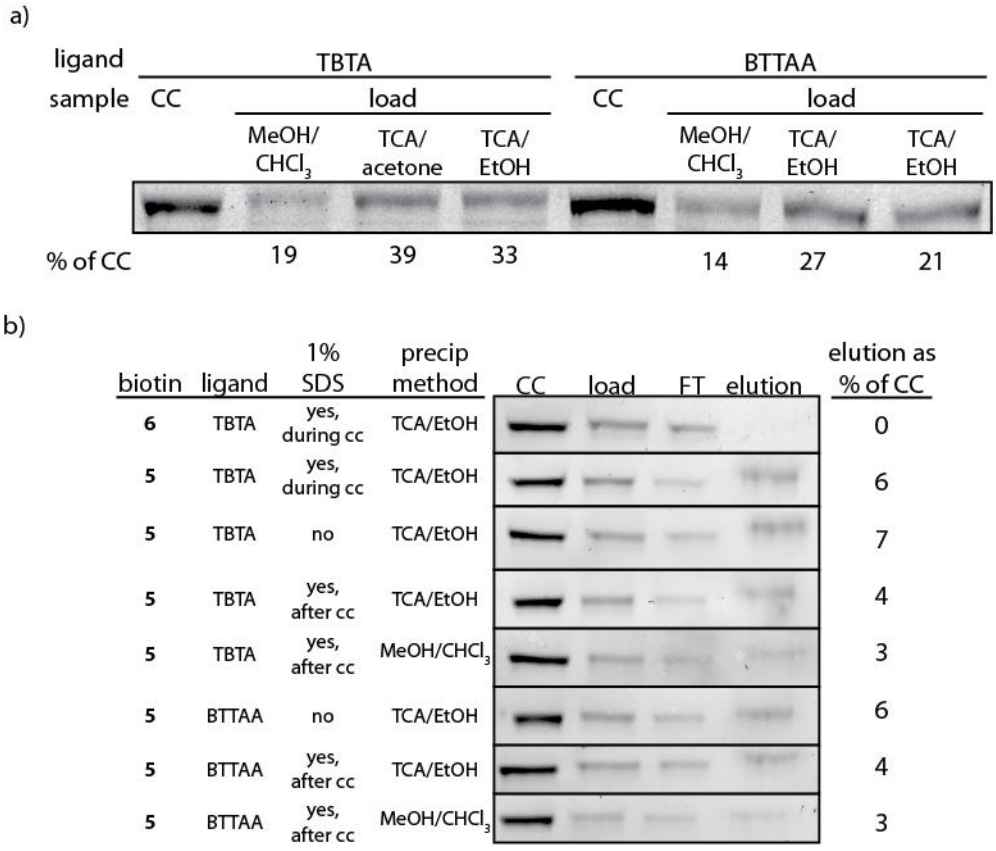

***Figure 7*:** Protein recovery with precipitation. a) ASH was labeled with biotin-azide (using the indicated ligands) and then precipitated using the indicated methods. Less than 40% of protein was recovered in all conditions. b) ASH was carried through the entire process in Figure 5 with the indicated conditions. Shown is the fluorescent gel from each condition, as well as the percentage of dl-ASH recovered from each experiment.

Most protocols published to date for streptavidin purification following click chemistry employ precipitation as a means to get rid of excess biotin because CuAAC with TBTA already precipitates a large portion of the protein. However, since we have observed that BTTAA and THPTA do not cause the protein to visibly precipitate, and that SDS can resolubilize protein precipitated in CuAAC with TBTA, we explored the use of desalting columns in place of precipitation (Figure 8).

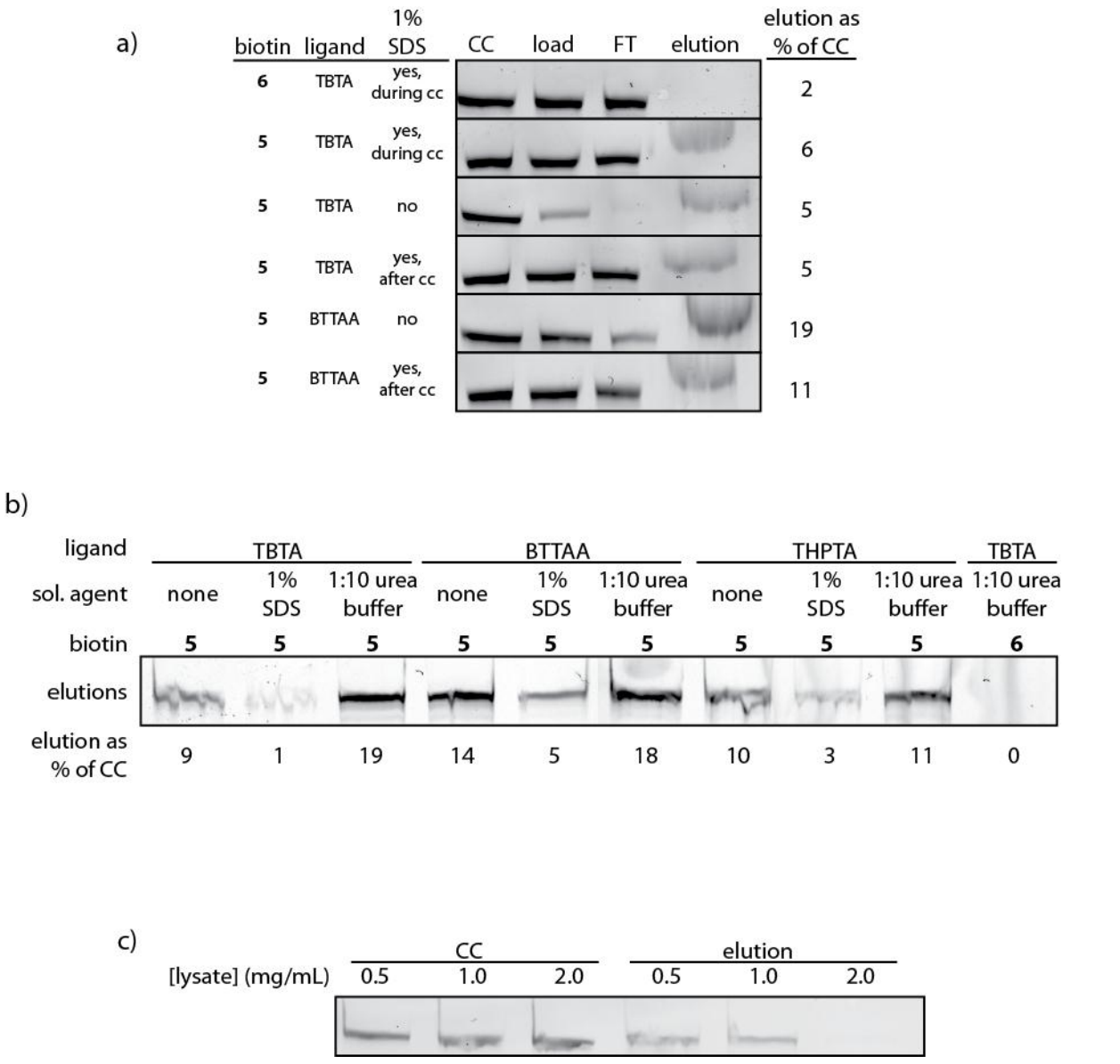

***Figure 8*:** Streptavidin bead recovery when using desalting in place of precipitation. a) Comparison of conditions for streptavidin bead recovery, focused on variations of click chemistry and desalting, showing markedly better recovery with BTTAA CuAAC. b) Comparison of CuAAC ligands and post-click chemistry solubilization agents for streptavidin bead recovery of dl-ASH. c) Analysis of the effect of lysate concentration on elution, showing use of 2.0 mg/mL lysate in CuAAC leads to no recovery of dl-ASH

Strikingly, the “load” sample for each reaction was nearly identical to the CC sample, showing the desalting columns provided efficient protein recovery. The one exception is when no SDS is used before or after CuAAC with TBTA. This is unsurprising, as the dense precipitate generated in this condition is not expected to be able to pass through the desalting resin, while addition of SDS provides a clear solution. However, most of the SDS-solubilized protein comes out in the flow-through, leading to very little recovery in the elution. Since the streptavidin beads are known to be stable at the SDS concentrations used here, we suspect that the SDS forms micelles that bring the excess biotin-azide through the desalting column, competing for the streptavidin binding sites. Notably, in the case of CuAAC with TBTA and no SDS, there is a comparable elution in spite of most of the protein not being recovered from the desalting column; what protein is soluble appears to be efficiently captured and released. When BTTAA was used as the ligand in CuAAC, recovery from the streptavidin beads is higher, achieving nearly 20% recovery, indicating that prevention of precipitation is key to recovery in this system. Once again, addition of SDS decreases this recovery substantially.

Given that SDS appears to be undesirable for use with desalting columns, we wondered if urea could resolubilize the proteins without drawing the biotin through the columns. We therefore compared CuAAC with each ligand, after which the reaction received either no additive, SDS (final 1%), or urea buffer (final 0.6 M urea, 0.2 M thiourea; experiments with higher urea concentrations gave comparable results). TBTA reactions with no additive were very cloudy in appearance; SDS addition provided completely clear reactions (no visible precipitate); and urea addition provided reactions of intermediate cloudiness. Consistent with our hypothesis that SDS

draws the biotin-azide through the desalting column, the yellow color of the cleavable biotin-azide was noticeable in the "load" samples when SDS had been used in contrast to reactions without SDS. As expected, therefore, the reactions that had received SDS had very little recovered dl-ASH. Reactions with no additive gave results consistent with the solubility of proteins in the CuAAC conditions: TBTA provides little dl-ASH recovery, but BTTAA and THPTA give 14% and 10% recovery, respectively. Addition of urea to all reactions results in increased recovery (up to 19%, 18%, and 11% for TBTA, BTTAA, and THPTA, respectively). While this increase is most noticeable for TBTA, this degree of recovery was somewhat variable in other replicates of the experiment, but BTTAA recovery is consistently around 20%. Given that THPTA tends to cause substantial non-specific labeling (Fig 4a), we decided to pursue recovery of dl-ASH from cell lysate with the ligand BTTAA. These experiments are ongoing.

Conclusion

In this study, we have explored for the first time the water-soluble ligands BTTAA and THPTA as reagents for maximal labeling of alkynylated proteins, and provide quantitative comparison of these ligands to TBTA. Through the use of the ASH protein, we have shown that all three ligands can provide labeling of up to 70% of alkynylated proteins with rhodamine-azide. When CuAAC is used to biotinylate alkynylated protein, up to 20% of the alkynylated protein can be recovered under our scheme with BTTAA as the ligand in CuAAC, and a desalting column to eliminate excess biotin. It is as yet unresolved whether the active site of SNAP-tag can be labeled to the same degree as the Halo-tag binding site. If not all fluorescein labeled ASH is also alkynylated, it is possible that an even greater percentage of alkynylated protein is purified in this scheme.

The choice of ligand for click chemistry, therefore, will be dependent on the choice of application. If no purification is needed, TBTA is attractive as a highly efficient ligand, which can be used at low concentrations (1/20th of the concentrations of BTTAA and THPTA), is synthetically tractable, and is commercially available. However, if proteins must be largely soluble after click chemistry (as for the streptavidin purification we describe), BTTAA or THPTA would be required. THPTA is more synthetically accessible, but CuAAC reactions with THPTA lead to labeling of non-alkynylated proteins. BTTAA provides clean reactions and is robust to a variety of conditions, particularly higher protein concentrations and the presence of Triton X-100.

Experimental

Synthesis

TMR* **1**,[18] Benzylguanine-alkyne **2**,[19] rhodamine-azide **3**,[20] Fluorescein-hexylchloride **4**,[11] cleavable biotin-azide **5**[16] and non-cleavable biotin-azide **6**,[21] fluorescein-benzylguanine **7**,[22] TBTA,[5] THPTA,[23] and BTTAA[15] were synthesized as previously described.

Preparation of mammalian cell lysate

Three 25-cm plates of HEK293 cells were grown to ~95% confluency using standard tissue culture procedure. The supernatant was removed, and 2 mL of PBS were added to each plate. The cells were collected and combined in a centrifuge tube. Cells were spun down (5 min, 2K

rpm) and the supernatant was removed. Cells were resuspended in 5 mL of lysis buffer (PBS containing Roche EDTA-free protease inhibitor cocktail). Lysis was achieved by pulling the suspension in and out of a 1-mL syringe with a 25-guage needle 40 times. Cell lysate was cleared by centrifugation in a microcentrifuge (10 min, maximum speed, 4° C), and then quantitated by Bradford assay and found to be at 3.8 mg/mL. Aliquots were snap-frozen in liquid N_2 and stored at -80° C.

Comparison of click chemistry conditions

ASH labeling reactions were prepared by combining 10x SNAP-tag labeling buffer (50 mM Tris buffer, pH 7.5, 100 mM NaCl, 0.1% Tween 20), water, fresh DTT (100 mM stocks, 2 mM final), and ASH (21.5 μM stock, 1 μM final). 19.5 uL of this protein solution was removed and received TMR* **1** (500 μM stock, 12.5 μM final) and incubated at rt for 2-3 hrs. Reaction was stopped by the addition of SDS loading buffer to create a "maximal labeling" sample. The remaining protein solution received benzylguaninine-alkyne **2** (500 μM stock, 12.5 μM final). This was incubated for 2 hrs at rt. For each condition, three replicates were set up simultaneously (though pipetted independently). Under order A conditions, components were sequentially combined: lysis buffer (to final volume 66.3 μL), lysate (3.8 mg/mL stock, to indicated final concentrations), ASH-alkyne labeling reaction (1 μM, to 38 nM final), detergents (20% (m/v) SDS or 10% (v/v) Triton x-100 stocks, to 1% final), aminoguanidine (50 mM aminoguanidine-HCl, to 1 mM final), rhodamine-azide (2.5 mM stock in DMSO, 0.1 mM final), reducing agent (50 mM TCEP or sodium ascorbate, freshly made in water, to 1 mM or 2.5 mM final, respectively), ligand (3.4 mM TBTA in 1:4 DMSO:*tert*-butanol and 50 or 5 mM BTTAA or THPTA in water, to indicated final concentrations), and finally $CuSO_4$ (50 mM, freshly made in

water, to 1 mM final). Under condition B conditions, components were sequentially combined: ligand (3.4 mM TBTA in 1:4 DMSO: *tert*-butanol and 50 or 5 mM BTTAA or THPTA in water, for indicated final concentrations) and $CuSO_4$ (50 mM, freshly made in water, for indicated final concentration) were pre-mixed in a tube and set aside. Then lysis buffer, lysate, ASH-alkyne, detergents, aminoguanidine, and rhodamine-azide were combined as for order A. The premixed copper/ligand were added to this alkyne/azide containing mixture, followed by the reducing agent (50 mM TCEP or sodium ascorbate, freshly made in water, to 1 mM or 2.5 mM final, respectively). Reactions were briefly mixed after each component was added. After incubating at rt for 1 hr, the reactions were stopped by addition of SDS loading buffer with EDTA (final [EDTA] = 5 mM). 20 μL of each reaction were loaded on 10-well 10% SDS-PAGE gels and run for about 60 min at 200V. Gels were scanned on a GE Typhoon under TAMARA settings, PMT at 600 V to obtain fluorescence scans. Gels were then transferred to nitrocellulose by standard Western blot.

In vitro biotin labeling and streptavidin recovery

Labeling and click chemistry

The entire experiment was performed without direct light to prevent photobleaching of the fluorescein components. ASH was labeled as above. Click chemistry reactions were assembled as for Order A above, adding detergents as indicated. All reactions had 0.5 mg/mL final lysate concentration. After being subjected to click chemistry conditions for 1 hr at rt, SDS or urea was added to the indicated reactions. No reactions with BTTAA were found to be cloudy at the end of precipitation, whereas all TBTA-containing reactions without SDS were quite cloudy with protein precipitate (including reactions with Triton X-100). After addition of SDS at the end of

click chemistry, that reaction went from being cloudy to being clear. At the end of click chemistry, an aliquot was removed as “CC” sample.

Precipitation and resolubilization

Precipitation protocols were carried out according to published protocols.[24] To each protein pellet, 60 μL of 1.2% SDS in PBS was added. Reactions were sonicated in a warm water bath for 5 min, then boiled on a heat block for 5 min to resolubilize all proteins. Reactions were then diluted to 0.2% SDS by addition of 300 μL of PBS, mixed, and centrifuged (4 min, rt, 16.1 K x *g*) again to remove any insoluble protein. An aliquot was removed here as “loaded” sample.

Streptavidin bead purification

Streptavidin beads were washed 3 times with PBS and prepared in a 50% (v/v) mixture in PBS. 40 μL of the bead mixture was added to the remaining resolubilized protein, and this slurry was twirled for 1 hr at room temp. Beads were spun down (1 min, rt, 2 K x *g*, as for all subsequent spins) and washed. All washes were in a volume of 500 μL, and twirled for 1 min before being spun down. Three washes were performed with 1% SDS in PBS, followed by 3 washes in urea buffer (6 M urea, 2 M thiourea, 10 mM HEPES pH 8.0). A fresh solution of 300 mM $Na_2S_2O_4$ and 1% SDS in PBS was prepared. 50 μL of this solution was added to the washed beads and twirled at 30 °C (to maintain $Na_2S_2O_4$ in solution) for 20 min. After incubation, beads were spun down and the supernatant was removed. This was performed twice. After removal of the second 50 μL of the dithionite solution, 25 μL of the sodium dithionite solution was added to the beads, mixed briefly, and spun down. The combined 125 μL of elutions were combined and received SDS loading buffer. All samples were run on gels and scanned for fluorescein fluorescence.

References

(1) Kolb, H. C.; Finn, M. G.; Sharpless, K. B. *Angew. Chem. Int. Ed. Engl.* **2001**, *40*, 2004-2021.

(2) Agard, N. J.; Baskin, J. M.; Prescher, J. A.; Lo, A.; Bertozzi, C. R. *ACS Chem. Biol.* **2006**, *1*, 644-8.

(3) Agard, N. J.; Baskin, J. M.; Prescher, J. A.; Lo, A.; Bertozzi, C. R. *ACS Chem Biol* **2006**, *1*, 644-8.

(4) Hong, V.; Presolski, S. I.; Ma, C.; Finn, M. G. *Angew Chem Int Ed Engl* **2009**, *48*, 9879-83.

(5) Chan, T. R.; Hilgraf, R.; Sharpless, K. B.; Fokin, V. V. *Org Lett* **2004**, *6*, 2853-5.

(6) Weerapana, E.; Speers, A. E.; Cravatt, B. F. *Nat. Protoc.* **2007**, *2*, 1414-25.

(7) Besanceney-Webler, C.; Jiang, H.; Zheng, T.; Feng, L.; Soriano Del Amo, D.; Wang, W.; Klivansky, L. M.; Marlow, F. L.; Liu, Y.; Wu, P. *Angew Chem Int Ed Engl*.

(8) Gronemeyer, T.; Chidley, C.; Juillerat, A.; Heinis, C.; Johnsson, K. 2006; Vol. 19, p 309-316.

(9) Juillerat, A.; Gronemeyer, T.; Keppler, A.; Gendreizig, S.; Pick, H.; Vogel, H.; Johnsson, K. *Chemistry & biology* **2003**, *10*, 313-317.

(10) Los, G. V.; Encell, L. P.; McDougall, M. G.; Hartzell, D. D.; Karassina, N.; Zimprich, C.; Wood, M. G.; Learish, R.; Ohana, R. F.; Urh, M.; Simpson, D.; Mendez, J.; Zimmerman, K.; Otto, P.; Vidugiris, G.; Zhu, J.; Darzins, A.; Klaubert, D. H.; Bulleit, R. F.; Wood, K. V. *ACS Chem. Biol.* **2008**, *3*, 373-82.

(11) Brigham, J., Perera, G., Maly, D. *Manuscript in preparation*.

(12) Witte, M. D.; Walvoort, M. T.; Li, K. Y.; Kallemeijn, W. W.; Donker-Koopman, W. E.; Boot, R. G.; Aerts, J. M.; Codee, J. D.; van der Marel, G. A.; Overkleeft, H. S. *Chembiochem*, *12*, 1263-9.

(13) Kaschani, F.; Verhelst, S. H.; van Swieten, P. F.; Verdoes, M.; Wong, C. S.; Wang, Z.; Kaiser, M.; Overkleeft, H. S.; Bogyo, M.; van der Hoorn, R. A. *Plant J.* **2009**, *57*, 373-85.

(14) Hong, V.; Steinmetz, N. F.; Manchester, M.; Finn, M. G. *Bioconjug. Chem.* **2010**, *21*, 1912-6.

(15) Besanceney-Webler, C.; Jiang, H.; Zheng, T.; Feng, L.; Soriano Del Amo, D.; Wang, W.; Klivansky, L. M.; Marlow, F. L.; Liu, Y.; Wu, P. *Angew. Chem. Int. Ed. Engl.*

(16) Szychowski, J.; Mahdavi, A.; Hodas, J. J.; Bagert, J. D.; Ngo, J. T.; Landgraf, P.; Dieterich, D. C.; Schuman, E. M.; Tirrell, D. A. *J. Am. Chem. Soc.* **2010**, *132*, 18351-60.

(17) Verhelst, S. H.; Fonovic, M.; Bogyo, M. *Angew. Chem. Int. Ed. Engl.* **2007**, *46*, 1284-6.

(18) Kindermann, M., Schwab, M. USA, 2006.

(19) Banala, S.; Arnold, A.; Johnsson, K. *Chembiochem* **2008**, *9*, 38-41.

(20) Hintersteiner, M.; Kimmerlin, T.; Garavel, G.; Schindler, T.; Bauer, R.; Meisner, N. C.; Seifert, J. M.; Uhl, V.; Auer, M. *Chembiochem* **2009**, *10*, 994-8.

(21) Onizuka, K.; Shibata, A.; Taniguchi, Y.; Sasaki, S. *Chem. Commun. (Camb.)*, *47*, 5004-6.

(22) Keppler, A.; Kindermann, M.; Gendreizig, S.; Pick, H.; Vogel, H.; Johnsson, K. *Methods* **2004**, *32*, 437-44.

(23) Hong, V.; Presolski, S. I.; Ma, C.; Finn, M. G. *Angew. Chem. Int. Ed. Engl.* **2009**, *48*, 9879-83.

(24) Lebendiker, M. 2002.

Curriculum Vitae

Education

University of Washington, Seattle, Washington, 2006-present
Ph.D. Chemistry, 2012 (expected)

Portland State University, Portland, Oregon, 2004-2006
M.S. Chemistry, 2006

Oregon State University, Corvallis, Oregon, 1998-2002
Honors B.S. Chemistry, 2002, Magna cum Laude
Honors B.S. Biochemistry/Biophysics, 2002, Magna cum Laude

Awards and Presentations

Poster presentation, ASBMB conference, April 2012
Molecular Biophysics Training Grant graduate fellowship, Univ. of Washington, 2006-2008
Merck Award, Dept. of Chemistry, Oregon State University, 2002
Undergraduate Research, Innovation, Scholarship & Creativity, Oregon St. Univ., 2001
Ray and Fran Cripps fellowship, Oregon State University, 2001

Research Experience

Graduate Research: Organic Chemistry Division, Department of Chemistry, University of Washington (advisor: Dustin Maly)

- Organic synthesis of new probes for the study of protein kinases
- Method development for purification, labeling, and identification of protein complex members
- Tissue culture for the study of protein kinases in mammalian cell lines

Graduate Research: Biochemistry Department, University of Washington (advisor: Tamir Gonen)

- Purification and crystallization of endogenous aquaporin 0 for electron crystallography
- Yeast expression and purification of aquaporin 7

Graduate Research: Department of Chemistry, Portland State University (advisor: David Peyton)

- Design and synthesis of novel antimalarial drugs

Undergraduate Research: College of Pharmacy, Oregon State University (advisor: Bill Gerwick)

- Isolation and identification of a novel cytotoxic terpenoid from an alga

Teaching Experience

Lab TA (16 quarters): Department of Chemistry, University of Washington and Portland State University. Prepared and presented lectures, guided student activities, and evaluated student performance at all levels of organic chemistry lab, from BA- level classes to Honors classes. Also, taught 1 quarter each of general chemistry lab, biochemistry lab, and spectroscopic analysis lab, with similar duties.

Biochemistry Lecture TA (1 quarter): Conducted study sections, including summarizing the week's material, and answering student questions.

Biochemistry study section leader (2 quarters): Volunteered time to lead study section of first-year medical student biochemistry class. Duties included presenting research papers and guiding student presentations of papers.

TA/RA Conference (Fall 2011): Volunteered time to lecture and lead discussion for incoming TAs and RAs about graduate school experiences and duties.

Publications

ZB Hill, BG Perera, **S Andrews**, DJ Maly, "Targeting Diverse Signaling Interaction Sites Allows the Rapid Generation of Bivalent Kinase Inhibitors." ACS Chemical Biology 2011 Dec 22 (Epub ahead of print)

S Andrews, SJ Burgess, D Skaalrud, JX Kelly, DH Peyton, "Reversal agent and linker variants of reversed chloroquines: activities against Plasmodium falciparum," Journal of Medicinal Chemistry 2010 **53** (2), 916-919

S Andrews, SL Reichow, T Gonen, "Electron crystallography of aquaporins," IUBMB Life 2008 **60** (7), 430-436

H Zheng, AS Olia, M Gonen, **S Andrews**, G Cingolani, T Gonen, "A conformational switch in bacteriophage p22 portal protein primes genome injection," Molecular Cell 2008 **29** (3), 376-383

OMM Sabry, **S Andrews**, KL McPhail, DE Goeger, A Yokochi, KT LePage, TF Murray, WH Gerwick, "Neurotoxic meroditerpenoids from the tropical marine brown alga Stypopodium flabelliforme." Journal of Natural Products 2005 **68** (7), 1022-1030